

**R-01-17**

## **Partitioning and transmutation**

### **Annual Report 2000**

S Andersson, C Ekberg, Å Enarsson, J-O Liljenzin,  
C Mesmin, M Nilsson and G Skarnemark

Department of Nuclear Chemistry  
Chalmers University of Technology, Göteborg

March 2001

**Svensk Kärnbränslehantering AB**

Swedish Nuclear Fuel  
and Waste Management Co  
Box 5864

SE-102 40 Stockholm Sweden

Tel 08-459 84 00  
+46 8 459 84 00

Fax 08-661 57 19  
+46 8 661 57 19



ISSN 1402-3091

SKB Rapport R-01-17

# **Partitioning and transmutation**

## **Annual Report 2000**

S Andersson, C Ekberg, Å Enarsson, J-O Liljenzin,  
C Mesmin, M Nilsson and G Skarnemark

Department of Nuclear Chemistry  
Chalmers University of Technology, Göteborg

March 2001

This report concerns a study which was conducted for SKB. The conclusions and viewpoints presented in the report are those of the author(s) and do not necessarily coincide with those of the client.

## CONTENTS

1	INTRODUCTION .....	1
2	SOLVENT EXTRACTION RESEARCH.....	2
3	COLLABORATIONS.....	4
4	MEETINGS AND LECTURES .....	5
5	PERSONNEL.....	5
6	REFERENCES .....	5

## APPENDICIES

### Articles/Reports

- I** M. G. B. Drew, P. B. Iveson, M. J. Hudson, J. O. Liljenzin, L. Spjuth, P.-Y. Cordier, Å. Enarsson, C. Hill, C. Madic, "Separation of americium(III) from europium(III) with tridentate heterocyclic nitrogen ligands and crystallographic studies of complexes formed by 2,2':6',2"-terpyridine with the lanthanides", *J. Chem. Soc., Dalton Trans.*, 821-830, 2000
- II** G. Meinrath, C. Ekberg, A. Landgren, J.O. Liljenzin, "Assessment of Uncertainty in Parameter Evaluation and Prediction", *Talanta*, 51, 231-246, 2000
- III** C. Gustafsson, "Extraction Studies of Ag, Co, Cs, Fe and U by Terpyridine - 2-bromodecanoic Acid Mixtures", *Diploma Thesis, Department of Nuclear Chemistry, Chalmers University of Technology, January 2000*
- IV** L. Spjuth, J.O. Liljenzin, M.J. Hudson, M.G.B. Drew, P.B. Iveson, C. Madic, "Comparison of extraction behaviour and basicity of some substituted malonamides", *Solv. Extr. & Ion Exch.*, 18, 1-23, 2000
- V** M. Nilsson, "Influence of Organic Phase Composition on the Extraction of Trivalent Actinides", *Diploma Thesis, Department of Nuclear Chemistry, Chalmers University of Technology, November 2000*

## 1 INTRODUCTION

The research on partitioning and transmutation at the Department of Nuclear Chemistry, Chalmers, is focused on the separation using solvent extraction.

For an efficient transmutation process it is essential that the nuclides intended for transmutation (i.e. the actinides and selected fission products) be separated from the rest of the fission products or else too many neutrons will be lost transmuting nuclides that are already short-lived or stable.

In the proposed process the separation is accomplished in at least two steps. First actinides and lanthanides are co-extracted from high concentration nitric acid and then the trivalent actinides and the lanthanides are back-extracted into a nitric acid solution of lower concentration. These are then separated from each other in a second step. All reagents used in this future process should follow the so-called CHON-principle, i.e. consist of only carbon, hydrogen, oxygen and nitrogen atoms, to be completely incinerable and thereby minimising the secondary waste produced.

The main part of the studies at the Department of Nuclear Chemistry, Chalmers, during this year has concerned the later part of the separation process, i.e. the separation of trivalent actinides from lanthanides.

## 2 SOLVENT EXTRACTION RESEARCH

Extractants that coordinate to the metal ion with one (or several) nitrogen atoms have a higher selectivity for actinides over lanthanides than extractants coordinating with oxygen.

Several nitrogen-containing extractants, together with carboxylic acids, have been studied in the past, e.g. substituted oligopyridines and triazines, and more are being synthesized at the University of Reading within the PARTNEW project. The objective is to find an extractant that can separate trivalent actinides from lanthanides as well as possible at as high nitric acid concentration as possible.

Terpyridine, which is commercially available, has been used as a reference molecule in synergy with 2-bromodecanoic acid (HA) in *tert*-butylbenzene to learn more about the synergistic extraction mechanism with this group of extractants. It has also been used to develop experimental procedures and methods for investigation of physical properties, e.g. solubility and basicity. These methods can then be used to examine new molecules of similar kind. The aim is to be able to relate the physical properties to the extraction and separation ability for better understanding and to synthesize new better molecules.

M.Sc. student Charlotta Gustafsson finished her diploma thesis in January 2000. She examined the extraction of several metal ions in the synergetic system of terpyridine and 2-bromodecanoic acid in *tert*-butylbenzene from nitric acid (Appendix III). For these ions she determined the extracted complexes (Table 2-1) and the possibilities for separation.

**Table 2-1. Extracted complexes for some metal ions in the terpyridine-HA system (TBB-nitric acid) (Appendix III)**

Metal ion	Extracted complex with 2-bromodecanoic acid (HA)	Extracted complex with terpyridine (T) and 2-bromodecanoic acid (HA)
Cs <sup>+</sup>	CsA(HA) <sub>2</sub>	CsA(HA) <sub>2</sub>
Ag <sup>+</sup>	AgAHA	(AgA(HA)) <sub>2</sub> T
Co <sup>2+</sup>	CoA <sub>2</sub> (HA) <sub>3</sub>	CoA <sub>2</sub> (HA) <sub>3</sub> T <sub>2</sub>
Fe <sup>3+</sup>	FeA <sub>3</sub>	FeA <sub>3</sub> T
UO <sub>2</sub> <sup>2+</sup>	UO <sub>2</sub> A <sub>2</sub>	UO <sub>2</sub> A <sub>2</sub> T <sub>2</sub> + UO <sub>2</sub> A <sub>2</sub> T

A second M.Sc. student, Mikael Nilsson, studied the influence of diluents, and mixtures of diluents, on the extraction of Am, Cm and Pm with terpyridine and 2-bromodecanoic acid from nitric acid and developed a model based on Hansen solubility parameters to predict the extraction with other organic phase compositions. He finished his diploma thesis in November 2000 (Appendix V). The model gives a good agreement between calculated and experimental values except for strong polar solvents e.g. nitrobenzene (fig 2-1).

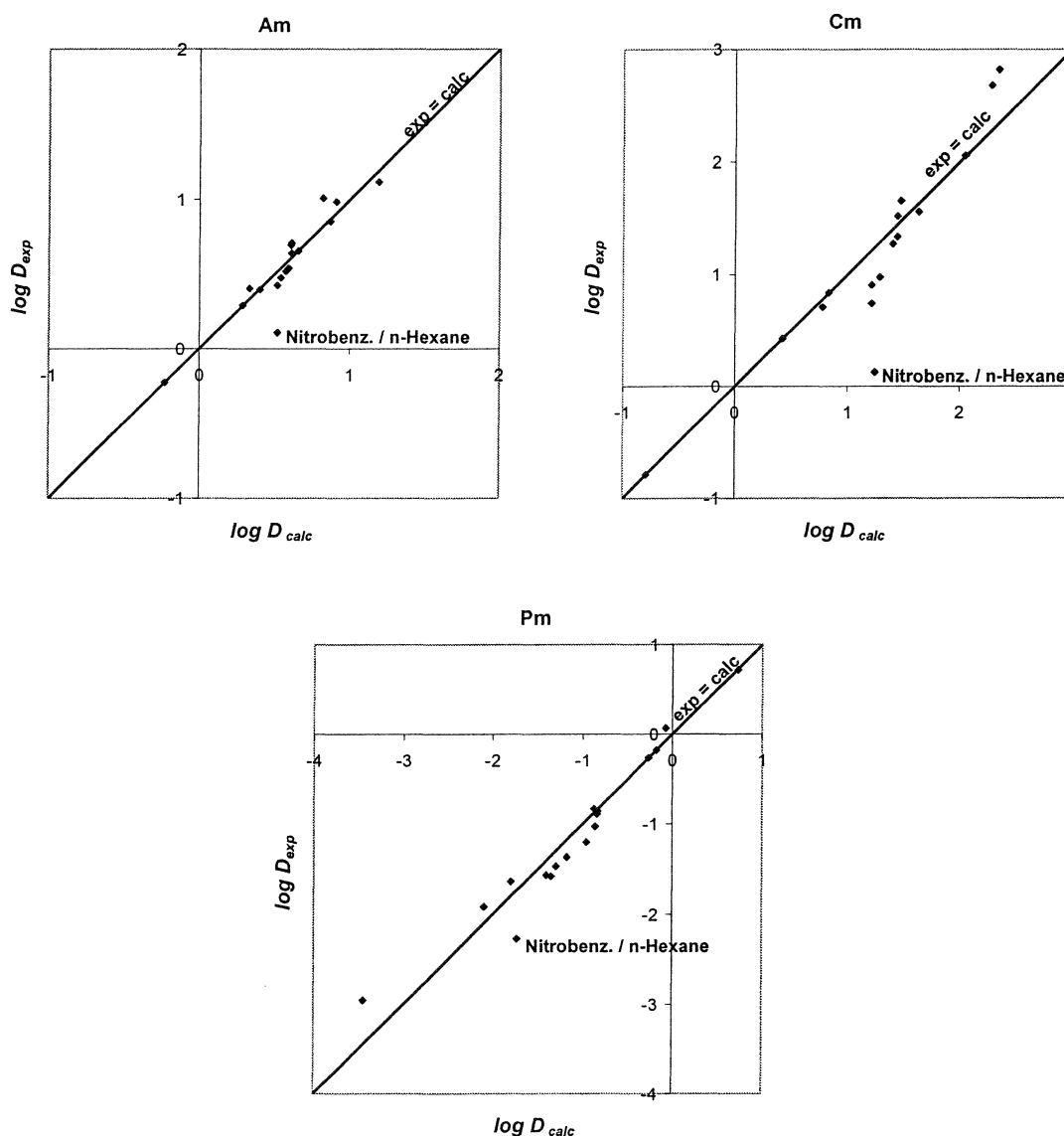


Fig 2-1. Comparison between calculated and experimental values of distribution.

To accomplish a better understanding of the mechanisms of actinide separation different extractants have been studied to determine their basic physical properties. The stability constants of protonated terpyridine have been derived through liquid-liquid extraction experiments with different compositions of the aqueous phase. The distribution of extractant is (among other things) dependent on the hydrogen ion concentration and can be determined spectrophotometrically since terpyridine forms a strong coloured complex with copper(II)-ions. Three protonation constants of terpyridine were found. Literature values of the protonation constants of terpyridine, found by titration, only include the two first protonation steps [Sch84]. When the same method was applied on TPTZ problems with solubility and complex distribution arose. Different organic solvents have and will be tested as well as other metal ions for the complex formation. Hopefully the final method can be applied to new nitrogen ligands produced within the PARTNEW project.

### 3 COLLABORATIONS

#### *Sweden*

The Swedish Spallator Network (SSN) is a national network with the objective to inform internally and externally about Swedish and international research concerning accelerator-driven transmutation systems. The network consists of representatives from different universities and institutes;

- \* Chalmers University of Technology, Göteborg
- \* Royal Institute of Technology, Stockholm
- \* Uppsala University
- \* Lund University.

#### *Europe*

A three-year European contract started in September 2000 concerning new partitioning techniques within the Nuclear Fission Safety program (PARTNEW FIKW-CT2000-00087). There are ten participating institutes from six different European countries;

- \* Department of Nuclear Chemistry, Chalmers (Sweden)
- \* CEA (France)
- \* University of Reading (UK)
- \* Transurium Institute (Germany)
- \* ENEA (Italy)
- \* Politecnico di Milano (Italy)
- \* Forschungszentrum Karlsruhe (Germany)
- \* Forschungszentrum Jülich (Germany)
- \* CIEMAT (Spain)
- \* Universidad Autonoma de Madrid (Spain).

This project is a continuation of the NEWPART contract from the Forth Framework Programme. Project meetings are held every 6th month.

### *England*

The University of Reading has an important role in the European contract as a “supplier” of new extractants. The department also performs co-ordination chemistry and molecular modelling of these new ligands.

### *France*

There have been a lot of contacts between the CEA laboratory in Marcoule and Chalmers since the work performed at the two laboratories are closely connected. There is a continuous exchange of new ligands and discussion of new results.

## **4 MEETINGS AND LECTURES**

A Kick off meeting for the European collaboration project PARTNEW were held in Marcoule, France, in October.

## **5 PERSONNEL**

In the first half of this year Jan-Olov Liljenzin was the only active member of the Partitioning and Transmutation group. Åsa Enarsson has been on maternity leave this year. In May Sophie Andersson started her Ph D studies and in September Post Doc Claire Mesmin joined the group. In the fall Mikael Nilsson concluded his M Sc degree and has now started his Ph D studies.

Jan-Olov Liljenzin, Gunnar Skarnemark and Christian Ekberg have been supervising.

## **6 REFERENCES**

- Sch84 Schildt A., Wong S-W., Protonation Constants of 2,6-bis(2pyridyl)pyridine) and 2,4,6-tris(2-pyridyl)-1,3,5-Triazine and Formation Constants of their Binary and Ternary Iron(II)Complexes, J. Inorg. Nucl. Chem., 13, 337 (1984)

# Appendix I

# Separation of americium(III) from europium(III) with tridentate heterocyclic nitrogen ligands and crystallographic studies of complexes formed by 2,2':6',2''-terpyridine with the lanthanides

Michael G. B. Drew,<sup>\*a</sup> Peter B. Iveson,<sup>a</sup> Michael J. Hudson,<sup>a</sup> Jan Olov Liljenzin,<sup>b</sup> Lena Spjuth,<sup>b</sup> Pierre-Yves Cordier,<sup>c</sup> Åsa Enarsson,<sup>b</sup> Clément Hill<sup>c</sup> and Charles Madic<sup>c</sup>

<sup>a</sup> Department of Chemistry, University of Reading, Whiteknights, Reading, UK RG6 6AD.  
E-mail: m.g.b.drew@reading.ac.uk

<sup>b</sup> Department of Nuclear Chemistry, Chalmers University of Technology, S-41296 Göteborg, Sweden

<sup>c</sup> Commissariat à l'Energie Atomique, Direction du Cycle du Combustible, B.P. 171, 30207 Bagnols-sur-Cèze cedex, France

Received 1st September 1999, Accepted 14th January 2000

Phenyl-substituted derivatives of 2,2':6',2''-terpyridine and a corresponding bipyridine-pyrazine derivative have been shown to have metal extraction properties and separation factors for americium(III) over europium(III) which are comparable to those previously obtained for 2,2':6',2''-terpyridine ( $L^1$ ). The extracting agents in either *tert*-butylbenzene (TBB) or hydrogenated tetrapropene (TPH) gave  $D_{Am}/D_{Eu}$  separation factors (SFs) between 7 and 9 when used to extract the metal ions from 0.01–0.1 M nitric acid solution in synergistic combination with 2-bromodecanoic acid. In contrast to  $L^1$ , the new hydrophobic ligands have little or no solubility in the aqueous phase. In an effort to better understand the nature of the species which may be involved in the extraction process, a series of metal- $L^1$  complexes which cover the lanthanides have been prepared. Five different structural types have been established for the lanthanide coordination complexes. In type 1,  $[M(NO_3)_3(L^1)(H_2O)]$  ( $M = Nd$ ), the metal is 10-coordinate being bonded to one terdentate  $L^1$  ligand, three bidentate nitrates and a water molecule. In type 2,  $[M(NO_3)_2(L^1)_2]^+[M(NO_3)_4(L^1)]^-$  ( $M = Nd, Sm, Tb, Dy$  and  $Ho$ ), the metal atom in the cation is 10-coordinate, being bonded to two terdentate  $L^1$  ligands and two bidentate nitrates; in the anion the metal is also 10-coordinate, being bonded to one terdentate  $L^1$  ligand and four nitrates, of which three are bidentate and one unidentate. In type 3,  $[M(NO_3)_3(L^1)(H_2O)] \cdot L^1$  ( $M = Ho, Er, Tm$  and  $Yb$ ), the metal is 10-coordinate, being bonded to three bidentate nitrates, one terdentate  $L^1$  and a water molecule. In addition, an  $L^1$  ligand is found in the asymmetric unit which is hydrogen-bonded to the coordinated water molecule. In type 4,  $[M(NO_3)_3(L^1)(H_2O)]$  ( $M = Tm$ ), the metal is 9-coordinate, being bonded to two bidentate nitrates, one unidentate nitrate, one terdentate  $L^1$  ligand and a water molecule. In type 5,  $[M(NO_3)_3(L^1)]$  ( $M = Yb$ ), the metal is 9-coordinate, being bonded to three bidentate nitrates and one terdentate  $L^1$  ligand. A sixth structural type was observed for  $M = La$  in the crystal structure  $[(H_2L^1)(NO_3)]^+[(H_2L^1)]^{2+}[La(NO_3)_6]^{3-}$ . The metal is not bound to  $L^1$  but instead forms the well-known hexanitrate anion. This complex may give some indication of the type of species which could be formed at higher acid concentrations in the aqueous phase, where protonation of  $L^1$  can occur.

## Introduction

One of the aims in nuclear reprocessing is the conversion or transmutation of the long-lived minor actinides, such as americium, into short-lived isotopes by irradiation with neutrons.<sup>1</sup> In order to achieve this transmutation it is necessary to separate the trivalent minor actinides from the trivalent lanthanides by solvent extraction because otherwise the lanthanides absorb neutrons effectively and, hence, prevent neutron capture by the transmutable actinides. For many years, we have been designing and testing ligands for the co-extraction of lanthanides and actinides from nuclear waste and their subsequent separation.<sup>2–4</sup> Various aza-aromatic bases have been shown to selectively extract actinides in preference to lanthanides from a nitric acid solution into an organic phase.<sup>5,6</sup> Nitric acid is used in the extraction experiments because it is envisaged that the An(III)–Ln(III) separation process will take place after the existing PUREX process and the proposed DIAMEX process.<sup>1</sup> The PUREX process is already used to separate uranium and plutonium from a concentrated nitric acid solution and the DIAMEX process will be used to coextract the trivalent lanthanide and actinide ions prior to their separation.

One of the tested ligands, 2,2':6',2''-terpyridine ( $L^1$ ) shown in Fig. 1, in synergistic combination with 2-bromodecanoic acid, gave an Am(III)/Eu(III) separation factor of 7 at 0.01 M  $HNO_3$ .<sup>6</sup> This promising result is tempered by the fact that the ligand has some solubility in the aqueous phase, even in its unprotonated form. In this work, we have used three, more hydrophobic, derivatives of terpyridine which should have little or no solubility in the aqueous phase. Thus, 4'-(4-nitrophenyl)-2,2':6',2''-terpyridine ( $L^2$ ), 4'-(4-tolyl)-2,2':6',2''-terpyridine ( $L^3$ ) and 4'-(4-dodecyloxyphenyl)-2,2':6',2''-terpyridine ( $L^4$ ) have been synthesised and their Am(III)/Eu(III) separation-extraction performance has been determined. A fourth ligand was also tested, 6'-pyrazin-2-yl-4'-(4-heptyloxyphenyl)-2,2'-bipyridinyl ( $L^5$ ) in which one of the pyridine groups was replaced by pyrazine. All of the synthesised ligands are shown in Fig. 1.

In an effort to determine the nature of the species which may be involved in the extraction process, we have structurally characterised a series of lanthanide complexes formed with  $L^1$ . It proved impossible to obtain crystals of complexes with ligands  $L^2$  to  $L^5$  but it seems likely that complexes with similar stoichiometries and coordination geometries will be found for the ligands  $L^1$  to  $L^5$  inclusive, as the bite angles of these planar

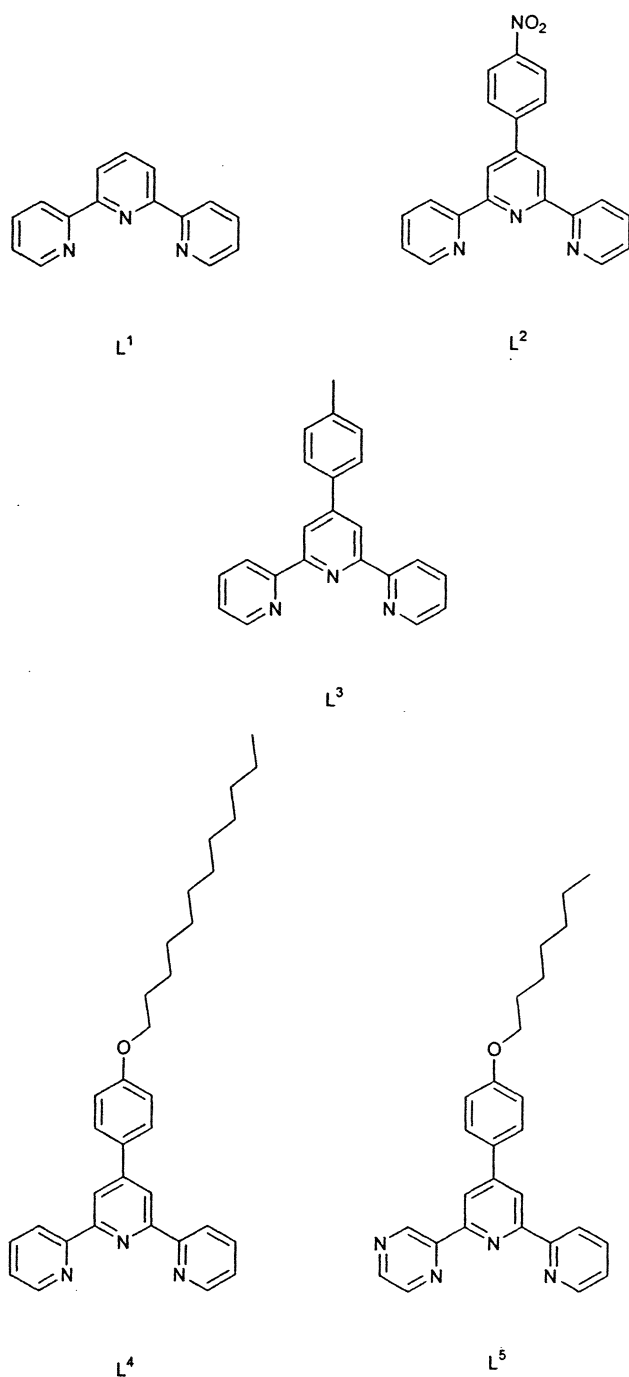


Fig. 1 Structures of the ligands.

terdentate ligands will be equivalent. Our aim is to gain an understanding of the processes involved in the extraction and, hence, to establish the best possible ligands for use in the An–Ln separations.

## Experimental

Lanthanum nitrate hexahydrate (99.9%), neodymium nitrate hexahydrate (99.9%), samarium nitrate hexahydrate (99.9%), terbium nitrate pentahydrate (99.9%), dysprosium nitrate pentahydrate (99.9%), holmium nitrate pentahydrate (99.9%), erbium nitrate pentahydrate (99.9%), thulium nitrate pentahydrate (99.9%), ytterbium nitrate pentahydrate (99.9%), 2-acetylpyridine, 2,2':6',2''-terpyridine (all Aldrich), 2-acetylpyrazine, 4-heptyloxybenzaldehyde, 4-dodecyloxybenzaldehyde (Lancaster Synthesis), *tert*-butylbenzene (TBB; Acros), 2-bromodecanoic acid (Fluka) and hydrogenated tetrapropene, an industrial aliphatic diluent with highly branched chains,

(TPH; Prochrom, France) were used as received. Acetonitrile was dried and stored over 3 Å molecular sieves. NMR spectra were run on a JEOL JNM-EX 400 spectrometer. Microanalyses were carried out by Medac Ltd., Brunel Science Centre and mass spectra were run on a VG autospec machine. Uncorrected melting points were obtained on a Stuart melting point apparatus.

## Preparation of ligands

4'-(4-Nitrophenyl)-2,2':6',2''-terpyridine ( $L^2$ ) and 4'-(4-tolyl)-2,2':6',2''-terpyridine ( $L^3$ ) were prepared according to the literature methods.<sup>7,8</sup>

**4'-(4-Dodecyloxyphenyl)-2,2':6',2''-terpyridine ( $L^4$ ).** A mixture of *N*-[1-oxo-2-(2-pyridyl)ethyl]pyridinium iodide<sup>9</sup> (8.29 g, 0.0254 mol), 1-(2-pyridyl)-3-[4-dodecyloxyphenyl]propen-1-one (10 g, 0.0254 mol)<sup>10</sup> and ammonium acetate (19.3 g) in 190 cm<sup>3</sup> methanol was heated at reflux for 6 h. After removal of the solvent, the residue was partitioned between CH<sub>2</sub>Cl<sub>2</sub> and water. The organic layer was separated and then the aqueous layer was extracted twice more with CH<sub>2</sub>Cl<sub>2</sub>. The combined organic extracts were then dried with sodium sulfate and the solvent was removed *in vacuo*. The oil was purified by column chromatography on Al<sub>2</sub>O<sub>3</sub> with CH<sub>2</sub>Cl<sub>2</sub> as eluant. The resulting yellow solid was recrystallised twice from ethanol to give 4.2 g (33%) of  $L^4$ . Mp 85–87 °C. Found: C, 80.36; H, 8.10; N, 8.37. C<sub>33</sub>H<sub>39</sub>N<sub>3</sub>O requires C, 80.29; H, 7.96; N, 8.51%. <sup>1</sup>H NMR (CDCl<sub>3</sub>): δ 0.88 (3H, t), 1.17–1.41 (8H, m), 1.47 (2H, qt), 1.81 (2H, qt), 4.01 (2H, t), 7.00–7.03 (2H, m), 7.32–7.36 (2H, m), 7.84–7.88 (4H, m), 8.65–8.74 (6H, m).

**1-(2-pyrazinyl)-3-[4-(heptyloxy)phenyl]propen-1-one.** 2-Acetylpyrazine (0.5 g, 0.0041 mol) was added dropwise to a stirred emulsion of 4-heptyloxybenzaldehyde (0.90 g, 0.0041 mol) containing 10 cm<sup>3</sup> EtOH and 5 cm<sup>3</sup> 1.5 M NaOH. After stirring overnight at room temperature under a nitrogen atmosphere, the yellow solid was filtered and recrystallised from MeOH to give 0.5 g (38%) of pure product. Mp 92–94 °C. Found: C, 73.77; H, 7.36; N, 8.56. C<sub>20</sub>H<sub>23</sub>N<sub>2</sub>O<sub>2</sub> requires C, 74.28; H, 7.17; N, 8.66%. <sup>1</sup>H NMR (CDCl<sub>3</sub>): δ 0.91 (3H, t), 1.25–1.41 (8H, m), 1.81 (2H, qt), 4.07 (2H, t), 6.88–6.98 (2H, m), 7.60–7.73 (2H, m), 7.90–8.10 (2H, m), 8.65–8.80 (2H, m), 9.38 (1H, s).

**6'-Pyrazin-2-yl-4'-(4-heptyloxyphenyl)-2,2'-bipyridinyl ( $L^5$ ).** A mixture of *N*-[1-oxo-2-(2-pyridyl)ethyl]pyridinium iodide (5.03 g, 0.0154 mol), 1-(2-pyrazinyl)-3-[4-(heptyloxy)phenyl]propen-1-one (5 g, 0.0154 mol) and ammonium acetate (12 g) in 120 cm<sup>3</sup> methanol was heated at reflux for 6 h. After cooling, a small amount of a light green solid precipitated. This was filtered, washed with water and dried under vacuum (yield 1.1 g, 17%). Mp 119–121 °C. Found: C, 76.33; H, 6.66; N, 13.26. C<sub>27</sub>H<sub>28</sub>N<sub>4</sub>O requires C, 76.39; H, 6.65; N, 13.26%. <sup>1</sup>H NMR (CDCl<sub>3</sub>): δ 0.92 (3H, t), 1.02–1.57 (8H, m), 1.84 (2H, qt), 4.02 (2H, t), 7.00–7.08 (2H, m), 7.33–7.41 (1H, m), 7.80–7.94 (3H, m), 8.60–8.78 (6H, m), 9.89 (1H, m).

## Preparation of metal complexes of $L^1$

The complexes are numbered as *n*-M, where M is the metal and *n* the structure type.

**1-Nd.** Nd(NO<sub>3</sub>)<sub>3</sub>·6H<sub>2</sub>O (0.0186 g, 0.04 mM) in 1 cm<sup>3</sup> of CH<sub>3</sub>CN was added dropwise to a stirred solution containing  $L^1$  (0.0099 g, 0.04 mM) dissolved in 1 cm<sup>3</sup> CH<sub>3</sub>CN. Crystals suitable for structure analysis formed after standing overnight (yield 14 mg, 60%). Found: C, 31.03; H, 2.28; N, 14.61. C<sub>15</sub>H<sub>13</sub>N<sub>6</sub>O<sub>10</sub>Nd requires C, 30.98; H, 2.25; N, 14.45%.

**2-Nd.** Nd(NO<sub>3</sub>)<sub>3</sub>·6H<sub>2</sub>O (0.0186 g, 0.04 mM) in 1 cm<sup>3</sup> of CH<sub>3</sub>CN was added dropwise to a stirred solution containing  $L^1$

(0.0397 g, 0.17 mM) dissolved in 1 cm<sup>3</sup> CH<sub>3</sub>CN. Crystals suitable for structure analysis formed almost immediately (yield 6 mg, 11%). Found: C, 39.92; H, 2.46; N, 15.45. C<sub>45</sub>H<sub>33</sub>N<sub>15</sub>O<sub>18</sub>Nd<sub>2</sub> requires C, 39.73; H, 2.44; N, 15.44%. Thus, the two acetonitrile molecules found in the crystal structures were not present in the analysed sample.

**2-Sm.** Sm(NO<sub>3</sub>)<sub>3</sub>·6H<sub>2</sub>O (0.0189 g, 0.04 mM) in 7 cm<sup>3</sup> of CH<sub>3</sub>CN (at approx. 60 °C) was added dropwise to a stirred solution containing L<sup>1</sup> (0.0397 g, 0.17 mM) dissolved in 7 cm<sup>3</sup> of CH<sub>3</sub>CN at the same temperature. Crystals suitable for X-ray crystallography were obtained after 2 days at room temperature (yield 16 mg, 29%). Found: C, 39.19; H, 2.43; N, 15.39. C<sub>45</sub>H<sub>33</sub>N<sub>15</sub>O<sub>18</sub>Sm<sub>2</sub> requires C, 39.38; H, 2.42; N, 15.30%.

**2-Tb.** Tb(NO<sub>3</sub>)<sub>3</sub>·5H<sub>2</sub>O (0.0185 g, 0.04 mM) in 2 cm<sup>3</sup> of CH<sub>3</sub>CN (at approx. 60 °C) was added dropwise to a stirred solution containing L<sup>1</sup> (0.0397 g, 0.17 mM) dissolved in 2 cm<sup>3</sup> of CH<sub>3</sub>CN at the same temperature. Crystals formed after standing overnight (yield 19 mg, 32%). Found: C, 38.75; H, 2.42; N, 15.30. C<sub>47</sub>H<sub>38</sub>N<sub>16</sub>O<sub>20</sub>Tb<sub>2</sub> requires C, 38.54; H, 2.61; N, 15.29%. The sample sent for analysis indicated the presence of one water molecule and one acetonitrile rather than the two acetonitriles that were observed in the crystal structure.

**2-Dy and 2-Ho.** The dysprosium (2-Dy) and holmium (2-Ho) complexes were prepared in the same way as the Tb complex (yield: Dy 10 mg, 17%; Ho 21 mg, 36%). Found: C, 38.55; H, 2.49; N, 15.88. C<sub>47</sub>H<sub>38</sub>N<sub>16</sub>O<sub>19</sub>Dy<sub>2</sub> requires C, 38.77; H, 2.63; N, 15.39%. Found: C, 38.33; H, 2.49; N, 15.10. C<sub>47</sub>H<sub>38</sub>N<sub>16</sub>O<sub>19</sub>Ho<sub>2</sub> requires C, 38.64; H, 2.62; N, 15.34%. In both 2-Dy and 2-Ho, one additional acetonitrile and one water molecule were found in the analysed samples which were not observed in the crystal structures.

**3-Ho.** 3-Ho was prepared in a similar manner to 2-Ho except that the metal solution was added to the L<sup>1</sup> solution at room temperature. On mixing, a precipitate began to form so a further 3 cm<sup>3</sup> of CH<sub>3</sub>CN was added and the solution was heated to redissolve the solid. Small crystals of 3-Ho appeared after standing overnight at room temperature.

**3-Er.** 3-Er was prepared according to the method described above for 2-Tb. Crystals appeared after slowly evaporating the solvent for one week at room temperature (yield 14 mg, 39%). Found: C, 42.80; H, 2.83; N, 14.93. C<sub>30</sub>H<sub>24</sub>N<sub>9</sub>O<sub>10</sub>Er requires C, 43.01; H, 2.89; N, 15.04%. The three solvent acetonitrile molecules found in the crystal structure were not found in the analysis of the bulk sample.

**3-Tm and 4-Tm.** Tm(NO<sub>3</sub>)<sub>3</sub>·5H<sub>2</sub>O (0.0189 g, 0.04 mM) in 1.5 cm<sup>3</sup> of CH<sub>3</sub>CN (at approx. 60 °C) was added dropwise to a stirred solution containing L<sup>1</sup> (0.0397 g, 0.17 mM) dissolved in 1.5 cm<sup>3</sup> of CH<sub>3</sub>CN at the same temperature. A precipitate appeared on standing overnight at room temperature and, on closer inspection, there appeared to be two different crystal forms whose structures were determined to be those of 3-Tm and 4-Tm (yield 15 mg). The elemental analysis indicated that the mixture was almost all 3-Tm with a small amount of 4-Tm. As in the 3-Er case, the solvent acetonitrile molecules found in the crystal structure were not found in the bulk sample. Found: C, 42.32; H, 2.87; N, 14.98. C<sub>30</sub>H<sub>22</sub>N<sub>9</sub>O<sub>9</sub>Tm (3-Tm) requires C, 42.92; H, 2.88; N, 15.01%.

**3-Yb and 5-Yb.** A mixture of 3-Yb and 5-Yb was prepared in a similar manner to the mixture of 3-Tm and 4-Tm. Only crystals of 5-Yb were suitable for a structure determination even though the analysis indicated that the precipitate was almost exclusively 3-Yb (yield 17 mg). Found: C, 42.31; H, 2.75;

N, 14.27. C<sub>30</sub>H<sub>22</sub>N<sub>9</sub>O<sub>9</sub>Yb (3-Yb) requires C, 42.71; H, 2.87; N, 14.94%.

An attempt was then made to prepare pure 5-Yb by adding one mole equivalent of L<sup>1</sup> to the metal. The analysis indicated that the formula of the precipitated complex is Yb(NO<sub>3</sub>)<sub>3</sub>·(L<sup>1</sup>)·H<sub>2</sub>O (yield 6 mg, 24%). Found: C, 29.33; H, 2.20; N, 13.57. C<sub>15</sub>H<sub>13</sub>N<sub>6</sub>O<sub>10</sub>Yb requires C, 29.52; H, 2.15; N, 13.77%. If the water molecule is coordinated the product could be structure type 4, if H<sub>2</sub>O is uncoordinated then it is likely to be type 5.

**6-La.** Diprotonated L<sup>1</sup> was prepared as described previously.<sup>4</sup> 6-La was prepared using the same method as for 3[H<sub>2</sub>L<sup>1</sup>]<sup>2+</sup>·2[La(NO<sub>3</sub>)<sub>6</sub>]<sup>3-</sup>·3H<sub>2</sub>O.<sup>4</sup> It appears that the initial solid diprotonated L<sup>1</sup> must have contained more nitric acid than the previous sample used to prepare 3[H<sub>2</sub>L<sup>1</sup>]<sup>2+</sup>·2[La(NO<sub>3</sub>)<sub>6</sub>]<sup>3-</sup>·3H<sub>2</sub>O. This resulted in the formation of a different product, [(H<sub>2</sub>L<sup>1</sup>)(NO<sub>3</sub>)]<sup>+</sup>[(H<sub>2</sub>L<sup>1</sup>)(CH<sub>3</sub>CN)]<sup>2+</sup>[La(NO<sub>3</sub>)<sub>6</sub>]<sup>3-</sup>, in which NO<sub>3</sub><sup>-</sup> and CH<sub>3</sub>CN were located in the diprotonated L<sup>1</sup> cavities, as compared to 3[H<sub>2</sub>L<sup>1</sup>]<sup>2+</sup>·2[La(NO<sub>3</sub>)<sub>6</sub>]<sup>3-</sup>·3H<sub>2</sub>O in which only water molecules were found in the L<sup>1</sup> cavity. The sample sent for analysis contained an additional mole of water. Found: C, 34.73; H, 2.65; N, 17.55. C<sub>32</sub>H<sub>29</sub>N<sub>14</sub>O<sub>21</sub>La·H<sub>2</sub>O requires C, 34.85; H, 2.87; N, 17.79%.

### Solvent extraction experiments

Mixtures of 2-bromodecanoic acid and the oligopyridine extractant in either TBB or TPH were vigorously shaken with aqueous phases containing tracer amounts of <sup>241</sup>Am and <sup>152</sup>Eu for 5 min (TBB) or 30 min (TPH). After phase disengagement by centrifugation at 4500 rpm, aliquots of each phase were withdrawn for radiometric analysis. The  $\gamma$ -activities at 59.54 and 121.78 keV, for <sup>241</sup>Am and <sup>152</sup>Eu, respectively, were measured using a HPGe detector (EG&G ORTEC or Eurysis Mesures). Distribution ratios  $D_M$  were calculated according to the equation  $D_M = [\text{Activity}]_{\text{org}}/[\text{Activity}]_{\text{aq}}$ , where  $[\text{Activity}]_{\text{org}}$  and  $[\text{Activity}]_{\text{aq}}$  are the radioactivity in counts s<sup>-1</sup> of <sup>241</sup>Am and <sup>152</sup>Eu at equilibrium for equal volumes of organic and aqueous phases respectively. Separation factors, SF<sub>Am/Eu</sub>, were calculated as the  $D_{\text{Am}}/D_{\text{Eu}}$  ratio for the same experimental conditions.

### Crystallography

The crystal structures of 12 lanthanide metal complexes of 2,2':6',2''-terpyridine (L<sup>1</sup>) were determined. 1-Nd is [M(L<sup>1</sup>)(NO<sub>3</sub>)<sub>3</sub>(H<sub>2</sub>O)], 2-Nd, 2-Sm, 2-Tb, 2-Dy and 2-Ho are [M(L<sup>1</sup>)<sub>2</sub>(NO<sub>3</sub>)<sub>2</sub>][M(L<sup>1</sup>)(NO<sub>3</sub>)<sub>4</sub>], 3-Ho, 3-Er, 3-Tm are [M(L<sup>1</sup>)(NO<sub>3</sub>)<sub>3</sub>(H<sub>2</sub>O)]·L<sup>1</sup>, 4-Tm is [M(L<sup>1</sup>)(NO<sub>3</sub>)<sub>3</sub>(H<sub>2</sub>O)], 5-Yb is [M(L<sup>1</sup>)(NO<sub>3</sub>)<sub>3</sub>] and 6-La is [(H<sub>2</sub>L<sup>1</sup>)(NO<sub>3</sub>)]<sup>+</sup>(H<sub>2</sub>L<sup>1</sup>)<sup>2+</sup>[La(NO<sub>3</sub>)<sub>6</sub>]<sup>3-</sup>. Crystal data for 1-Nd, 2-Nd, 2-Sm, 2-Tb, 2-Dy, 2-Ho, 3-Ho, 3-Er, 3-Tm, 4-Tm, 5-Yb and 6-La are given in Table 1, together with refinement details. Data for all 12 crystals were collected with Mo-K $\alpha$  radiation using the MARresearch Image Plate System. The crystals were positioned at 70 mm from the image plate. 95 frames were measured at 2° intervals with a counting time of 2 min. Data analysis was carried out with the XDS program.<sup>11</sup> Structures were solved using direct methods with the SHELX86 program.<sup>12</sup> All non-hydrogen atoms in the metal complexes were refined anisotropically. Hydrogen atoms on the carbon and nitrogen atoms were included in calculated positions and given thermal parameters equivalent to 1.2 times those of the atom to which they were attached. Hydrogen atoms on water molecules were not included. Heavy atoms in solvent molecules were refined anisotropically or isotropically where appropriate. Empirical absorption corrections were made for all structures using the DIFABS program.<sup>13</sup> All structures were refined on  $F^2$  until convergence, using SHELXL.<sup>14</sup> All calculations were carried out on a Silicon Graphics R4000 Workstation at the University of Reading. Bond lengths in the metal coordination sphere of each structure are shown in Table 2. Hydrogen bonds are detailed in Table 3.

Table 1 Crystal data and structure refinement for the compounds

Code	1-Nd	2-Nd	2-Sm	2-Tb	2-Dy	2-Ho	3-Ho	3-Er	3-Tm	4-Tm	5-Yb	6-La
Empirical formula	C <sub>15</sub> H <sub>13</sub> N <sub>6</sub> <sup>-</sup> NdO <sub>10</sub>	C <sub>49</sub> H <sub>39</sub> N <sub>17</sub> <sup>-</sup> Nd <sub>2</sub> O <sub>18</sub>	C <sub>45</sub> H <sub>33</sub> N <sub>15</sub> <sup>-</sup> Sm <sub>2</sub> O <sub>18</sub>	C <sub>49</sub> H <sub>39</sub> N <sub>17</sub> <sup>-</sup> O <sub>18</sub> Tb <sub>2</sub>	C <sub>45</sub> H <sub>33</sub> N <sub>15</sub> <sup>-</sup> O <sub>18</sub> Dy <sub>2</sub>	C <sub>45</sub> H <sub>33</sub> N <sub>15</sub> <sup>-</sup> O <sub>18</sub> Ho <sub>2</sub>	C <sub>36</sub> H <sub>33</sub> <sup>-</sup> HoN <sub>12</sub> O <sub>10</sub>	C <sub>36</sub> H <sub>33</sub> <sup>-</sup> ErN <sub>12</sub> O <sub>10</sub>	C <sub>34</sub> H <sub>28</sub> N <sub>11</sub> <sup>-</sup> O <sub>10</sub> Tm	C <sub>15</sub> H <sub>13</sub> N <sub>6</sub> <sup>-</sup> O <sub>10</sub> Tm	C <sub>15</sub> H <sub>11</sub> N <sub>6</sub> <sup>-</sup> O <sub>9</sub> Yb	C <sub>32</sub> H <sub>29</sub> LaN <sub>14</sub> <sup>-</sup> O <sub>21</sub>
Formula weight	581.56	1442.45	1372.54	1471.81	1396.86	1401.72	958.67	961	919.60	606.24	592.34	542.30
Crystal system, space group	Triclinic, <i>P</i> $\bar{1}$	Triclinic, <i>P</i> $\bar{1}$	Triclinic, <i>P</i> $\bar{1}$	Triclinic, <i>P</i> $\bar{1}$	Triclinic, <i>P</i> $\bar{1}$	Triclinic, <i>P</i> $\bar{1}$	Triclinic, <i>P</i> $\bar{1}$	Triclinic, <i>P</i> $\bar{1}$	Triclinic, <i>P</i> $\bar{1}$	Monoclinic, <i>P</i> <sub>2</sub> / <i>n</i>	Monoclinic, <i>P</i> <sub>2</sub> / <i>n</i>	Monoclinic, <i>P</i> <sub>2</sub> / <i>n</i>
Unit cell dimensions/Å, °												
<i>a</i>	8.327(9)	11.189(14)	10.518(12)	11.087(12)	10.452(13)	10.463(11)	9.994(12)	10.017(12)	10.263(19)	8.655(10)	9.090(9)	10.385(14)
<i>b</i>	10.985(12)	16.059(17)	15.595(17)	16.01(2)	15.531(17)	15.525(17)	14.967(17)	14.742(17)	14.487(17)	8.833(10)	16.693(17)	41.89(5)
<i>c</i>	11.160(14)	16.320(17)	16.116(17)	16.266(17)	16.107(19)	16.131(17)	14.954(17)	14.936(17)	14.816(17)	25.31(3)	13.636(15)	10.757(12)
$\alpha$	93.76(1)	106.58(1)	100.72(1)	106.01(1)	101.06(1)	100.88(1)	70.01(1)	69.49(1)	64.87(1)	(90)	(90)	(90)
$\beta$	94.44(1)	95.16(1)	106.15(1)	95.80(1)	106.14(1)	106.22(1)	78.05(1)	78.11(1)	73.94(1)	90.86(1)	111.11(1)	115.70(1)
$\gamma$	101.42(1)	95.87(1)	95.78(1)	95.87(1)	95.84(1)	95.81(1)	79.78(1)	79.78(1)	78.88(1)	(90)	(90)	(90)
Volume/Å <sup>3</sup>	994	2774	2462	2728	2431	2438	2006	2008	1909	1934	1140	4216
Z, Calculated density/Mg m <sup>-3</sup>	2, 1.943	2, 1.727	2, 1.851	2, 1.792	2, 1.908	2, 1.910	2, 1.587	2, 1.589	2, 1.600	4, 2.082	4, 2.038	4, 1.709
Absorption coefficient/mm <sup>-1</sup>	2.680	1.940	2.455	2.662	3.144	3.004	3.336	3.144	2.393	4.657	4.909	1.114
Reflections measured	3414	8908	7591	8460	8252	8371	5583	6861	5396	3494	5514	11752
Unique reflections ( <i>R</i> <sub>int</sub> )	3414	8908	7591	8460	8252	8371	5583	6861	5396	2111 (0.0566)	3449 (0.0756)	6846 (0.0689)
Data/restraints/parameters	3414/0/290	8908/0/763	7591/0/722	8460/0/767	8252/0/722	8252/0/722	5583/0/536	6861/0/491	5396/0/478	2111/54/290	3449/0/281	6846/36/616
Final <i>R</i> indices ( <i>I</i> > 2σ( <i>I</i> ))	<i>R</i> <sub>1</sub> 0.0733	0.0593	0.0800	0.0423	0.0700	0.0452	0.0638	0.0610	0.0949	0.0604	0.0652	0.1111
<i>wR</i> <sub>2</sub>	0.1979	0.1617	0.2042	0.1144	0.2000	0.1201	0.1623	0.1941	0.2208	0.1822	0.1852	0.2245
<i>R</i> indices (all data)	<i>R</i> <sub>1</sub> 0.1199	0.0781	0.1879	0.0582	0.1214	0.0735	0.1258	0.0748	0.2745	0.0720	0.0797	0.1372
<i>wR</i> <sub>2</sub>	0.2179	0.1783	0.2471	0.1237	0.2306	0.1405	0.1887	0.2100	0.2859	0.1945	0.2014	0.2367
Largest diff. peak and hole/e Å <sup>-3</sup>	0.888, -1.492	1.656, -2.125	2.719, -1.477	1.976, -1.116	2.767, -1.650	1.542, -0.965	1.993, -1.588	1.924, -2.492	0.927, -0.655	1.180, -1.505	3.447, -3.278	1.214, -2.924

**Table 2** Bond lengths (Å) in the metal coordination spheres

Type 1: 1-Nd					
Nd(1)–O(100)	2.488(8)				
Nd(1)–O(41)	2.530(9)				
Nd(1)–O(42)	2.553(10)				
Nd(1)–O(62)	2.556(9)				
Nd(1)–O(52)	2.560(8)				
Nd(1)–O(61)	2.570(8)				
Nd(1)–N(31)	2.586(10)				
Nd(1)–N(11)	2.625(10)				
Nd(1)–O(51)	2.632(9)				
Nd(1)–N(21)	2.703(13)				
Type 2: 2-Nd, 2-Sm, 2-Tb, 2-Dy and 2-Ho					
Cation	2-Nd	2-Sm	2-Tb	2-Dy	2-Ho
M(1)–O(22)	2.526(5)	2.475(13)	2.462(5)	2.440(10)	2.421(6)
M(1)–O(11)	2.550(6)	2.483(12)	2.479(6)	2.413(10)	2.405(6)
M(1)–N(31)	2.592(7)	2.609(13)	2.542(7)	2.539(9)	2.538(7)
M(1)–O(12)	2.591(6)	2.598(13)	2.539(6)	2.596(9)	2.598(6)
M(1)–O(21)	2.598(6)	2.550(12)	2.541(6)	2.555(10)	2.545(6)
M(1)–N(41)	2.630(6)	2.572(14)	2.563(6)	2.543(10)	2.559(7)
M(1)–N(11)	2.631(6)	2.583(15)	2.567(6)	2.587(10)	2.558(7)
M(1)–N(61)	2.638(7)	2.675(15)	2.585(6)	2.613(11)	2.605(7)
M(1)–N(51)	2.645(6)	2.621(13)	2.586(6)	2.560(9)	2.560(7)
M(1)–N(21)	2.651(6)	2.555(13)	2.587(6)	2.528(9)	2.541(7)
Anion					
M(2)–O(31)	2.644(7)	2.547(13)	2.645(7)	2.507(10)	2.509(6)
M(2)–O(32)	2.548(6)	2.497(12)	2.468(6)	2.428(9)	2.439(6)
M(2)–O(41)	2.598(6)	2.613(13)	2.567(6)	2.580(11)	2.580(7)
M(2)–O(42)	2.571(7)	2.570(13)	2.514(7)	2.488(10)	2.495(8)
M(2)–O(51)	2.567(7)	2.497(13)	2.520(6)	2.460(9)	2.435(7)
M(2)–O(52)	2.559(6)	2.596(13)	2.466(6)	2.573(11)	2.556(7)
M(2)–O(61)	2.434(7)	2.370(14)	2.374(6)	2.346(10)	2.323(6)
M(2)–N(71)	2.600(6)	2.556(14)	2.528(6)	2.527(10)	2.531(7)
M(2)–N(81)	2.591(7)	2.590(13)	2.513(6)	2.554(11)	2.544(7)
M(2)–N(91)	2.577(7)	2.561(16)	2.519(6)	2.506(10)	2.541(7)
Types 3 and 4: 3-Ho, 3-Er, 3-Tm and 4-Tm					
	3-Ho	3-Er	3-Tm	4-Tm	
M(1)–O(100)	2.328(7)	2.326(6)	2.317(12)	2.313(10)	
M(1)–O(41)	2.478(10)	2.451(8)	2.407(14)	2.500(14)	
M(1)–O(42)	2.463(9)	2.460(7)	2.444(13)	2.371(14)	
M(1)–O(51)	2.518(9)	2.523(7)	2.480(12)	2.402(14)	
M(1)–O(52)	2.436(8)	2.435(6)	2.473(14)	2.410(13)	
M(1)–O(61)	2.431(8)	2.414(8)	2.313(16)	2.251(13)	
M(1)–O(62)	2.725(11)	2.858(12)	[3.534(20)]	[3.576(16)]	
M(1)–N(11)	2.503(11)	2.478(7)	2.494(19)	2.441(15)	
M(1)–N(21)	2.545(8)	2.505(7)	2.463(17)	2.482(17)	
M(1)–N(31)	2.510(9)	2.489(7)	2.475(16)	2.526(14)	
Type 5: 5-Yb					
Yb(1)–O(42)	2.364(8)				
Yb(1)–O(61)	2.373(8)				
Yb(1)–O(52)	2.382(10)				
Yb(1)–O(41)	2.385(7)				
Yb(1)–N(21)	2.395(8)				
Yb(1)–O(62)	2.406(10)				
Yb(1)–N(11)	2.417(7)				
Yb(1)–N(31)	2.419(8)				
Yb(1)–O(51)	2.456(9)				
Type 6: 6-La					
La(1)–O(42)	2.624(10)				
La(1)–O(21)	2.646(11)				
La(1)–O(12)	2.653(10)				
La(1)–O(51)	2.645(10)				
La(1)–O(62)	2.659(9)				
La(1)–O(32)	2.658(10)				
La(1)–O(41)	2.660(10)				
La(1)–O(22)	2.667(10)				
La(1)–O(11)	2.672(11)				
La(1)–O(31)	2.678(11)				
La(1)–O(52)	2.685(10)				
La(1)–O(61)	2.742(20)				

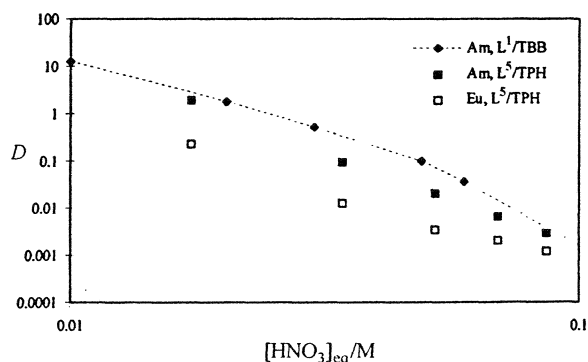
**Table 3** Hydrogen bonds (Å) in the structures

1-Nd			
O(100)···O(64) <sup>a</sup>	2.92		
O(100)···O(52) <sup>b</sup>	2.96		
O(100)···O(62) <sup>b</sup>	2.97		
3-M	M = Ho	M = Er	M = Tm
O(100)···N(41)	2.87	2.87	2.83
O(100)···N(51)	2.97	2.93	2.92
O(100)···N(61)	2.81	2.80	2.79

Angle (°) between adjacent pyridine rings of uncoordinated L<sup>1</sup> in 3-M

	23.8, 29.9	22.8, 31.4	16.9, 27.2
4-Tm			
O(100)···O(62) <sup>c</sup>	2.75		
O(100)···O(51) <sup>d</sup>	2.84		
6-La			
N(11)···N(100)	2.91		
N(31)···N(100)	2.91		
N(41)···O(71)	2.73		
N(61)···O(71)	2.76		

Symmetry operations: <sup>a</sup> 1 - x, -y, -z; <sup>b</sup> -x, -y, -z; <sup>c</sup> -x + 1/2, y - 1/2, -z + 1/2; <sup>d</sup> 1/2 - x, y + 1/2, 1/2 - z.

**Fig. 2** Distribution ratios for the extraction of americium(III) and europium(III) with 0.02 M L<sup>2</sup>–L<sup>4</sup> and 1 M 2-bromodecanoic acid in TBB.

CCDC reference number 186/1805.

See <http://www.rsc.org/suppdata/dt/a9/a907077j/> for crystallographic files in .cif format.

## Discussion

### Solvent extraction

Solvent extraction studies were carried out with the different nitrogen heterocycles (L<sup>2</sup>–L<sup>5</sup>) in synergy with 2-bromodecanoic acid (HA) in *tert*-butylbenzene (TBB) or hydrogenated tetrapropene (TPH). Distribution ratios (*D*) for the extraction of Am(III) and Eu(III) from aqueous solutions containing HNO<sub>3</sub> (ca. 0.005–0.1 M) by 1 M 2-bromodecanoic acid and by 0.02 M solutions of ligands L<sup>1</sup>–L<sup>4</sup> containing 1 M 2-bromodecanoic acid in *tert*-butylbenzene are shown in Fig. 2. The extraction of Am(III) and Eu(III) when 0.02 M of L<sup>5</sup> in synergistic combination with 1 M 2-bromodecanoic acid was used in TPH is shown in Fig. 3, together with the data previously obtained for L<sup>1</sup> in TBB.<sup>6</sup> The data for L<sup>1</sup> extracted from initial HNO<sub>3</sub> are included in Fig. 3 for comparison, even though the data for L<sup>5</sup> are plotted *versus* the equilibrium HNO<sub>3</sub> concentration.

Metal extraction with TPH and *tert*-butylbenzene has been shown to be almost identical when using L<sup>1</sup> and 2-bromo-

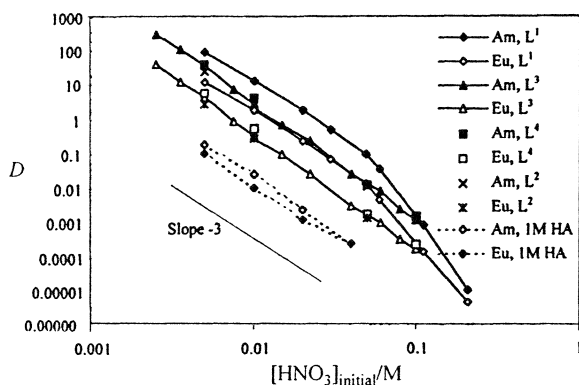


Fig. 3 Distribution ratios for the extraction of americium(III) and europium(III) with 1 M 2-bromodecanoic acid and either 0.02 M L<sup>1</sup> (in TBB) or 0.02 M L<sup>5</sup> (in TPH).

decanoic acid<sup>6</sup> and the extractions presented in Fig. 2 and 3 are thus comparable. It has been previously shown that Am(III) and Eu(III) extraction by L<sup>1</sup> itself is negligible.<sup>6</sup> Fig. 2 shows that 2-bromodecanoic acid (HA) only extracts to a small degree and an Am(III)/Eu(III) separation factor around 2 is obtained at low acid concentrations. The synergistic combination of L<sup>1</sup>–L<sup>5</sup> and 2-bromodecanoic acid, however, results in increased distribution coefficients and Am(III)/Eu(III) separation factors between 7 and 9 are observed. In each case, the extraction decreases with increasing HNO<sub>3</sub> concentration. This would seem to indicate that all of the ligands become protonated, at higher acid concentrations. It has been previously shown that when L<sup>1</sup> becomes protonated, it can pass into the aqueous phase although the amount passing into the aqueous phase is reduced in the presence of the synergist 2-bromodecanoic acid.<sup>6</sup> In the case of the more hydrophobic ligands L<sup>2</sup> and L<sup>3</sup>, precipitates were observed at higher nitric acid concentrations indicating that the protonated species were not soluble in either the aqueous or organic phases. Substitution with a hydrophobic group on the terpyridine was expected to increase the Am and Eu distribution ratios because the hydrophobic derivatives would be more likely to remain in the organic phase during the extractions. The opposite was, however, observed and treatment with the unsubstituted terpyridine (L<sup>1</sup>) shows a slightly higher metal extraction when compared to those using the substituted nitrogen heterocycles (L<sup>2</sup>–L<sup>5</sup>). It seems more likely that a factor such as the basicity of the ligand has a bigger effect than hydrophobicity on the Am and Eu distribution ratios. The extraction results show that substitution of one terminal pyridine with pyrazine does not change either the distribution ratios or the separation factors to any significant degree. It seems likely that further substitution by pyrazine or by a more weakly basic heterocyclic nitrogen ligand such as triazine or triazole will be necessary before an effect can be seen. This was shown in a recently published study involving the separation of Am and Eu by 2,6-di(5,6-dipropyl-1,2,4-triazin-3-yl)pyridine, which gave  $D_{Am}$  values of between 22 and 45 and  $SF_{Am/Eu}$  of 131–143 when 0.034 M of the ligand in modified TPH was used to extract from 0.9–0.3 M HNO<sub>3</sub>.<sup>15</sup> The substituted terpyridines whose efficacies are compared in Fig. 2 and 3 also show similar nitric acid dependency, distribution ratios and separation factors for americium and europium. The different substituents on the central pyridyl groups do not seem to affect the extraction considerably. These results indicate that the nature of the metal complexes formed by ligands L<sup>1</sup> to L<sup>5</sup> with the lanthanide series are likely to be equivalent and the following crystallographic studies were only carried out on complexes containing the unsubstituted terpyridine (L<sup>1</sup>). Acetonitrile was found to be an excellent solvent for the crystallisation of all the studied lanthanide complexes.

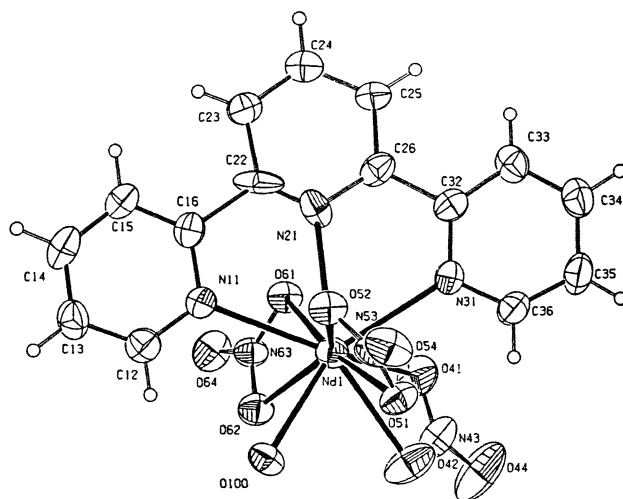


Fig. 4 The structure of 1-Nd with the atomic numbering scheme. Ellipsoids at 30% probability.

### Solid state structures

When this work was initiated there were very few lanthanide structures containing L<sup>1</sup>, apart from a series of 1 : 1 lanthanide chloride–L<sup>1</sup> complexes.<sup>16</sup> However in the last year a systematic survey has been reported of lanthanide structures containing L<sup>1</sup> with a variety of anions, such as acetate, trichloroacetate<sup>17</sup> and perchlorate<sup>18</sup> as well as nitrate.<sup>19</sup> Remarkably, although 7 structures containing nitrate are reported in 3 groups, not one was the same as those reported here, despite all having a metal : L<sup>1</sup> ratio of 1 : 1. While the preparations were subtly different, the variations in stoichiometry are clearly significant and indicate the complexity of the lanthanide–nitrate–L<sup>1</sup> system.

The complex 1-Nd was prepared by adding the metal to the ligand in a ratio of 1 : 1 and shows the metal ion coordinated to three bidentate nitrates, one tridentate L<sup>1</sup> ligand and a water molecule (Fig. 4). By contrast, the previously determined complexes<sup>19</sup> with lanthanide, nitrate, L<sup>1</sup> and water have structures  $[ML^1(NO_3)_2(H_2O)_n](NO_3)_n$ , with  $n = 3$  for the La, Eu and Gd compounds, which are 10-coordinate and form an isomorphous set, and  $n = 2$  for the Tb, Lu and Yb products, which are nine-coordinate and form another isomorphous set. A previous structure determination of the Gd complex has also been published.<sup>20</sup> In all these compounds then, one nitrate remains unbound to the metal and it seems likely, though the Nd complex was not studied, that a 10-coordinate complex of formulation  $[NdL^1(NO_3)_2(H_2O)_3](NO_3)$  does exist in solution and in the solid state. The only difference between this cation and 1-Nd is that two water molecules in the former are replaced by one nitrate in the latter to form a neutral complex but the coordination number remains at 10. An interesting feature of the coordination sphere, as has been previously observed,<sup>17,19</sup> is the close interaction between C(12) and O(100) of 3.13 Å [H(12)···O(100) 2.48 Å] (see Fig. 4), which is indicative of a stabilising intramolecular hydrogen bond between L<sup>1</sup> and water in the coordination sphere. The water molecule is only 0.59 Å from the plane of the pyridine ring. The dimensions in 1-Nd are as expected. The shortest metal–ligand bond is to the water molecule [2.488(8) Å] with similar bond lengths to the three nitrates [2.530(9)–2.632(9) Å]. The Nd–N bond lengths show some variation, such that the Nd–N<sub>c</sub> [c = central, thus N(21)] bond length of 2.703(13) Å is significantly longer than Nd–N<sub>o</sub> [o = outer, thus N(11), N(31)] at 2.625(10) and 2.586(10) Å.

The complex 2-Nd was prepared by adding the metal nitrate to the ligand in a ratio of 1 : 4 and shows the presence of both a cation and an anion in the asymmetric unit, with a formulation of  $[Nd(NO_3)_2(L^1)_2][Nd(NO_3)_4(L^1)]$ . As shown in Fig. 5(a), the cation  $[Nd(NO_3)_2(L^1)_2]^+$  is 10-coordinate with the metal bonded to two tridentate L<sup>1</sup> ligands and two bidentate nitrate anions.

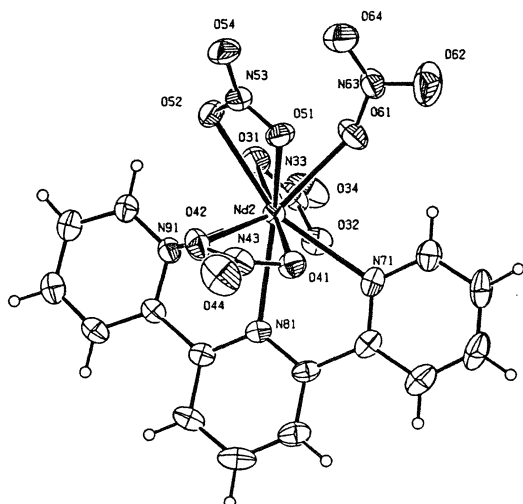
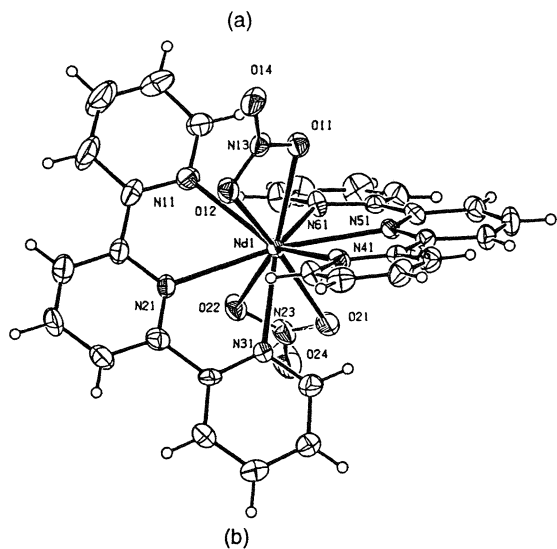


**Fig. 5** The structure of (a) the cation and (b) the anion in 2-Nd with the atomic numbering scheme. Ellipsoids at 30% probability. The structures of 2-Sm, 2-Tb, 2-Dy and 2-Ho are similar.

The two  $L^1$  ligands intersect at  $55.7^\circ$ . The dimensions in the cation are remarkably regular, with Nd–O ranging from 2.526(5)–2.598(6) Å and Nd–N from 2.592(7)–2.651(6) Å. The anion  $[\text{Nd}(\text{NO}_3)_4(L^1)]^-$ , shown in Fig. 5(b), is also 10-coordinate with the metal bonded to only one tridentate  $L^1$  and four nitrate anions, one of which is unidentate. The bond lengths in the anion show a greater variation than in the cation, with a short bond to the unidentate nitrate [Nd(2)–O(61) 2.434(7) Å], but the other Nd–O distances [2.548(6)–2.644(7) Å] and Nd–N distances [2.577(7)–2.600(6) Å] are more regular. There is a weak C–H $\cdots$ O interaction to the unidentate nitrate (H $\cdots$ O 2.55 Å), but there are no such contacts in the cations. The asymmetric unit is completed by two solvent acetonitrile ligands, but these are not involved in intermolecular hydrogen bonding. This  $[\text{M}(\text{NO}_3)_2(L^1)_2][\text{M}(\text{NO}_3)_4(L^1)]$  formulation has been observed before for  $\text{M}=\text{La}$ ,<sup>21</sup> with the significant difference that the metal atom in the anion is 11-coordinate with all 4 nitrates bidentate.

Lanthanides bonded to more than one  $L^1$  ligand are relatively rare in the literature. Apart from this example,<sup>21</sup> the others all show three  $L^1$  ligands bonded to a 9-coordinate metal ion. Examples include  $[\text{Ln}(L^1)_3](\text{ClO}_4)_3$ , Ln = Eu<sup>22</sup> and Ce, Pr, Sm, Eu (form A), Eu, Lu and Y (form B).<sup>18</sup> Both forms A and B show similar discrete  $[\text{Ln}(L^1)_3]^{3+}$  cations. The fact that these cations have only been found in the presence of a weakly coordinating anion such as perchlorate is significant particularly as they have not been observed in the presence of the more

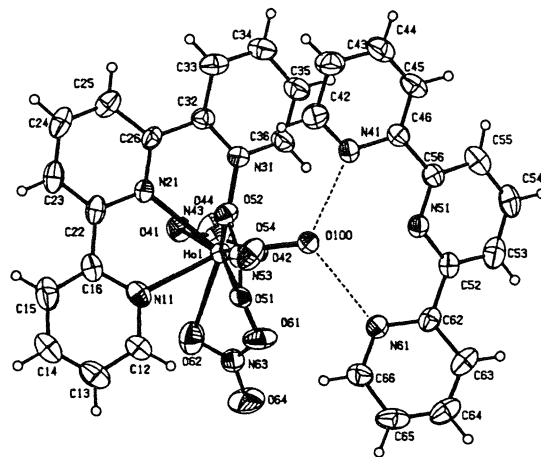


**Fig. 6** The structure of 3-Ho with the atomic numbering scheme. Ellipsoids at 30% probability. Hydrogen bonds shown as dotted lines. The structures of 3-Er and 3-Tm are similar.

strongly coordinating nitrate ion or indeed of the acetate and trichloroacetate anions.<sup>17</sup>

The structure of 2-Sm is equivalent to that of 2-Nd, but while the unit cell is similarly triclinic, the lattice dimensions are different and there is no solvent in the unit cell. We have analysed Ln $L^1$  structures in the Cambridge Structural Database<sup>23</sup> as implemented at the Daresbury Laboratory<sup>24</sup> and have found that, on average, when the  $\text{M}-\text{N}_c$  distances are greater than 2.58 Å,  $\text{M}-\text{N}_o < \text{M}-\text{N}_c$ , and for distances less than 2.58 Å,  $\text{M}-\text{N}_o > \text{M}-\text{N}_c$ . While distances in 1-Nd conform to this pattern, the distances in 2-M are much more disparate, no doubt because of the steric constraints of the coordination sphere and because the differences will be small as  $\text{M}-\text{N}_c$  distances are close to 2.58 Å for these early lanthanides. The structure of 2-Tb is isomorphous with that of 2-Nd, while 2-Dy and 2-Ho are both isomorphous with 2-Sm. The only noticeable difference in structure is that in 2-Tb and 2-Nd, both  $L^1$  ligands are closely planar (inter-pyridine angles  $< 10^\circ$ ) while in 2-Dy, 2-Ho and 2-Sm, one of the  $L^1$  ligands is highly distorted (inter-pyridine angles *ca.*  $25^\circ$ ) while the other is more closely planar (angles  $< 10^\circ$ ).

It is interesting that the anions in all five ionic complexes contain three bidentate nitrates and one unidentate nitrate. A search of the CSD<sup>23,24</sup> shows the presence of only a few examples of the unidentate nitrate with lanthanides although the recent study of acetate and trichloroacetate structures<sup>17</sup> did show many unidentate anions. Dimensions of the metal coordination spheres in the five compounds are compared in Table 2; the only differences are due to the decrease in metal size with the lanthanide series.

The structure of 3-Ho is shown in Fig. 6. The asymmetric unit contains  $[\text{Ho}(L^1)(\text{NO}_3)_3(\text{H}_2\text{O})]$  together with an unbonded  $L^1$  molecule. The metal atom is 10-coordinate, being bonded to three bidentate nitrate anions, one tridentate  $L^1$  and a water molecule. However, the bond to O(62), at 2.725(11) Å, is much longer than the other nitrate bonds [range 2.431(8)–2.518(9) Å], suggesting that this particular nitrate is intermediate between unidentate and bidentate. The water molecule forms the shortest bond at 2.328(7) Å. The uncoordinated  $L^1$  molecule in the asymmetric unit forms hydrogen bonds to the water molecule which is coordinated to the holmium. The O(100) $\cdots$ N(41) and O(100) $\cdots$ N(61) distances are 2.87 and 2.81 Å, while O(100) $\cdots$ N(51) is 2.97 Å, thus suggesting that water hydrogen atoms form donating hydrogen bonds to the outer two nitrogen atoms. Previous calculations<sup>4</sup> have shown that a water molecule (or equivalent) is necessary to stabilise this conformation of the uncoordinated  $L^1$  where the nitrogen atoms are mutually *cis* (the *cis, cis* conformation) because in its absence the *trans, trans* conformation is found, which reduces steric interactions. The

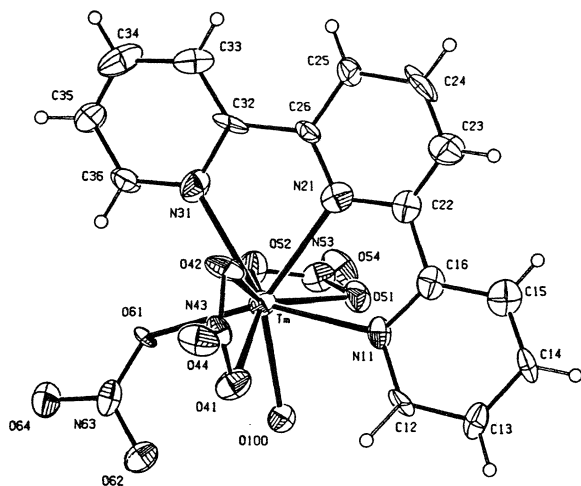


Fig. 7 The structure of 4-Tm with the atomic numbering scheme. Ellipsoids at 30% probability.

angles between adjacent rings in the uncoordinated  $L^1$  are 23.8 and 29.9°, compared to 10.4 and 4.0° in the coordinated  $L^1$ . It is noteworthy that O(100) also forms a weak interaction of 2.59 Å with H(35) and could be considered to form an acceptor hydrogen bond from C(35)–H, as well as the two donor hydrogen bonds to N(41) and N(61). Indeed, the two pyridine rings 3 and 4 are stacked (angle of intersection 21.3°) with a closest contact of 3.28 Å between the two hydrogen bonded atoms N(41) and C(35) (Fig. 6). Rather surprisingly, the three acetonitrile solvent molecules do not form any intermolecular hydrogen bonds.

It is interesting that 2-Ho and 3-Ho were prepared under almost identical conditions. It has been noted previously that the complexation properties of lanthanides with soft N-donor ligands are very sensitive to the conditions under which the reaction takes place and, in particular, the nature of the solvent and the solvent:water ratio. The results obtained here for Ho indicate that the volume of solvent and temperature are also important factors which may have an influence on the precipitated complex.<sup>25</sup>

3-Er and 3-Tm are isomorphous with 3-Ho, although in 3-Tm there are only two acetonitrile solvent molecules and the unit cell is significantly smaller by *ca.* 2%. In 3-Er the bonds are just slightly shorter than for 3-Ho (see Table 2), except for the M–O(62) bond which is 2.858(12) Å. This is not unexpected as it indicates that the smaller size of Er compared to Ho forces the nitrate to be more unidentate. This pattern is also observed in 3-Tm, but here the nitrate is clearly unidentate, with a Tm–O(62) distance of 3.534(20) Å, so that the metal is 9-coordinate. The Tm–O(61) bond, at 2.313(16) Å, is remarkably short, and indeed comparable to the Tm–O(100) water molecule bond of 2.317(12) Å. In both 3-Er and 3-Tm, the hydrogen bond pattern and twist in the uncoordinated ligand is similar to that observed in the 3-Ho structure. Details are provided in Table 3. It is interesting that in all three structures the oxygen atom of the unidentate nitrate forms a shorter bond to the metal than any oxygen atoms of the bidentate nitrates.

The structure of 4-Tm is shown in Fig. 7. Here the metal atom is also 9-coordinate, being bonded to three nitrates, one of which is unidentate, one  $L^1$  ligand and one water molecule. The dimensions are given in Table 2. It is interesting that two different structures are obtained for Tm, one with an extra  $L^1$  ligand (3-Tm) and one without (4-Tm). It is noteworthy that the dimensions of the metal coordination spheres are very similar, indicative of the fact that the size of the metal ion is consistent with a 9-coordinate metal environment. In 4-Tm, the Tm–O(61) bond to the unidentate nitrate is even shorter at 2.251(13) Å. This oxygen atom is in the  $ML^1$  plane and forms a hydrogen bond to C(12)–H (H...O 2.36 Å). In the absence of the extra  $L^1$  molecule, the water molecule in 4-Tm is hydrogen bonded to

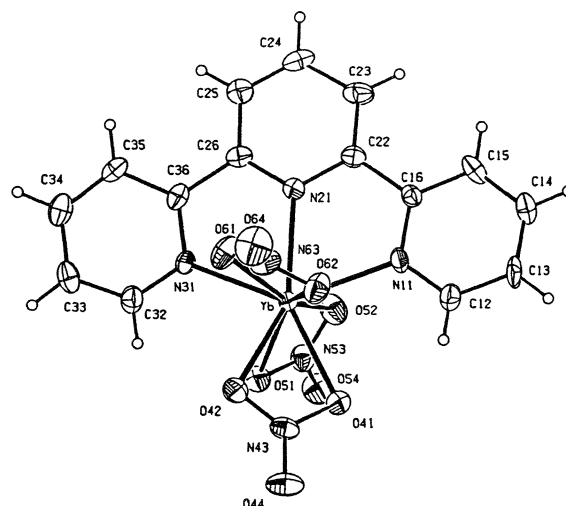


Fig. 8 The structure of 5-Yb with the atomic numbering scheme. Ellipsoids at 30% probability.

two oxygen atoms from two different nitrates coordinated to two different metal atoms (Table 3), at distances of 2.75 and 2.84 Å. The stoichiometry of 4-Tm is equivalent to that of 1-Nd but, in the latter case, the large size of the cation permits the formation of a 10-coordinate complex with  $L^1$ , three bidentate nitrates and a water molecule all bonded to the metal.

The structure of 5-Yb (Fig. 8) shows that the metal ion is bonded to three bidentate nitrates and one terdentate  $L^1$  ligand. There is a short C(12)–H...O(41) contact of 2.48 Å, indicative of weak hydrogen bond formation. The Yb–O distances range from 2.364(8)–2.406(10) Å, apart from Yb–O(51) which is 2.456(9) Å. The Yb–N<sub>o</sub> distances, at 2.417(7) and 2.419(8) Å, are just larger than the M–N<sub>c</sub> distance of 2.395(8) Å, which is consistent with the pattern observed in the CSD. Analysis of the precipitate obtained on addition of four mol equivalents of the ligand indicates that it contains a mixture of complexes and that the majority of the mixture is made up of 3-Yb. A further preparation involving the addition of only one molar equivalent of  $L^1$  produced a precipitate of formula Yb(NO<sub>3</sub>)<sub>3</sub>·( $L^1$ )·H<sub>2</sub>O, which is consistent with a formulation as 1-, 4- or 5-M. It is unlikely to be 1-M as the smaller Yb(III) generally forms complexes with coordination numbers of nine or less, which are observed in both 4-M and 5-M, but it could also be an example of the [M(NO<sub>3</sub>)<sub>2</sub>( $L^1$ )(H<sub>2</sub>O)](NO<sub>3</sub>) family of ref. 19.

The prevalence of the unidentate nitrate in the present work is unprecedented. A search of the CSD for structures containing the nitrate anion bonded to a lanthanide found 729 examples. The mean difference between the two shortest Ln–O distances was calculated as 0.069 Å. There were only eight examples with a difference greater than 1.00 Å and none with a difference between 0.5 and 1.0 Å. In this work alone we have almost doubled the number of examples of the unidentate nitrate anion. It seems likely a significant reason for these is the relative inflexibility of the  $L^1$  ligand which is necessarily terdentate and planar. Thus, the Ln( $L^1$ )(NO<sub>3</sub>)<sub>3</sub>(H<sub>2</sub>O) formulation with three bidentate nitrates is too crowded for all but the largest lanthanide and stable complexes can be formed either by excluding one nitrate from the coordination sphere<sup>19</sup> or by one of the nitrates becoming unidentate.

The crystal structure of the 6-La structure is shown in Fig. 9 together with the atomic numbering scheme. There are two independent (H<sub>2</sub> $L^1$ )<sup>2+</sup> cations, an [La(NO<sub>3</sub>)<sub>3</sub>]<sup>3-</sup> anion, a nitrate ion and a solvent acetonitrile in the asymmetric unit. In the hexanitrate anion, the metal ion is 12-coordinate, with La–O dimensions ranging from 2.62(1) to 2.74(2) Å. As is usually found for diprotonated  $L^1$  cations, the two outer nitrogens are protonated and form donor hydrogen bonds to atoms that are encapsulated within the plane of the ligand. One cation forms

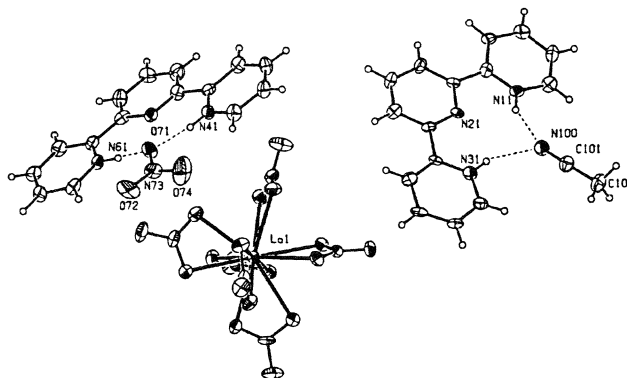


Fig. 9 The structure of 6-La with the atomic numbering scheme. Ellipsoids at 30% probability. Hydrogen bonds shown as dotted lines.

two N-H...N hydrogen bonds to the acetonitrile with distances of 2.91(2) and 2.91(2) Å and the other to an oxygen atom of a free nitrate of 2.73(2) and 2.76(2) Å.

It would appear that the most important factors in determining which complex is precipitated from solution for the lanthanide series 1-Ln–5-Ln, are the amount of added L<sup>1</sup>, the size of the metal ion and the crystallization solvent used. The addition of more than one molar equivalent of L<sup>1</sup> favoured the formation of the ion-pair for the larger lanthanides [Ln(NO<sub>3</sub>)<sub>2</sub>(L<sup>1</sup>)] [Ln(NO<sub>3</sub>)<sub>4</sub>(L<sup>1</sup>)] and [Ln(L<sup>1</sup>)(NO<sub>3</sub>)<sub>3</sub>(H<sub>2</sub>O)]·L<sup>1</sup> for the smaller lanthanides. Under these conditions, however, it seems likely that there are a number of species present in solution. This was confirmed in a multi-nuclear NMR study of La(NO<sub>3</sub>)<sub>3</sub>–L<sup>1</sup> solutions in CH<sub>3</sub>CN.<sup>21</sup> The authors interpreted the NMR results as showing the presence of seven different La(III) species, of which two did not contain L<sup>1</sup>, *viz.* La(NO<sub>3</sub>)<sub>3</sub>(MeCN)<sub>4</sub> and La(NO<sub>3</sub>)<sub>3</sub>(MeCN)<sub>3</sub>(H<sub>2</sub>O) and five did, *viz.* La(NO<sub>3</sub>)<sub>3</sub>(L<sup>1</sup>)(MeCN), La(NO<sub>3</sub>)<sub>3</sub>(L<sup>1</sup>)(H<sub>2</sub>O), [La(NO<sub>3</sub>)<sub>4</sub>(L<sup>1</sup>)(MeCN)]<sup>–</sup>, [La(NO<sub>3</sub>)<sub>4</sub>(L<sup>1</sup>)(H<sub>2</sub>O)]<sup>–</sup> and [La(NO<sub>3</sub>)<sub>2</sub>(L<sup>1</sup>)<sub>2</sub>]<sup>+</sup>. It was proposed that the anionic complex in solution was an equilibrium between [La(NO<sub>3</sub>)<sub>4</sub>(L<sup>1</sup>)(MeCN)]<sup>–</sup>, [La(NO<sub>3</sub>)<sub>4</sub>(L<sup>1</sup>)(H<sub>2</sub>O)]<sup>–</sup> and [La(NO<sub>3</sub>)<sub>2</sub>(L<sup>1</sup>)<sub>2</sub>]<sup>+</sup>, while in the solid state the coordinated MeCN or H<sub>2</sub>O solvent molecule becomes uncoordinated. The structural data presented here and in previous work confirm the plethora of species likely to be present in solution.

The difference in the nature of the 1:1 complexes found in our work and in ref. 19 is interesting, particularly as ostensibly similar preparations were used. However, in ref. 19 the procedure was to prepare the complex in acetonitrile and recrystallise from water. The alternative procedure for the Gd complex<sup>20</sup> was to prepare the crystals at the interface between water and chloroform. Our preparations were carried out under more anhydrous conditions (*vide supra*) and this may account for the difference in obtaining [Ln(NO<sub>3</sub>)<sub>3</sub>(L<sup>1</sup>)(H<sub>2</sub>O)<sub>*n*</sub>]<sup>+</sup> (*n* = 1, 0) rather than [Ln(NO<sub>3</sub>)<sub>2</sub>(L<sup>1</sup>)(H<sub>2</sub>O)<sub>*n*</sub>](NO<sub>3</sub>)<sup>–</sup> (*n* = 3, 2) but it seems likely that the two types coexist in solution. There are, however, common features in these two series. The coordination number of the lower larger lanthanides is 10 and that of the higher smaller lanthanides is 9. 10-Coordination is achieved *via* the terdentate L<sup>1</sup> ligand, two nitrates and a water molecule with either an additional nitrate or two water molecules completing the metal environment. 9-Coordination is achieved *via* the terdentate L<sup>1</sup> ligand, two nitrates, with either an additional nitrate or two water molecules completing the metal coordination sphere.

It is noteworthy that in studies with acetate (ac) or trichloroacetate (tca) these same authors<sup>17</sup> also found structures of the type [Lu(ac)<sub>2</sub>(L<sup>1</sup>)(H<sub>2</sub>O)<sub>2</sub>]<sup>+</sup>(NO<sub>3</sub>)<sup>–</sup>, but additionally identified neutral complexes with unidentate acetates, *viz.* [Ln(tca)<sub>3</sub>(L<sup>1</sup>)(OMe)]<sup>–</sup> (Ln = Lu, Yb), in which two acetates were unidentate giving rise to 8-coordinate metal environments. An interesting comparison can be made between the structures of La(NO<sub>3</sub>)<sub>3</sub>(L<sup>1</sup>)(MeOH)<sub>2</sub><sup>20</sup> and Er(NO<sub>3</sub>)<sub>3</sub>(L<sup>1</sup>)(EtOH).<sup>26</sup> The

former is 11-coordinate with three bidentate nitrates while the latter is 9-coordinate with 1 unidentate nitrate. This pattern is similar to the differences between 2-La and 2-Nd and between 1-Nd and 4-Tm, which are also just due to changes in the denticity of the nitrate anion.

## Conclusion

We have shown that the ligands L<sup>2</sup>–L<sup>4</sup> show comparable extraction performance to L<sup>1</sup>. Metal extraction with L<sup>1</sup> is slightly better compared to the substituted terpyridines L<sup>2</sup>–L<sup>4</sup>. Very little difference in distribution ratios was observed between the ligands L<sup>2</sup>–L<sup>4</sup>. Substitution of more hydrophobic groups or more electron withdrawing groups did not effect the distribution coefficients or separation factors to any significant degree. Similar results were obtained when one of the pyridine groups was substituted with a pyrazine (L<sup>3</sup>). Although previous studies have shown that a number of 2-bromodecanoic acid molecules may also be present in the extracting species, our studies give some indication of the different types of complexes which can be formed across the lanthanide series with L<sup>1</sup> and, by implication, with L<sup>2</sup>–L<sup>5</sup>. It was earlier shown that for identical experimental conditions, *D<sub>M</sub>* values increase with atomic Ln number (*Z*), *D<sub>La</sub>* < *D<sub>Nd</sub>* < *D<sub>Eu</sub>* ≈ *D<sub>Tb</sub>*, which is connected with the decrease in ionic radius of Ln(III) with increasing *Z*, which induces an increase in ionic potential of the lighter Ln(III) ions.<sup>6</sup> Our complexation studies indicate that the type of complexes formed changes across the series and this may be another reason for the observed change in extraction performance. The type of complex formed was found to be dependent on the concentration of L<sup>1</sup> and on the size of the lanthanide. An increase in L<sup>1</sup> concentration is more likely to result in the formation of ion-pairs for the heavier elements in the lanthanide series, in which more than one terpyridine ligand is bound to the metal-ion. The lighter elements are more likely to form simple 1:1 complexes, although it is possible that an “extra” associated L<sup>1</sup> molecule can be precipitated. The presence of more than one L<sup>1</sup> molecule in the precipitated lanthanide complexes is consistent with the observation that the extracting species found at higher L<sup>1</sup> concentrations may contain two L<sup>1</sup> molecules. In this case the extracting species was tentatively assigned as MA<sub>3</sub>(L<sup>1</sup>)<sub>2</sub>, where A is the synergistic extractant 2-bromodecanoic acid.<sup>6</sup>

## Acknowledgements

We are grateful for financial support from the European Union Nuclear Fission Safety Programme (Contract FI41-CT-96-0010). We would also like to thank the EPSRC and the University of Reading for funding of the image plate system. We wish also to acknowledge the use of the EPSRC Chemical Database Service at Daresbury.

## References

- 1 Proceedings of the 5<sup>th</sup> OECD/NEA Information Exchange Meeting on Actinide and Fission Product Partitioning and Transmutation, Mol, Belgium, 1998, EUR 18898 EN; *Solvent Extraction and Ion Exchange in the Nuclear Fuel Cycle*, eds. D. H. Logsdail and A. L. Mills, Ellis Horwood, Chichester, 1985.
- 2 G. Y. S. Chan, M. G. B. Drew, M. J. Hudson, N. S. Isaacs, P. Byers and C. Madic, *Polyhedron*, 1996, **15**, 3385.
- 3 G. Y. S. Chan, M. G. B. Drew, M. J. Hudson, P. B. Iveson, J.-O. Liljenzin, M. Skålberg, L. Spjuth and C. Madic, *J. Chem. Soc., Dalton Trans.*, 1997, 649.
- 4 M. G. B. Drew, M. J. Hudson, P. B. Iveson, M. L. Russell, J.-O. Liljenzin, M. Skålberg, L. Spjuth and C. Madic, *J. Chem. Soc., Dalton Trans.*, 1998, 2973.
- 5 P. Y. Cordier, C. Hill, P. Baron, C. Madic, M. J. Hudson and J.-O. Liljenzin, *J. Alloys Compd.*, 1998, **271**, 738.
- 6 I. Hagström, L. Spjuth, Å. Enarsson, J. O. Liljenzin, M. Skålberg, M. J. Hudson, P. B. Iveson, C. Madic, P. Y. Cordier, C. Hill and N. Francois, *Ion Exch. Solvent Extr.*, 1999, **17**, 221.

- 7 V.-M. Mikkala, M. Helenius, I. Hemmilä, J. Kankare and H. Takalo, *Helv. Chim. Acta*, 1993, **76**, 1361.
- 8 C. Chamchoumis and P. G. Potvin, *J. Chem. Res. (S)*, 1998, 180.
- 9 F. Kröhnke and K. F. Gross, *Chem. Ber.*, 1959, **92**, 22.
- 10 F. Neve, A. Crispini and S. Campagna, *Inorg. Chem.*, 1997, **36**, 6150.
- 11 W. Kabsch, *J. Appl. Crystallogr.*, 1988, **21**, 916.
- 12 G. M. Sheldrick, *Acta Crystallogr., Sect. A*, 1990, **46**, 467.
- 13 N. Walker and D. Stuart, *Acta Crystallogr., Sect. A*, 1983, **39**, 158.
- 14 G. M. Sheldrick, Program for crystal structure refinement, University of Göttingen, 1993.
- 15 Z. Kolarik, U. Mullich and F. Gassner, *Ion Exch. Solvent Extr.*, 1999, **17**, 23.
- 16 C. J. Kepert, Lu Wei-Min, B. W. Skelton and A. H. White, *Aust. J. Chem.*, 1994, **47**, 365.
- 17 C. J. Kepert, Lu Wei-Min, L. I. Semenova, B. W. Skelton and A. H. White, *Aust. J. Chem.*, 1999, **52**, 481.
- 18 L. I. Semenova, A. N. Sobolev, B. W. Skelton and A. H. White, *Aust. J. Chem.*, 1999, **52**, 519.
- 19 L. I. Semenova and A. H. White, *Aust. J. Chem.*, 1999, **52**, 507.
- 20 P. C. Leverd, M. C. Charbonnel, J. P. Dognon, M. Lance and M. Nierlich, *Acta Crystallogr., Sect. C*, 1999, **55**, 368.
- 21 M. Frechette and C. Bensimon, *Inorg. Chem.*, 1995, **34**, 3520.
- 22 G. H. Frost, F. A. Hart, C. Heath and M. B. Hursthouse, *J. Chem. Soc. D*, 1969, 1421.
- 23 F. H. Allen and O. Kennard, *Chem. Des. Auto. News*, 1993, **8**, 1.
- 24 D. A. Fletcher, R. F. McMeeking and D. Parkin, *J. Chem. Inf. Comput. Sci.*, 1996, **36**, 746.
- 25 C. V. Krishnamohan and R. D. Rogers, *Chem. Commun.*, 1999, 83.
- 26 S. A. Cotton and P. R. Raithby, *Inorg. Chem. Commun.*, 1999, **2**, 86.

Paper a907077j

# Appendix II

Reprinted from

# Talanta

---

Talanta 51 (2000) 231–246

## Assessment of uncertainty in parameter evaluation and prediction

G. Meinrath <sup>a,b,c,\*</sup>, C. Ekberg <sup>d</sup>, A. Landgren <sup>d</sup>, J.O. Liljenzin <sup>d</sup>

<sup>a</sup> Faculty of Chemistry and Physics, Institute of Inorganic Chemistry, Technical University Mining Academy Freiberg, D-09596 Freiberg, Germany

<sup>b</sup> Department of Hydrogeology, Faculty of Geology, Technical University Mining Academy Freiberg, D-09596 Freiberg, Germany

<sup>c</sup> RER Consultants, Schießstattweg 3a, D-94032 Passau, Germany

<sup>d</sup> Department of Nuclear Chemistry, Chalmers University of Technology, S-41296 Gothenburg, Sweden



ELSEVIER

## Assessment of uncertainty in parameter evaluation and prediction

G. Meinrath<sup>a,b,c,\*</sup>, C. Ekberg<sup>d</sup>, A. Landgren<sup>d</sup>, J.O. Liljenzin<sup>d</sup>

<sup>a</sup> Faculty of Chemistry and Physics, Institute of Inorganic Chemistry, Technical University Mining Academy Freiberg, D-09596 Freiberg, Germany

<sup>b</sup> Department of Hydrogeology, Faculty of Geology, Technical University Mining Academy Freiberg, D-09596 Freiberg, Germany

<sup>c</sup> RER Consultants, Schießstattweg 3a, D-94032 Passau, Germany

<sup>d</sup> Department of Nuclear Chemistry, Chalmers University of Technology, S-41296 Gothenburg, Sweden

Received 2 April 1999; received in revised form 23 August 1999; accepted 25 August 1999

### Abstract

Like in all experimental science, chemical data is affected by the limited precision of the measurement process. Quality control and traceability of experimental data require suitable approaches to express properly the degree of uncertainty. Noise and bias are nuisance effects reducing the information extractable from experimental data. However, because of the complexity of the numerical data evaluation in many chemical fields, often mean values from data analysis, e.g. multi-parametric curve fitting, are reported only. Relevant information on the interpretation limits, e.g. standard deviations or confidence limits, are either omitted or estimated. Modern techniques for handling of uncertainty in both parameter evaluation and prediction are strongly based on the calculation power of computers. Advantageously, computer-intensive methods like Monte Carlo resampling and Latin Hypercube sampling do not require sophisticated and often unavailable mathematical treatment. The statistical concepts are introduced. Applications of some computer-intensive statistical techniques to chemical problems are demonstrated. © 2000 Elsevier Science B.V. All rights reserved.

**Keywords:** Computer-intensive methods; Monte Carlo resampling; Uncertainty analysis; Latin Hypercube sampling

### 1. Introduction

The comparability of experimentally determined parameter estimates from different laboratories and/or different methods requires the assignment of meaningful uncertainty limits to

such parameters. Traceability of results to accepted reference standard materials is understood as a crucial element of quality assessment in analytical chemistry [1–4].

Extracting model parameters from experimental data and predicting future events on basis of model parameters is a common task in science and technology. It is general practice to fit models to experimental data by suitable computer pro-

\* Corresponding author. Tel./fax: +49-851-70372.

E-mail address: meinrath@geo.tu-freiberg.de (G. Meinrath)

grams that minimise the difference between experimental data points and model functions. A variety of minimisation routines are available. Newton–Raphson algorithm [5], variable metric methods, especially the Davidon–Fletcher–Powell implementation [6–8] and the SIMPLEX algorithm [9–11] are among the most commonly applied procedures. The task of a fitting routine is in most cases to minimise the sum of squared differences between the measured dependent data points and calculated values for the given regressors. More formally spoken, the data are measured as a function of a certain variable, called the regressor variable or independent variable, for which responses or dependent variables are obtained. This is expressed by Eq. (1)

$$\text{SOR} = \sum w_i (y_{m,i} - f(x_i, p_n))^2 \quad (1)$$

where SOR, sum of squared residuals;  $w_i$ , weight;  $y_{m,i}$ , response measured at the  $i$ -th regressor;  $x_i$ ,  $i$ -th regressor;  $p_n$ , parameter estimates of the model function;  $f()$ , model function of  $n$  parameters assumed to be a satisfactory model for the relationship between regressor  $x$  and response  $y$

Regressors  $x_i$  may be multi-dimensional (e.g. represent two variables pH and temperature). However, in the present discussion, the regressors are assumed to be scalars. In other words, however, a model function is not just  $y_i = f(x_i)$ , but actually is

$$y_i = f(x_i, p_n) + \beta_i + \varepsilon_i \quad (2)$$

where  $\varepsilon_i$  is some stochastic error like random noise and  $\beta_i$  is the bias. Statistical literature refers to the  $\varepsilon_i$  as disturbances. Here, we will abbreviate this an ‘error’. It should be emphasized that these ‘errors’ are unavoidable contributions and represent the stochastic nature of our perception of the world. These errors infer doubt about the correctness of the derived parameter estimates. In contrast, bias refers to systematic errors that should be avoided or at least minimised as far as possible—even though they might be very difficult to detect. Not included into the models according to Eq. (2) are outliers. Outliers are more common than usually anticipated and have given rise to the so-called robust statistical methods. Outliers are

briefly considered, but the reader might be further enlightened by reading Ref. [12].

Prediction is a task in science that grows more and more important. Complicated processes can be modelled due to the increasing abundance of high-speed computing systems. But here, too, prediction capability is limited by the uncertainty in the experimental data, from which the input parameters of a predicting code are derived from. Hence, assessment of uncertainty in a parameter estimate that is derived from experimental data is an essential task in order to recognize the limits of our prediction capability.

When only looking to the optimum parameter estimates  $p_n$  in Eq. (1), an important part of information obtained from the curve fitting procedure is ignored: while the optimum parameter estimates represent the new knowledge obtained from the experimental data, the errors  $\varepsilon_i$  carry the information on the limitations of this new knowledge, or the doubt in the new knowledge, expressed by the probability distribution of the parameter estimate. Information enclosed in the errors  $\varepsilon_i$  however is essential not only in, e.g. assigning confidence limits to parameter estimates, but also e.g. to provide objective criteria on the number of parameters that can be estimated reasonably from a given data set at all. Thus statistical analysis of information enclosed in the errors  $\varepsilon_i$  is indispensable in order to test significance of results obtained from data modelling.

Scientists take considerable efforts to obtain information on the system under study in form of numerical data. To extract information from data (as well as avoiding over-interpretation) is a subject of statistics. A large amount of concepts and techniques are available in statistical literature. Each attempt to summarise these statistical techniques in a manuscript is futile. Hence, in the following the authors will concentrate on some effective procedures that have been proven to be of merit during their past efforts in empirical model building and data analysis of chemical, especially thermodynamic, systems. However, fitting models to data, especially by regression methods, is a science of its own and the reader is referred to some instructive sources directed to the needs of chemists [13–15].

Reading through many papers containing experimental results, it is obvious that the estimation of uncertainties and confidence limits of the fitted parameter estimates often is a subject not given its due importance. The consequences may be tough: the parameter estimates finally evaluated and eventually included into more complex models may not reflect the experimental findings at all or even worse, the inference made on the system under study is simply incorrect. From a metrological point of view, a result of measurement is nearly meaningless without a traceable statement of the measurement uncertainty [1]. In some cases, the lack of error analysis may be due to the fact that estimation of errors in parametric curve fitting does not appeal to experimentalists as being too cumbersome to interpret. However, nowadays, the computer allows simple and efficient data post-analysis. Easily implemented algorithms result in sound parameter uncertainties with a sophistication and ease unimaginable before [16].

## 2. Least-squares, distribution functions and non-linear regression

The use of the squared residuals is commonly accepted to find optimum parameter values, but there is a definite reason for preferring squared sums over, say, linear or cubic residuals. This preference results from the fact that under certain constraints the least squares parameters are those parameter estimates that have the highest probability to be correct. Thus, least squares parameters are the maximum likelihood parameters [17]. Some of the conditions, on which this maximum likelihood statement is based, are (I) the model function is a reasonable representation of the true (but unknown) functional relationship. (II) the  $\varepsilon_i$  are independently distributed with equal mean and equal variances (which requires the distribution function to be a Normal distribution), (III) the contribution of the errors and the model function to the experimentally observed response is additive (cf. Eq. (2)) and (IV) the regressors  $x_i$  themselves can be considered to be unaffected by errors and noise. However, for functions  $f(x)$

where the derivative with respect to  $x$  is sufficiently small and it is possible to assume that  $f(x)$  is linear in the given uncertainty interval, it is also possible to include uncertainties into the regressor. For non-linear functions, where the first derivative still depends on one or more parameters, the relationships are more complicated. The preference for squared residuals is not any longer a natural choice [17].

Thus, empirical model building will rely on independently and identically distributed (i.i.d.) errors  $\varepsilon_i$ . Hence, an important part of the data post-analysis deals with the question, whether the  $\varepsilon_i$  may be reasonably considered to be normally distributed. A further issue that should deserve special attention is the number of data points on which the statistical analysis is based. The experimental data not only has to allow for an estimate of the parameters  $p_n$  (cf. Eq. (2)), but also has to be a representative sample for the stochastic errors  $\varepsilon_i$ . In order to apply standard statistics, the experimental distribution function, where the  $\varepsilon_i$  may be considered to result from, is required to asymptotically approximate a Normal distribution if  $i$  is increasing to infinity. However, from experiments usually a quite limited number of data points and, hence, errors  $\varepsilon$ 's are obtained. Furthermore, the  $\varepsilon$ 's may be drawn from a distribution that is not normal at all due to non-linearity of the model function. Hence, it is desirable to visualise the empirical distribution function (edf) and to have numerical methods at hand to compare this edf to a normal distribution. Undue differences between edf and normal distribution may indicate, e.g. a poor model function. Poor model functions in turn may result from inclusion of too few or too many parameters in the data analysis. Thus, the stochastic errors  $\varepsilon_i$  may also carry information on the correct number of parameters to be included into the data analysis.

### 2.1. Estimation of standard deviations by the $\chi^2$ (Chi-square) method

The basic idea behind the  $\chi^2$  method is the assumption that errors  $\varepsilon_i$  are normally distributed according to Eq. (3):

$$N_i = \frac{y_{m,i} - y_i}{k_i} \quad (3)$$

where  $N_i$  is a weighted residual and  $k_i$  is a weight factor. The sum of squared normal distributions

$$\chi^2 = \sum_i N_i^2 \quad (4)$$

is said to be  $\chi^2$  distributed. This sum, divided by its degrees of freedom (df), gives a measure of the overall quality of the fit. The degree of freedom is defined by Eq. (5):

$$\text{df} = m - n \quad (5)$$

where  $m$ , number of data points;  $n$ , number of parameters fitted.

An experimentally obtained  $\chi^2$  may be compared to the expectation value of the  $\chi^2$  distribution, which is just the degree of freedom itself. The variance of the  $\chi^2$  is twice the expectation value. Thus, in a first approach, variance in  $\chi^2$  may be used to estimate the variance for the fitted parameters. The procedure is simple to implement: each parameter value in the model has to be changed step by step from its 'best-fit' value and the respective increase in  $\chi^2$  has to be followed until  $\chi^2$  is twice its minimum value. The difference between a parameter's 'best-fit' value and its value corresponding to two times  $\chi^2$  minimum value is an estimate for the parameters variance. The square root of that difference is assigned to the parameter estimate as its standard deviation.

The weighing parameter  $k_i$  in Eq. (3) is usually chosen as the variance of the data point  $y_i$  [18]. If these data (which often requires considerable additional information) is not available,  $k_i$  is set to unity. The parameters  $N_i$  in Eqs. (3) and (4) then are the residuals  $\varepsilon_i$  themselves.

## 2.2. Marginal confidence limit and Student's $t$

Often not only the standard deviation is desired but an information on the confidence limit. The fitted mean value is, within the constraints I–IV, the most likely parameter estimate, but only on basis of the measurement(s) performed. If the measurement is repeated, the mean value of the new measurement(s) will differ somewhat from the previous one, because of the random contribu-

tions in the errors  $\varepsilon_i$ . Hence, the experimentalist should be interested in what range the parameter estimates might vary from experiment to experiment, with, say, 95% probability. This 95% confidence region does not only depend on the standard deviation  $\sigma$  of the parameter estimate but also on the degree of freedom df. The smaller df, the more limited is our knowledge of the distribution function of the errors  $\varepsilon_i$ . It must be considered, that the few  $\varepsilon_i$  have a high probability to be obtained close to the maximum of the distribution. Hence, these  $\varepsilon_i$  do not carry information about the tails of the distribution. This point has been discussed in all details in Ref. [19] and has given rise to a parameter that corrects for this kind of bias, called Student's  $t$ . Student's  $t$  is tabulated in almost all text books on statistics:

$$\text{CI}_\tau = 2t_{\text{df}, \tau} \sigma_i \quad (6)$$

CI $_\tau$ , confidence interval, centred at the parameter mean value;  $\tau$ , confidence level.

A studentised distribution function is broader than the normal distribution but gradually approaches the normal distribution with increasing df. As a rule of thumb the difference between studentised distribution and normal distribution becomes negligible if  $\text{df} > 30$ . To give an example, if  $\text{df} > 30$ ,  $t_{\text{df}, \tau} = 1.96$  at  $\tau = 95\%$  but if df is only 3,  $t_{3, 95\%} = 3.18$ . The problem of inference on small data sets in chemistry has been addressed by e.g. Dean and Dixon [20].

## 3. Outliers and hypothesis testing

"An outlying observation, or outlier, is one that appears to deviate markedly from the other members of the sample in which it occurs" [12]. Such a definition immediately directs to the most vulnerable point in discussion of outliers: it's very much a subjective one. Collett and Lewis [22] extensively discuss criteria to deal with the problem of extraneous data in an objective way. Outliers may result from natural variability or experimental mistakes and weaknesses. To identify outliers is therefore an important topic in data post-analysis. Many methods for rejecting data as extraneous are build on the assumption of some

fundamental distribution function. However, rejection of data is only one strategy in statistics to deal with outliers. Outlier detection has a subjective element (already the decision to check for extraneous data carries the suspicion that some data might be outlying) and data with a large deviation from the sample mean have a very small but finite probability even when considering well-behaved normally distributed data. Incorporation of the data, e.g. by weighing the data or allowing for accommodation by alternative statistical concepts is then possible. It should be noted that rejection of data from small samples on statistical arguments only is a highly controversial issue.

Here, we will mention a rejection test for outlier detection, but the reader is directed to [21–25] for further reading. Especially Bayesian statistics offers a variety of interesting perspectives [26,27]. As outlined recently [28] the rejection  $Q$  test [29] has become the methodology of choice in analytical chemistry.  $Q$  test assumes that data are obtained from Gaussian distribution. Since ranges are compared, detailed knowledge of sample means and standard deviations are not required. The use of ranges makes the  $Q$  test less sensible to deviations from normal distribution [28].  $Q$  testing has been proposed for several possible situations. Here, only the ' $r_{10}$ ' situation will be discussed to illustrate the procedure. The ' $r_{10}$ ' situation means that only one of the extreme values, either highest or lowest data, is suspected outlying. There are also critical values for other situations, e.g. the ' $r_{21}$ ' situation, where two data at one extreme and one data at the other extreme are suspected outliers.

$$r_{10} = \frac{x_2 - x_1}{x_n - x_1} \quad (7)$$

Table 1  
Ten experimental data points used to illustrate the Dixon  $Q$ -test

4.25	2.43
3.12	2.33
2.99	2.01
2.66	1.98
2.59	1.91

Eq. (7) is valid for the situation that the first data in an ordered list of  $n$  data is suspected to be extraneous. The  $r_{10}$  ratio compares the difference between the suspected outlying data (naturally the largest or the lowest value in the ordered list) and its direct neighbour to the complete range of the tested data set including the suspected outliers.

In the framework of curve fitting, the  $x$ -values in Eq. (7) are typically the difference between experimental data and modelled values, squared or not. Tabulated critical values  $Q$  on different levels of significance are given in [28]. If  $r_{10}$  is larger than the corresponding  $Q$  at a given significance level, this test suggests rejection of this data point.

When ordering the 10 data in Table 1, the data 4.25 might be a suspected outlier. Using Eq. (7), we find  $r_{10} = 0.482$ . The critical value for a sample size of 10 is  $Q_{10, 80\%} = 0.349$  ( $\alpha = 0.20$ ),  $Q_{10, 95\%} = 0.466$  ( $\alpha = 0.05$ ) and  $Q_{10, 96\%} = 0.483$  ( $\alpha = 0.04$ ). Hence, the data 4.25 would be rejected on the 80 and 95% level but accepted on the 96% level. Thus, statistics offers objective criteria for decision — it does not necessarily take the burden of decision from the experimentalist.

The use of critical values, e.g.  $\chi^2$  expectation values, Student's  $t$ , Fisher variance ratio  $F$  [18] or Dixon's  $Q$  is always ambiguous. If we reject a hypothesis, e.g. the hypothesis that an extreme value is not an outlier, because e.g. Dixon's  $Q$  indicated 95% probability that the suspected data is actually an outlier, then we accept about 5% risk that our decision is wrong. If we are too cautious and require a 99% probability that a data is an outlier, we accept an increased risk that the data actually is an outlier. There is no automatic way to make decisions. If we accept experimental data, we accept errors. Statistics usually distinguishes two kinds of risks, the 'Type I' or ' $\alpha$  risk' to reject a value that is legitimate versus the 'Type II' or ' $\beta$  risk' that a value to be rejected is retained. More generally, statistics tests the so-called 'Null Hypothesis' that, for example, the difference between two groups of data is actually only due to random error and noise and the difference is actually not significant. Accepting the Null Hypothesis on the  $\alpha$  probability level always incorporates the  $\beta = 1 - \alpha$  risk that the decision is wrong.

#### 4. Non-normally distributed data and computational statistics

Normally distributed parameter estimates do have desirable properties: (I) the maximum of the normal distribution is also its mean value; (II) the distribution is symmetric with one single maximum, hence upper interval for standard deviation is equal to lower interval, resulting in the common  $\pm \sigma$  notation. It is, however, evident that most experimental data, available usually in limited number only, are not normally distributed. There are commonly significant differences between a normal distribution and the empirical distribution function of the experimental data. For the experimental scientist, hence, normal distribution is the exception, not the rule. Due to this importance of non-normally distributed data, there are a wide range of statistical tools for coping with non-normal data [30,31]. Some of these techniques strongly rely on computers' processing power. Powerful applications of the computer to the analysis of experimental data are resampling methods (also called 'computer-intensive' methods). They replace mathematical sophistication by brute computing power. Some of them shall be discussed in the following.

##### 4.1. The jackknife

In Section 2, it has been mentioned that, with respect to certain constraints, the parameter estimates resulting in the least sum of squared residuals have the highest probability to be the true parameters-however based on given experimental data. If an additional data would be measured and included into the data analysis, the optimum parameter estimates would in almost all cases vary a little bit. Given some experimental data, no additional data can be added, but the other way can be taken: omitting a datum. By analyzing the variation in the optimum parameter estimates as a consequence of this omission, information on the variability of the parameters due to error-affected experimental data can be obtained. A strategy that follows this line is the jackknife.

The jackknife [32–34] procedure of estimating parameter uncertainties may be introduced as a

resampling method. Since the jackknife doesn't require the errors  $\varepsilon_i$  to follow a certain distribution function, jackknife is a representative of non-parametric statistics. Resampling is done by using the  $m$  original measured data pairs  $(x_i, y_i)$  as adequate representation of the true but unknown distribution function. The properties of this distribution function are explored by creating sub-samples from the  $m$  data pairs. In the jackknife approach, each sub-sample contains  $m-1$  of the  $(x_i, y_i)$  data pairs. An algorithmic application of the jackknife for estimation of variance may be as follows:

1. obtain the parameter estimate  $p_n^*$  by fitting the model function  $f(x_i, p_n)$  (cf. Eq. (2)) to all  $m$  data points  $(x_i, y_i)$ .
2. create a sub-sample by omitting the  $k$ -th data pair in the  $k$ -th run, re-fit the sub-sample to obtain the sub-sample parameters  $p_{n,k}$ .
3. repeat step (b)  $m$  times
4. calculate the jackknife estimate of variance  $\sigma^2$  for each parameter estimate by Eq. (8)

$$\sigma^2 = \frac{m-1}{m} \sum_{k=1}^m (p_k - p^*)^2 \quad (8)$$

$p^*$ , parameter mean value;  $p_k$ , parameter value obtained from a reduced data set;  $m$ , total number of data sets  $(x, y)$ .

Eq. (8) is valid for each of the  $n$  parameters in Eq. (2) individually. The standard deviation  $\sigma$  is estimated as the square root of the variance  $\sigma^2$ . If there are many experimental data points ( $m$  is large), the jackknife may be abbreviated by randomly choosing  $j$  ( $j < m$ ) data pairs which are successively omitted during the above procedure (a–d). Of course,  $m$  has to be replaced by  $j$  in Eq. (8). Even though the jackknife procedure may look like a rough-and-ready statistical tool, it has a sound statistical basis reviewed, e.g. in [32]. It should be noted that jackknife estimates of variance are usually conservative. The jackknife approach requires  $m+1$  (or  $j+1$ ) replications of the fitting procedure. Taking the abundance of high-speed desktop computers nowadays, jackknifing even a large data set is done within minutes. There is one great advantage of the full jackknife approach because for each data point omitted a set of fitted parameter estimates is obtained. It is

thus possible to detect the effect of possible outlier data and their effect on the estimated parameters because this parameter estimate grossly deviates from the others. Such a suspicion may subsequently be substantiated, e.g. by Dixon's  $Q$  test.

#### 4.2. The bootstrap

The bootstrap may be introduced as a Monte Carlo resampling method. While the jackknife procedure creates sub-samples in a predictable way, bootstrap doesn't. Bootstrapping a data set means to create a large number  $N$  of sub-samples by randomly drawing data pairs  $(x_i, y_i)$  from the  $m$  measured data pairs. Large number is, e.g.  $N = 1000$  or even more sub-samples, for that the fitting procedure is repeated. In a bootstrap sample, a certain data pair, say  $(x_r, y_r)$ , can be found several times in a given sub-sample, while another data pair, say  $(x_w, y_w)$ , is not considered at all. In the next sub-sample however, the situation may be reversed. (Strictly speaking, this is the bootstrap with random regressors. Later, we will briefly discuss fixed regressor schemes). An algorithmic application of the bootstrap may be as follows

1. obtain the parameter estimate  $p_n^*$  by fitting the model function to the  $m$  data points  $(x_i, y_i)$
2. create another sample of  $m$  data points by selecting  $m$  times from the original data set with replacement and re-fit the new data set
3. repeat (b)  $N$  times ( $N$  large)
4. calculate the bootstrap estimate of variance  $\sigma^2$  by Eq. (9).

$$\sigma^2 = \frac{1}{N-1} \sum_{l=1}^N (p_l - p^*)^2 \quad (9)$$

In some cases, it might be advisable not to use the strategy outlined above for creating bootstrap samples. If in one of the generated sub-samples data points are missing in a range of the function that is important for the determination of, say, one of the function parameters, this parameter estimate may float arbitrarily. Even in this case, the bootstrap method is applicable, if the fixed-regressor bootstrap is applied. Here, the experimentally obtained data points  $y_i$  are replaced by the

'best-fit' data points  $y'_i$  obtained from the curve fitting procedure using all data pairs  $(x_i, y_i)$ . The difference  $(y_i - y'_i)^2$  is nothing else than the estimates of  $\varepsilon_i$ . Hence, for  $n$  data pairs  $(x_i, y_i)$   $n$  residuals  $\varepsilon_i$  are obtained. Now, new bootstrap samples are created by adding to the mean value  $y'$  an  $\varepsilon$ , randomly selected from the  $n$   $\varepsilon_i$ 's. In the fixed-regressor bootstrap, the  $x_i$  are not any longer selected by a random procedure but stay the same in each bootstrap sample—they are fixed. It should be noted that the fixed-regressor design must be applied only after a thorough analysis of the problem. While the standard bootstrap is quite robust, the fixed-regressor bootstrap is not necessarily so [35].

#### 4.3. The empirical cumulative distribution function and the Kolmogorov-Smirnov test

From a bootstrap analysis, a large number of statistically possible realizations of an experimental data set are created, stored and evaluated in a computer. Interpretation of such a great amount of valuable information by Eq. (9) is only a first step in analysing these informations. By applying Eq. (9), the common  $\pm \sigma$  standard deviations are obtained that are applicable properly to normally distributed parameter estimates only. From the bootstrap resamplings, more detailed informations on the distribution of the parameter estimates is available. The key to these informations is the empirical cumulative distribution function cdf. The cdf returns the fraction of times an event  $p_i$  smaller than a certain value  $p$  occurs. In a formal expression, the cdf  $F(p)$  is defined as

$$F(p) = \frac{1}{n} \sum_{j=i}^n H(p - p_j) \quad (10)$$

where  $H(u)$ , unit step function jumping from 0 to 1 at  $u = 0$ ;  $n$ , total number of observations.

The values of a cdf  $F(p)$  are fixed  $(0, 1/n, 2/n, \dots, n/n)$ . Hence, the form of  $F(p)$  is defined by the ordered set of events  $p_i$  [34]. In the present situation, an event is a parameter estimate smaller than a specified value.

Again, the cdf is best illustrated by an example. In Table 2, ten values of a parameter estimate  $P$  are given. What is the value of  $F(P)$  for  $P <$

Table 2  
Ten values of a parameter  $P$  for illustrating the cumulative distribution function

12.32	12.48
12.33	12.51
12.39	12.55
12.47	12.67
12.48	12.81

12.32. There is no event given with  $P < 12.32$ . Hence  $F(P < 12.32) = 0$ . What is  $F(P < 12.48)$ . There are four events from a total of ten. Hence,  $F(P < 12.48) = 0.4$ . It is obvious that a cdf is a stepwise function that rises at an event  $P$  by a fraction  $m/n$ , where  $n$  is the total number of events, while  $m$  represents the number of this event  $P$ . For example,  $m(12.48) = 2$ . The cdf  $F(P)$  is shown in Fig. 1. The cdf is an estimate of the true but unknown distribution function of a parameter. Hence, it is often called ‘empirical cumulative distribution function’.

The number of events from a bootstrap analysis is commonly much larger than only 10 and, hence, the cdf’s are much smoother. It has to be reminded that this ‘stepwise’ situation is unavoidable in science: all experimental data is obtained in digital form. The smooth distributions, e.g. the normal distribution, are obtained by mathematical extrapolation to infinity. Since the situation often occurs that only a limited number of experimental data is available, the a priori assumption

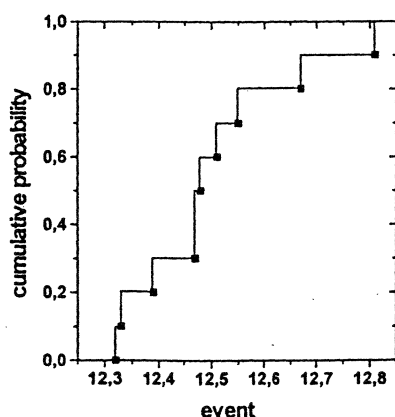


Fig. 1. Cumulative distribution function  $F(P)$  with data listed in Table 2.

of a normal distribution must be dropped. Therefore, it is desirable to test the degree of normality in a data set by an objective method. This information is available from the Kolmogorov-Smirnov (KS) test. KS test compares two arbitrary distributions. Hence, it is not limited to comparison with the normal distribution but able to assign a measure for the similarity of two arbitrary data sets [31]. In KS test, the largest discrepancy between two data sets is identified and the probability is calculated that this discrepancy is due to a stochastic variation. A detailed implementation instruction for KS test is available in Ref. [36]. Hence, no further discussion of this method is given.

The derivative of the cdf is the empirical probability density distribution edf. The edf directly shows the distribution of uncertainty for a parameter due to the limited precision of the experimental data. In frequent situations it is necessary to have an estimate, whether two different probability distributions differ only due to stochastic variations or are in fact significantly different. Here, the Wilcoxon–Mann-Whitney rank order (WMW) test on difference in location is a helpful instrument. The WMW test is advantageously demonstrated by a practical example and therefore will be introduced in Section 6.

## 5. The latin hypercube approach (LHS)

Experimentally obtained parameter estimates often are included into large data bases with the purpose to predict behaviour of complex systems. To take an example from chemistry, the geochemical data bases used to predict behaviour of substances in natural systems by reactive transport modelling include several hundred formation constants of relevant metal species. Each thermodynamic datum is obtained from experiment and hence affected by the limited precision of the measurement process [37]. However, even in the everyday practice of a scientist, it might be necessary to calculate uncertainty limits for a prediction based on input data with stated uncertainty. A simple example might be a speciation diagram that returns the relative distribution of certain

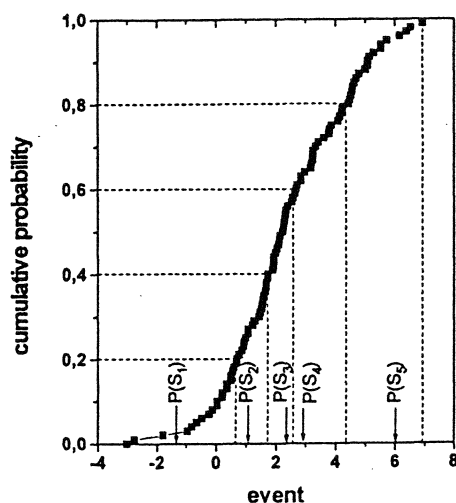


Fig. 2. Cumulative distribution function with five strata of equal probability. The representatives  $P(S_i)$  are randomly selected from each stratum and indicated by bottom arrows.

species calculated from experimentally determined formation constants. It is of course possible to use the Monte Carlo strategy in order to obtain confidence intervals for the speciation diagram, but the same strategy is not actually feasible for the geochemical modelling example. Even large main-frame computers need considerable time to finish a single run in full-scale three-dimensional transport modelling. In reactive transport modelling, only small-scale scenarios with a limited number of varied parameters are at the border of feasibility for Monte Carlo methods [38].

Here, the latin hypercube sampling approach (LHS) [39–42] is shown to reduce the computational burden considerable for the cost of some strategic planning. The Monte Carlo approach provides estimates of the cdf for parameter estimates, e.g. a thermodynamic constant. Even if there is only a confidence limit available, based on the assumption of normally distributed parameter estimate, the cumulative normal distribution is calculated from these both informations. With a cdf at hand, it is a numerically simple task to divide the cdf in a number of sections with equal probability. Each section is commonly called a 'stratum' and the complete procedure is called 'stratified sampling' in the statistical literature. Such strata are obtained for each parameter involved. A schematic representation is given in Fig. 2 for a cdf with five strata, S1–S5. The probability to observe a parameter in a stratum is 0.2 and equal for each of the five strata.

From each stratum, one representative parameter value, say  $P(S_i)$  is randomly selected. Thus a subsample is generated, where every region of the distribution function is represented in subsequent statistical procedure.

There are two options now to combine the  $i = 1 \dots c$  ( $i = \text{stratum index}$ ) representative parameter values  $P_n(S_i)$  obtained for each of the  $n = 1 \dots k$  error-affected parameter estimates into input data for the subsequent simulation, e.g. reactive transport modelling. The first strategy is to randomly select one of the  $P_n(S_i)$  for each of the  $k$  parameters. A possible outcome is shown in

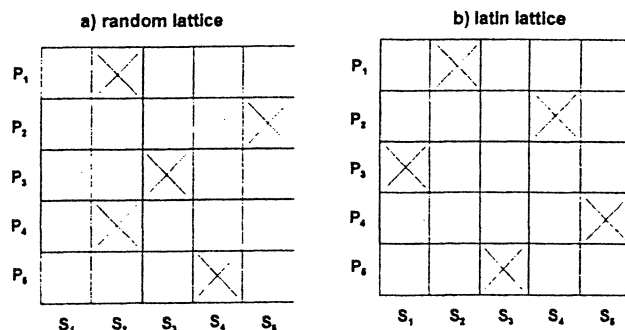


Fig. 3. Comparison of two strategies to generate input for a predictive code with five parameter estimates  $P_1$ – $P_5$  affected by uncertainty. Fig. 3a gives a possible input vector for a random selection. Here, strata may be left unconsidered, while other strata are used more often. Fig. 3b gives a latin lattice, where each stratum is applied with equal probability and not used twice.

Fig. 3a for a  $5 \times 5$  design: We have a lattice, where some stratum indices occur twice in a column, while some stratum indices do not occur at all. The second strategy requires that each index may occur only once in each column and each row. The resulting lattice is called a latin lattice. A latin lattice is shown in Fig. 3b. Each column of the both lattices defines one input vector for the subsequent operation. The LHS approach however requires more: for each column and each row, the same combination of indices ( $n, i$ ) may not occur again. Hence, in the  $5 \times 5$  design, there are five possible latin lattices only. After five replications, the possible permutations are exhausted. Information obtained from the strata of the input parameters via the representative  $S_i$  are used with equal probability.

If  $n$  is small, it might be advantageous to subdivide the edf in more strata than parameters are available ( $c > k$ ) and, consequently, more than  $k$  permutations are available. On the other hand, more parameters than strata ( $c < k$ ) is not allowed. In total, the subsequent operation has to be repeated  $c$  (the number of strata) times and a total number of  $c$  results are obtained. The mean value of the  $c$  outputs,  $Y$  (which may be, e.g. the time after which contaminant concentration in a well will exceed a threshold value) is calculated by Eq. (11)

$$Y = \frac{1}{c} \sum_{i=1}^c Y_i \quad (11)$$

The variance  $s^2(Y)$  is calculated according to Eq. (12)

$$s^2(Y) = \frac{1}{c} \sum_{i=1}^c (Y - Y_i)^2 + \left[ \frac{c-1}{c} \cdot \frac{1}{c^k(c-1)^k} \right] \sum_R (Y - Y_i)(Y - Y_j) \quad (12)$$

Here,  $R$  indicates that summation has to include only those permutations where no indices are in common.

An advantage of the LHS strategy becomes evident if a large number of error-affected input parameters have to be used in a simulation. If a random strategy would be applied here, several thousand repetitions of the predictive code would be needed in order to satisfactorily map the distribution of the input parameter estimates to the

output. Taking the duration of one run of a typical geochemical transport code in case of a real-world problem, this is not feasible. With the LHS strategy, the number of repetitions is given by number of uncertainty-affected input data, say in the order of hundreds. Combining LHS prediction with sensitivity analysis, the number of error-affected input parameters can often be reduced considerably [43].

## 6. Examples

### 6.1. Solvent extraction data

In the following, examples illustrate the enhanced information obtainable from computer intensive methods of statistics in chemical applications. The first example selected to demonstrate some of the different methods of uncertainty estimation in fitted parameter estimates are taken from the problem of determining chemical stability constants for some species by the use of solvent extraction. Solvent extraction is a separation method which uses that two immiscible liquids, e.g. water and toluene, are brought in contact with each other, e.g. in a separation funnel. The organic phase consists of a phase in which an extraction reagent with certain chemical properties is provided, while in the aqueous phase the element of interest is dissolved. By contacting the two phases, the element of interest will distribute between the two phases. The distribution of the element of interest can then be expressed in terms of the distribution ratio,  $D$ . In the present example, a radioactive tracer is used for concentration determination. By using the fact that the concentration of a radioactive element,  $M$ , is proportional to the specific radioactivity, Eq. (13) is obtained. Here  $M = M^{4+} = \text{Th}^{4+}$ .

$$\begin{aligned} D_M &= \frac{[M]_{\text{tot. org}}}{[M]_{\text{tot. aq}}} \\ &= \frac{\text{Total concentration of M in the organic phase}}{\text{Total concentration of M in the organic phase}} \\ &= \frac{\text{Specific radioactivity in the aqueous phase (Bq/ml)}}{\text{Specific radioactivity in the aqueous phase (Bq/ml)}} \\ &= \frac{S_{\text{org}}}{S_{\text{aq}}} \end{aligned} \quad (13)$$

Table 3  
Extraction data set from the Th-Aa<sup>-</sup> system [44] (Aa<sup>-</sup>:  
acetylacetonate)

[Aa <sup>-</sup> ] <sup>a</sup>	<i>D</i> <sub>Th</sub> <sup>b</sup>
4.37 × 10 <sup>-9</sup>	3.89 × 10 <sup>-4</sup>
4.70 × 10 <sup>-9</sup>	3.52 × 10 <sup>-4</sup>
9.30 × 10 <sup>-9</sup>	1.21 × 10 <sup>-3</sup>
1.65 × 10 <sup>-8</sup>	7.55 × 10 <sup>-3</sup>
3.48 × 10 <sup>-8</sup>	5.29 × 10 <sup>-2</sup>
4.91 × 10 <sup>-8</sup>	6.54 × 10 <sup>-2</sup>
7.12 × 10 <sup>-8</sup>	2.17 × 10 <sup>-1</sup>
1.67 × 10 <sup>-7</sup>	7.08 × 10 <sup>-1</sup>
1.86 × 10 <sup>-7</sup>	1.18 × 10 <sup>0</sup>
4.24 × 10 <sup>-7</sup>	4.11 × 10 <sup>0</sup>
5.10 × 10 <sup>-7</sup>	6.54 × 10 <sup>0</sup>
9.40 × 10 <sup>-7</sup>	1.57 × 10 <sup>1</sup>
1.76 × 10 <sup>-6</sup>	3.18 × 10 <sup>1</sup>
4.19 × 10 <sup>-6</sup>	8.90 × 10 <sup>1</sup>
5.08 × 10 <sup>-6</sup>	1.21 × 10 <sup>2</sup>
1.05 × 10 <sup>-5</sup>	1.96 × 10 <sup>2</sup>
3.25 × 10 <sup>-5</sup>	3.35 × 10 <sup>2</sup>
3.75 × 10 <sup>-5</sup>	3.39 × 10 <sup>2</sup>
2.26 × 10 <sup>-4</sup>	4.96 × 10 <sup>2</sup>
2.40 × 10 <sup>-4</sup>	5.11 × 10 <sup>2</sup>
1.02 × 10 <sup>-3</sup>	7.93 × 10 <sup>2</sup>
1.45 × 10 <sup>-3</sup>	6.27 × 10 <sup>2</sup>
2.76 × 10 <sup>-3</sup>	7.70 × 10 <sup>2</sup>
7.52 × 10 <sup>-3</sup>	7.68 × 10 <sup>2</sup>
8.67 × 10 <sup>-3</sup>	8.70 × 10 <sup>2</sup>
1.88 × 10 <sup>-2</sup>	9.01 × 10 <sup>2</sup>
2.89 × 10 <sup>-2</sup>	7.91 × 10 <sup>2</sup>
3.73 × 10 <sup>-2</sup>	9.28 × 10 <sup>2</sup>
3.86 × 10 <sup>-2</sup>	9.13 × 10 <sup>2</sup>
4.78 × 10 <sup>-2</sup>	8.03 × 10 <sup>2</sup>
6.04 × 10 <sup>-2</sup>	1.02 × 10 <sup>3</sup>

<sup>a</sup> Calculated from distribution equilibrium of HAA between organic and aqueous phase and pH; square brackets denote concentrations in mol l<sup>-1</sup>.

<sup>b</sup> Distribution ratio; measured by liquid scintillation counting.

In Eq. (13), 'org' and 'aq' denote the organic and aqueous phase respectively. The distribution ratio, *D*<sub>M</sub>, is not a constant since it depends on ligand concentration. Assuming that only mononuclear species exist and only the uncharged complex ML<sub>4</sub> is extractable where L<sup>-</sup> denotes the ligand, the distribution ratio, *D*<sub>M</sub>, can be expressed as

$$D_M = \frac{[ML_z]_{\text{org}}}{[M^{z+}] + [ML^{(z-1)}] + \dots + [ML_k^{(z-k)}]}$$

$$\begin{aligned} &= \frac{\lambda_z [ML_z]_{\text{aq}}}{[M^{z+}] + [ML] + \dots + [ML_k^{(z-k)}]} \\ &= \frac{\lambda_z \beta_z [M^{z+}][L^-]^z}{\sum_{i=0}^1 \beta_i [M^{z+}][L^-]^i} = \frac{\lambda_z \beta_z [L^-]^z}{\sum_{i=0}^1 \beta_i [L^-]^i} \end{aligned} \quad (14)$$

where  $\lambda_z$  is the distribution ratio of the uncharged species ML<sub>4</sub>, while  $\beta_i$  is the overall stability constant for the formation of the *i*-th complex. The  $\beta_i$  in Eq. (14) are obtained by multi-parameter curve fitting to the experimentally obtained distribution ratios for different ligand concentrations.

In present case the extraction reagent is acetylacetonate (HAA) which forms complexes of the type M(Aa)<sub>*i*</sub><sup>(4-*i*)</sup> with *i* = {1, ..., 4} with thorium in the aqueous phase. The extractable species is the uncharged complex with *i* = 4. To determine the constants for the system, thorium-acetylacetonate experiments were conducted with phases containing, apart from the inert electrolyte, thorium (< 10<sup>-5</sup> M) and 0.1 M acetylacetonate in toluene. The extraction procedure were performed in an AKUFVE unit ('apparatus for continuous investigation of distribution equilibrium using solvent extraction') [46]. An AKUFVE unit includes a palladium-passivated titanium vessel as central unit. Since the thorium stock solution was dissolved in 1 M HClO<sub>4</sub> the initial pH of the solution was about 2 and was increased during the experiment by additions of 1.0 M NaOH. The distribution of the acetylacetonate between the phases is known and taken into account by its respective distribution constant [45]. Samples were taken from each phase, and their activities were measured using a liquid scintillation counter. Calculations have shown that the effect of trace impurities in the <sup>232</sup>Th(NO<sub>3</sub>)<sub>4</sub> on the liquid scintillation measurements were negligible compared to the activity of the <sup>234</sup>Th. Further experimental details are already given in [44,45] and not repeated here.

The resulting experimental extraction data are shown in Table 3. For statistical treatment, data from Table 3 was selected according to the requirements of each sampling scheme:  $\chi^2$ , jackknife and bootstrap, resp. For the jackknife

Table 4  
Results from uncertainty calculations

Stability constant	Bootstrap	Jackknife	Chi-square
$\lg \beta_1$	$11.60 \pm 0.22$	$11.55 \pm 0.11$	$11.64 \pm 0.32$
$\lg \beta_2$	$19.63 \pm 0.19$	$19.53 \pm 0.12$	$19.62 \pm 0.17$
$\lg \beta_3$	$25.94 \pm 0.23$	$25.80 \pm 0.12$	$25.90 \pm 0.20$
$\lg \beta_4$	$30.32 \pm 0.18$	$30.23 \pm 0.12$	$30.32 \pm 0.10$

calculations, 31 subsamples were created, i.e. one data point was omitted in each run. For comparison purposes, 31 bootstrap samples were taken. The results are presented in Table 4, together with uncertainties estimated according to the  $\chi^2$  method. In the latter case an upper and a lower bound may be calculated since the  $\chi^2$  distribution is not symmetrical. The results presented here are the largest limit for one standard deviation interval. In this kind of application it is the logarithm of the value for the stability constants which is commonly used. The values are therefore in log-scale which also is asymmetrical with respect to a symmetrical linear scale, why also here the largest uncertainty intervals are selected.

Upon examining Table 4 it is clear that the methods give results in agreement with one another. The uncertainties are rather small but it must be remembered that errors in auxiliary data, e.g. pH, have not been considered which might have increased the uncertainty limit. However, it is not completely clear how

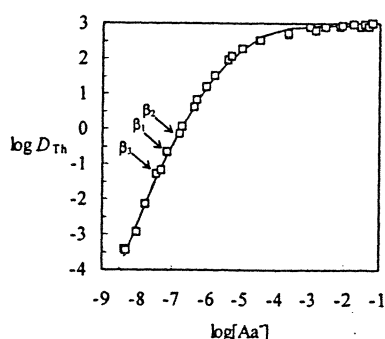


Fig. 4. Experimental points and fitted curve together with the most sensitive data for each parameter fitted.

such additional error contributions are to be included in the fitting procedure without often cumbersome progression of error calculations. Since this paper covers different methods for assigning uncertainties, there are no steps taken to address the problem of errors in auxiliary data mentioned above. However, it should be noted that Bootstrap methods are able to handle such additional error contributions.

The results from a jackknife estimation, e.g. tabulating the optimum parameter estimates obtained on omission of a certain data point, may be used to detect experimental data which will influence the result to a large extent. This information may be used to determine whether a suspected outlier might have any influence and ought to be reconsidered. Such an analysis has been done and the results are included in Fig. 4.

The data points whose omission leads to the strongest difference within all results for a given parameter, are indicated by arrows in Fig. 4. This method of ranking experimental data resulted in several points of equal importance for the fourth stability constants and, hence, such indication has been omitted for  $\beta_4$  in Fig. 1. Further analysis did not indicate outlying data.

## 6.2. Solubility data

Thermodynamic data is often determined repeatedly, e.g. in different laboratories. The question arises, whether the newly forwarded data is confirming or questioning previously reported results. It is a not uncommon observation that new data is claimed to be at least as accurate than existing data. Often, however, it has to be realised that the method of statistical analysis is not given at all.

Consider two experimental data sets in Fig. 5 on the solubility of  $\text{UO}_2\text{CO}_3(\text{s})$  in 0.1 M perchlorate medium in equilibrium with 100%  $\text{CO}_2$  [47,48]. It has been shown by detailed spectroscopic investigation [48] that the model function Eq. (15) is an adequate model for interpreting the both experimental data sets:

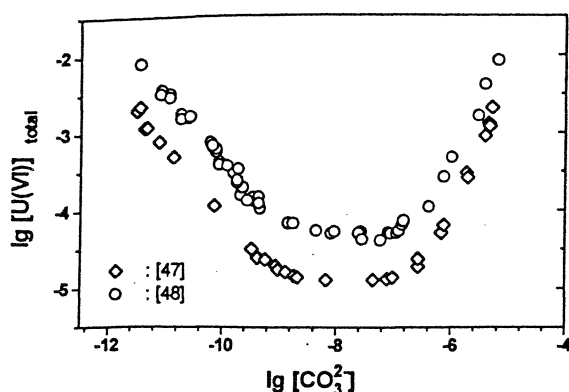


Fig. 5. Solubility of  $\text{UO}_2\text{CO}_3(\text{s})$  in 0.1 M perchlorate medium in equilibrium with 100%  $\text{CO}_2$  atmosphere [47,48].

$$Y_i = \frac{K'_{\text{sp}}}{[\text{CO}_3^{2-}]^2} (1 + \beta'_{101}[\text{CO}_3^{2-}]_i + \beta'_{102}[\text{CO}_3^{2-}]_i^2 + \beta'_{103}[\text{CO}_3^{2-}]_i^3) + \varepsilon_i \quad (15)$$

where  $Y_i$  is the measured total U(VI) concentration at free carbonate concentration  $[\text{CO}_3^{2-}]_i$ , and the parameters are  $K'_{\text{sp}}$  (solubility product of solid phase  $\text{UO}_2\text{CO}_3(\text{s})$ ) and formation constants  $\beta'_{10n}$  of the  $n$ -th carbonate species ( $\beta'_{10n} = [\text{UO}_2(\text{CO}_3)_n]^{(2-2n)} [\text{UO}_2^{2+}]^{-1} [\text{CO}_3^{2-}]^{-n}$ ). The random error is indicated by  $\varepsilon_i$ . A small contribution of the dimeric hydrolysis species  $(\text{UO}_2)_2(\text{OH})_2^{2+}$  will be neglected here (but not in the data analysis) for sake of simplicity.

The question arises, whether the both data sets give a common or differing picture of U(VI) solubility behaviour in carbonate solutions. It has to be emphasized that both data sets are obtained by comparable methods in different laboratories.

Both data sets are interpreted by 1000 bootstrap replicates. The empirical distribution functions

Table 5

Standard bootstrap estimates and standard deviations obtained from 1000 resampling cycles for  $\text{UO}_2\text{CO}_3(\text{s})$  solubility data from Refs. [47,48]

	[47]	[48]
$\lg K'_{\text{sp}}$	$-14.21_0 \pm 0.024_6$	$-13.46_2 \pm 0.020_7$
$\lg \beta'_{101}$	$9.27_1 \pm 0.034_9$	$9.12_8 \pm 0.033_5$
$\lg \beta'_{102}$	$15.42_9 \pm 0.159_8$	$15.41_8 \pm 0.174_7$
$\lg \beta'_{103}$	$21.99_8 \pm 0.050_2$	$21.78_0 \pm 0.087_4$

(edf) for each parameter in Eq. (15) are obtained for both data sets by numerical differentiation of the cumulative distribution function (cdf). The calculated parameter estimates according to the standard bootstrap procedure are given in Table 5.

The 1000 resamplings provide 1000 estimates for each of the four parameters in Eq. (15). These estimates are ranked (ordered according to their magnitude). From these ranked parameter estimates, the edf is easily obtained [33,34]. For illustration, the edf's for parameters  $\lg K'_{\text{sp}}$  and  $\lg \beta'_{102}$  are compared to each other in Fig. 6.

Fig. 6 visualizes clearly the relationship between the parameter estimates: while the solubility products are very accurate but clearly separated, the parameters  $\lg \beta'_{102}$  from the both studies are closely overlapping. All distributions are monomodal.

Are both distributions obtained from different experimental data significantly different or are the observed differences accidental? This question is answered by application of a rank test, e.g. the so-called Wilcoxon–Mann–Whitney (WMW) test

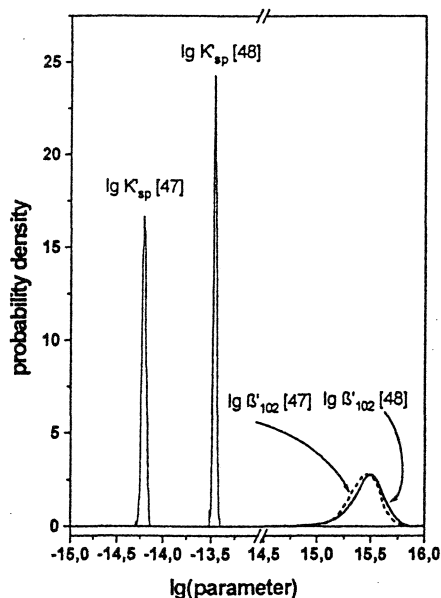


Fig. 6. A comparison of edf's of the parameters  $\lg K'_{\text{sp}}$  and  $\lg \beta'_{102}$ , obtained from 1000 bootstrap cycles. Note the x-axis break.

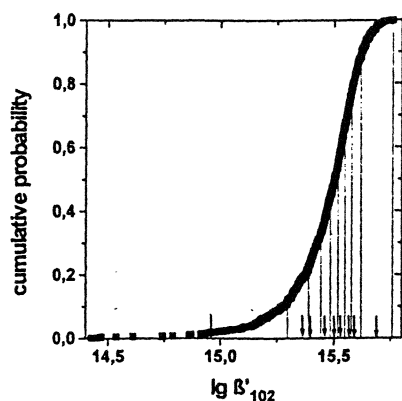


Fig. 7. Cumulative probability distribution function (cdf) of parameter  $\lg \beta'_{102}$ . The distribution is divided into nine strata of equal probability. The randomly selected representatives  $S_i$  of each stratum are indicated by bottom arrows. Note the skewness in the cdf. The edf of this distribution is shown in Fig. 6.

[31]. To perform a WMW test, the both sets of data are combined into one data set, generating a set of 2000 values for  $\lg \beta'_{102}$ . The data are then ranked. Hence, each data point becomes assigned a rank  $w$  between 1 and 2000, depending on its position in the ordered list. The important point is here, that it must be recognizable from which of the both initial data sets an individual data point is coming from. Now, the ranks  $w$  of all data coming from one of the both data sets are added, resulting in a statistics  $W$ :

$$W = \sum w_i \quad (16)$$

The statistics  $W^*$  is calculated by Eq. (17)

$$W^* = \frac{W - \frac{n_1(n_1 + n_2 + 1)}{2}}{\sqrt{\frac{n_1 n_2 (n_1 + n_2 + 1)}{12}}} \quad (17)$$

where  $n_1$  and  $n_2$  are number of data in data sets 1 and 2, resp. (both are 1000 in present case). Eq. (17) is applicable if  $(n_1 + n_2) > 20$  and  $n_1$  and  $n_2 > 5$ . This is definitively true in the present situation where  $n_1 = n_2 = 1000$ .

It is obvious that calculating WMW statistics  $W^*$  by hand is extremely tedious, but very simple by computer. In the present example,  $W^*$  was

found to be 3.57. Now, the statistics  $W^*$  is compared to the critical value. The hypothesis, that the difference between the both distributions obtained for  $\lg \beta'_{102}$  is not significant is rejected, if  $W^*$  is either too small or too large. For WMW rank test, the critical value can be directly obtained from a normal distribution, whose values are tabled in almost every textbook on statistics. The 95% cut-off value is 1.96, the 99% cut-off value is 2.57. Both critical values are smaller than  $W^*$ . Hence, it may be concluded that the difference between the both distributions of parameter  $\lg \beta'_{102}$  from different experiment is highly significant. The 'Type II' or  $\beta$  risk, that our conclusion is wrong may thus be expected to be smaller than 1%. Actually, the 99.9% cut-off point of the normal distribution is 3.29 — still smaller than 3.57 and thus reducing our  $\beta$  risk to almost 0.

A speciation diagram, giving the relative amount of each species at given pH, is not an experimentally measured information. It is predicted on basis of the experimentally obtained formation constants. Since these experimental data are affected by uncertainty, the speciation diagram will likewise carry an uncertainty for each species. The uncertainty in the relative contribution of each species can not be estimated by a straightforward procedure because the different parameter estimates are mutually coupled by the total amount of species. Here, latin hypercube sampling (LHS) offers an effective perspective. In Fig. 7, the cdf of the parameter  $\beta'_{102}$  is stratified into nine strata. From each stratum, a value is randomly selected to represent its stratum in the further procedure. These stratification is repeated for the three other parameters: a  $4 \times 9$  design is applied.

A realization of an LHS lattice is shown in Fig. 8, where each column represents an input vector used for calculation of a speciation diagram. Hence, the procedure of calculating the species diagram is repeated nine times, each time with a different choice of input data for the four parameters  $K'_{sp}$ ,  $\beta'_{101}$ ,  $\beta'_{102}$  and  $\beta'_{103}$ . This choice is designed according to the LHS strategy. Each figure in the array Fig. 7 gives the stratum number, from which the input data is chosen. Please note, that the same stratum number never occurs twice in

parameter	$K'_{sp}$	1	2	3	4	5	6	7	8	9
	$B'_{101}$	7	5	9	1	3	8	2	6	4
	$B'_{102}$	9	3	5	2	4	1	8	7	6
	$B'_{103}$	4	6	8	7	9	3	1	2	5
	run	1	2	3	4	5	6	7	8	9

Fig. 8. LHS array of nine input vectors for a  $4 \times 9$  design. The figures in each column represent a stratum number from the cdf of a row's parameter. The input data for each run are made up by the representatives  $S_i$  in the respective stratum. Please note that no stratum number occurs twice in both a column and a row. Several input vectors belong to the subspace  $R$  (cf. Eq. (12)). These are, among others, columns 1, 2 or columns 7, 9. These columns do not contain common stratum numbers.

both a column and a row. This is the LHS strategy.

Hence, the LHS strategy requires to repeat the prediction nine times. For the first run, the value selected for  $K'_{sp}$  in stratum 1, for  $\beta'_{101}$  the value from stratum 7, for  $\beta'_{102}$  in stratum 9 and for  $\beta'_{103}$  in stratum 4. Since the strata are based on the cdf of each parameter estimates, non-normality and skewness (as e.g. in  $\lg \beta'_{102}$  in Fig. 6) is taken into account.

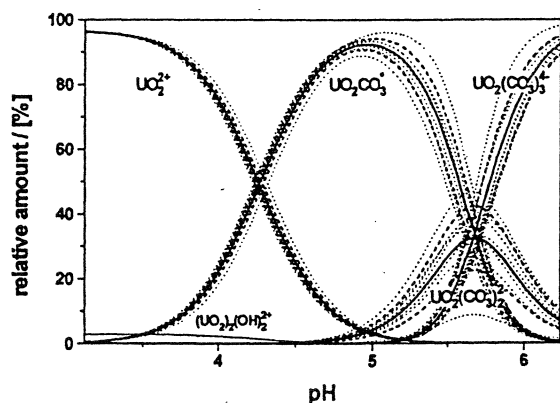


Fig. 9. Species distribution of the U(VI)-CO<sub>2</sub>-H<sub>2</sub>O system in 0.1 M perchlorate medium. The mean distribution is given by solid lines with dashed lines presenting the respective standard deviations. The diagram is based on the nine LHS calculations according to the scheme shown in Fig. 8. The calculations result in the nine runs that are given by dotted lines. The species  $(UO_2)_2(OH)_2^{2+}$  is taken into account by its mean value only.

The resulting speciation diagram with uncertainties is shown in Fig. 9, where the nine different species diagrams are given as dotted curves. From these nine realizations, the mean value (solid curves) and standard deviation (dashed curves) are estimated by Eqs. (11) and (12), resp. In this example, the bias correction (summing over subspace  $R$ ) turned out to be close to 0.

## 7. Conclusions

Uncertainty is an unavoidable part of experimental science. Computer-intensive methods of inference, e.g. bootstrap or jackknife, are recognized as powerful tools in judging data in complicated situations. Ignoring uncertainty is a waste of valuable information, sometimes even rendering forwarded conclusions void. Due to the ubiquity of computers, more and more complicated models are applied for numerical interpretation of experimental data. Often, the traditionally trained research worker is unaware of the powerful tools available to treat such data structures. According to our observation, statistical parameter estimates reported in thermodynamic literature, e.g. uncertainty limits, are often rather estimated than precisely determined. The present work intends to encourage the use of available statistical tools like  $\chi^2$  intervals or resampling methods that replace complicated (and often unavailable) parametric statistics by simple-to-implement computer algorithms. The procedures and examples discussed in the foregoing sections have been applied in recent research work [37,44] and have been forwarded helpful guidance especially in those situations, where judgement and decisions are not obvious. Intention of the present discussion is to illustrate the application of computer-intensive methods for data post-analysis and prediction. It is obvious that a manuscript is not able to cover the topic thoroughly. Therefore, the references have been selected to support an interested reader's initiative. An almost basic statement, however, should be given at the end: statistics is a tool that supplements a scientist's judgement. It is not recommended to use statistics 'as a drunk uses a

lamp-post — more for support than enlightenment' [49].

## References

- [1] Guide to the Expression of Uncertainty in Measurement, International Standardization Organisation, Geneva, Switzerland (1993).
- [2] S. Ellison, W. Wegscheider, A. Williams, *Anal. Chem.* 69 (1997) 607A.
- [3] P. Spitzer, R. Eberhardt, I. Schmidt, U. Sudmeier, *Fresenius J. Anal. Chem.* 356 (1996) 178.
- [4] L. Cortez, *Mikrochim. Acta* 119 (1995) 323.
- [5] J.C. Nash, *Compact Numerical Methods for Computers*, Adam Hilger, Bristol, UK, 1981.
- [6] R. Fletcher, M.J.D. Powell, *Comp. J.* 6 (1963) 163.
- [7] R. Fletcher, *Comp. J.* 13 (1970) 317.
- [8] D.R. Powell, J.R. MacDonald, *Comp. J.* 15 (1972) 148.
- [9] J.A. Nelder, R. Mead, *Comp. J.* 7 (1965) 308.
- [10] W. Spendley, Non-linear least squares fitting using a modified simplex minimization method, in: R. Fletcher (Ed.), *Optimization*, Institute of Mathematics and its Applications, Academic Press, London, UK, 1969, p. 259.
- [11] S.N. Deming, L.R. Parker, *Crit. Rev. Anal. Chem.* 7 (1978) 187.
- [12] R.J. Beckman, R.D. Cook, *Technometrics* 25 (1983) 119.
- [13] M. Otto, *Chemometrics*, VCH-Wiley, Weinheim, Germany, 1998.
- [14] M. Meloun, J. Militký, M. Forina, *Chemometrics for Analytical Chemistry*, vol. 2. Ellis Horwood, Chichester, UK, 1994.
- [15] S.J. Haswell (Ed.), *Practical Guide to Chemometrics*, Marcel Dekker Inc., New York, USA, 1992.
- [16] B. Efron, *SIAM Rev.* 21 (1979) 460.
- [17] D.M. Bates, D.G. Watts, *Nonlinear regression analysis and its application*, in: *Wiley Series in Probability and Mathematical Statistics*, Wiley and Sons, Chichester, UK, 1988 p. 365.
- [18] B.P. Korin, *Statistical Concepts for the Social Sciences*, Winthrop Inc, Cambridge, USA, 1975.
- [19] 'Student' (W. Gosset), *Biometrika* 6 (1908) 1.
- [20] R.B. Dean, W.J. Dixon, *Anal. Chem.* 23 (1951) 636.
- [21] F.E. Grubbs, *Technometrics* 11 (1969) 1.
- [22] D. Collett, T. Lewis, *Appl. Stat.* 25 (1976) 228.
- [23] B.M. Brown, *Biometrika* 62 (1975) 623.
- [24] G.S. Lingappaiah, *Metrika* 23 (1976) 27.
- [25] R.G. McMillan, *Technometrics* 13 (1971) 87.
- [26] I. Guttman, *Technometrics* 15 (1973) 723.
- [27] I. Guttman, C.G. Kaharti, A Bayesian approach to some problems involving the detection of spuriousity, in: R.P. Gupta (Ed.), *Applied Statistics Symposium*, North-Holland, Amsterdam, Netherlands, 1975, p. 111.
- [28] D.B. Rorabacher, *Anal. Chem.* 63 (1991) 139.
- [29] W.J. Dixon, *Ann. Math. Stat.* 21 (1950) 488.
- [30] W.J. Conover, *Practical nonparametric statistics*, in: *Wiley Series in Probability and Mathematical Statistics*, Wiley and Sons, Chichester, UK, 1980.
- [31] J.V. Desphande, A.P. Gore, A. Shanubhogue, *Statistical Analysis of Nonnormal Data*, Wiley & Sons, Chichester, UK, 1995 p. 255.
- [32] R.G. Miller, *Biometrika* 61 (1974) 1.
- [33] B. Efron, R.J. Tibshirani, *An Introduction to the Bootstrap*, Monographs on Statistics and Applied Probability 57, Chapman & Hall, London, UK, 1993 p. 436.
- [34] A.C. Davison, D.V. Hinkley, *Bootstrap methods and their application*, in: *Cambridge Series in Statistical and Probabilistical Mathematics*, Cambridge University Press, Cambridge, UKp. 582, 1997.
- [35] R. Stine, in: J. Fox, J. Scott-Long (Eds.), *Modern Methods of Data Analysis*, Sage Publications, Newbury Park, USA, 1990, p. 325.
- [36] W.H. Press, B.P. Flannery, S.A. Teukolsky, W.T. Vetterling, *Numerical Recipes — The Art of Scientific Computation*, Cambridge University Press, Cambridge, UK, 1989.
- [37] G. Meinrath, Y. Kato, T. Kimura, Z. Yoshida, *Radiochim. Acta* 84 (1999) 21.
- [38] O. Nitzsche, G. Meinrath, B. Merkel@, Data base uncertainty as limiting factor in reactive transport modelling, in press.
- [39] M.D. McKay, R.J. Beckman, W.J. Conover, *Technometrics* 1 (1979) 239.
- [40] R.L. Iman, *Trans. Am. Nucl. Soc.* 55 (1987) 309.
- [41] R.L. Iman, J.C. Helton, *Risk Anal.* 8 (1988) 71.
- [42] R.L. Iman, *Reliab. Techn.* 28 (1992) 153.
- [43] C. Ekberg, G. Skarnemark, A.T. Emrén, I. Lunden, *Mater. Res. Soc. Symp.* 412 (1996) 889.
- [44] I. Hagström, L. Spjuth, Å. Enarsson, J.O. Liljenzin, M. Skälberg, M.J. Hudson, P.B. Iveson, C. Madic, P.Y. Cordier, C. Hill, *Solvent Extr. Ion Exch.* 17 (1998) 221–242.
- [45] C. Ekberg, *Freiberg On-line Geoscience*, Vol. 2 (1999) (<http://www.geo.tu-freiberg.de/fog>).
- [46] J. Rydberg, *Acta Chem. Scand.* 23 (1969) 647.
- [47] G. Meinrath, T. Kimura, *J. Alloy Comp.* 202 (1993) 89.
- [48] G. Meinrath, *Wiss. Mitt. Geol. Freiberg* 4 (1997) 100.
- [49] R.A. Chalmers, *Talanta* 40 (1993) 121.

# Appendix III

**Extraction Studies of  
Ag, Co, Cs, Fe and U by  
terpyridine - 2-bromodecanoic acid mixtures**

**Charlotta Gustafsson  
2000**

**DIPLOMA WORK 20P**

**DEPARTMENT OF NUCLEAR CHEMISTRY  
CHALMERS UNIVERSITY OF TECHNOLOGY  
GÖTEBORG  
SWEDEN  
2000 01 21**

**Examinator: Prof. Jan-Olov Liljenzin  
Supervisors: M.Sc. Åsa Enarsson, Prof. Jan-Olov Liljenzin**

## Abstract

The storage of nuclear waste must be safe for millions of year if a deep geological repository is used. One way to decrease the time needed for the waste to decay to background level is to separate lanthanides, actinides and other fission products from each other and then transmute the actinides, which is mainly the most radiotoxic nuclides in a longer perspective, to more short-lived or stable isotopes. The background to this work is the separation of trivalent actinides and lanthanides from each other in the SANEX process, which is one part of the separation process for long-lived radionuclides. To be able to make a process simulation of the SANEX process the behaviour of the metals present in the feed must be studied. Thus, the extraction of Cs, Co, Fe, Ag and U with 2,2':6',2''-terpyridine (terpyridine, T) in a synergistic combination with 2-bromodecanoic acid (HA) dissolved in *tert*-butylbenzene (TBB) has been studied.

The results show a very high extraction of iron, but also a longer time to reach equilibrium than for the other studied metals. The extracted specie is probably  $\text{FeA}_3 \cdot \text{T}$ , three  $\text{A}^-$  to form a neutral iron complex and one terpyridine. When the nitric acid concentration is increased to 0.4 M the distribution ratio is not so much influenced by the terpyridine concentration but more by the HA concentration.

The distribution ratio for extraction of uranium and cobalt with terpyridine and HA is similar in the studied nitric acid interval. However, when terpyridine is absent there is almost no extraction of Co, while U on the other hand is extracted. The results for uranium implicates a change in the extracted complex when the nitric acid concentration increases. At low nitric acid concentration (0.01-0.03 M) the extracted uranium complex is probably  $\text{UO}_2\text{A}_2 \cdot 2\text{T}$  but when the nitric acid concentration is increased the complex loses first one terpyridine and at 0.4 M nitric acid concentration the other is also lost and the extracted specie is  $\text{UO}_2\text{A}_2$ . To determine the extracted complex of cobalt is more complicated. However, the extracted specie could possibly be  $\text{CoA}_2 \cdot 2\text{T}(\text{HA})_3$ .

The distribution ratio for silver is higher than for americium, curium and europium. The extracted specie is most likely  $(\text{AgA}(\text{HA}))_2 \cdot \text{T}$ . However, when the nitric acid concentration is increased the difference between the distribution ratios for extraction with terpyridine and HA compared to extraction with HA decreases, implicating less influence of terpyridine and an extracted specie of the type  $\text{AgAHA}$ .

There are no difference in the distribution ratio when cesium is extracted with a mixture of terpyridine and HA or with only HA. Thus, cesium is not extracted by terpyridine and the extracted complex is  $\text{CsA}(\text{HA})_2$ . The distribution ratios are also lower for cesium than for other studied metals when the nitric acid concentration is lower than 0.05 M.

The separation factor between fission products (Fe, Ag and Co) and the actinides (Am and Cm) is higher than 38 at a nitric acid concentration of approximately 0.07M. Furthermore, the separation factor between uranium and the actinides (Am and Cm) is higher than 50. At 0.02 M nitric acid the separation factor between europium and cesium is 38.

<b>INTRODUCTION .....</b>	<b>1</b>
1.1 WASTE HAZARD .....	1
1.2 THE SEPARATION AND TRANSMUTATION CONCEPT.....	2
1.3 SEPARATION PROCESS .....	3
<b>2. THEORY.....</b>	<b>4</b>
2.1 SEPARATION PROCESS .....	4
2.2 DISTRIBUTION RATIO.....	5
2.3 EXTRACTION MECHANISM FOR THE 2,2':6',2''-TERPYRIDINE AND 2-BROMODECANOIC ACID SYSTEM.....	7
2.3.1 Protonation of terpyridine .....	8
2.3.2 Adduct formation between terpyridine and 2-bromodecanoic acid.....	8
2.3.3 Distribution of 2-bromodecanoic acid.....	8
2.4 CORRECTION FOR DECAY.....	10
<b>3. EXPERIMENTAL .....</b>	<b>11</b>
3.1 MATERIALS .....	11
3.2 RADIONUCLIDES.....	11
3.3 PREPARATION OF <sup>233</sup> U, <sup>59</sup> Fe, <sup>60</sup> Co, AND <sup>137</sup> Cs TRACER SOLUTIONS .....	11
3.4 TITRATION OF RADIOACTIVE TRACERS.....	11
3.5 DETERMINATION OF EXTRACTION CURVES FOR DIFFERENT NITRIC ACID CONCENTRATIONS WITH CONSTANT CONCENTRATIONS OF 2,2':6',2''-TERPYRIDINE AND 2-BROMODECANOIC ACID IN TERT-BUTYLBENZENE.....	12
3.6 DETERMINATION OF EXTRACTION CURVES FOR CONSTANT NITRIC ACID CONCENTRATION WITH DIFFERENT CONCENTRATIONS OF 2,2':6',2''-TERPYRIDINE AND CONSTANT 2-BROMODECANOIC ACID CONCENTRATION IN TERT-BUTYLBENZENE.....	12
3.7 DETERMINATION OF EXTRACTION CURVES FOR CONSTANT NITRIC ACID CONCENTRATION WITH DIFFERENT 2-BROMODECANOIC ACID CONCENTRATIONS AND CONSTANT 2,2':6',2''- TERPYRIDINE CONCENTRATION IN TERT-BUTYLBENZENE.....	12
3.8 DETERMINATION OF EXTRACTION CURVES FOR DIFFERENT NITRIC ACID CONCENTRATIONS WITH CONSTANT CONCENTRATION OF 2-BROMODECANOIC ACID IN TERT-BUTYLBENZENE.....	13
3.9 DETERMINATION OF EXTRACTION CURVE FOR <sup>137</sup> Cs FOR CONSTANT NITRIC ACID CONCENTRATION WITH DIFFERENT CONCENTRATION OF 2-BROMODECANOIC ACID IN TERT-BUTYLBENZENE.....	13
3.10 MEASURING CONDITIONS .....	13
3.10.1 Preparation of sample before measuring.....	13
3.10.2 Uranium.....	14
3.10.3 Iron .....	14
3.10.4 Cobalt .....	14
3.10.5 Cesium .....	14
3.10.6 Silver.....	14
<b>4. RESULTS AND DISCUSSION .....</b>	<b>15</b>
4.1 URANIUM .....	15
4.1.1 Uranium extraction with 2-bromodecanoic acid.....	15
4.1.2 Uranium extraction with 2,2':6',2''-terpyridine and 2-bromodecanoic acid.....	15
4.2 IRON.....	17
4.2.1 Iron extraction with 2-bromodecanoic acid .....	17
4.2.2 Iron extraction with 2,2':6',2''-terpyridine and 2-bromodecanoic acid .....	18
4.3 COBALT.....	19
4.3.1 Cobalt extraction with 2-bromodecanoic acid .....	19
4.3.2 Cobalt extraction with 2,2':6',2''-terpyridine and 2-bromodecanoic acid .....	20
4.4 CESIUM .....	21
4.4.1 Cesium extraction with 2-bromodecanoic acid .....	21
4.4.2 Cesium extraction with 2,2':6',2''-terpyridine and 2-bromodecanoic acid .....	22

4.5 SILVER .....	23
4.5.1 Silver extraction with 2-bromodecanoic acid .....	23
4.5.2 Silver extraction with 2,2':6',2''-terpyridine and 2-bromodecanoic acid .....	23
4.6 SEPARATION PROCESS POSSIBILITIES .....	25
<b>5. CONCLUSIONS .....</b>	<b>27</b>
5.1 DETERMINED EXTRACTED COMPLEXES .....	27
5.2 POSSIBILITIES FOR SEPARATION .....	27
<b>6. FUTURE WORK .....</b>	<b>28</b>
<b>7. ACKNOWLEDGEMENTS .....</b>	<b>29</b>
<b>8. REFERENCES .....</b>	<b>30</b>

**APPENDICES 1-19**

# 1. Introduction

## 1.1 Waste hazard

The radioactive waste from nuclear fuel is a problem in all countries where electricity is produced with nuclear reactors. There are different ideas on how the radioactive waste is to be treated in the future. One solution is deposition of waste in a deep geological repository, where the rock will prevent the radiotoxic nuclides from reaching the biosphere for hundreds of thousand of years. A complement to this deep geological storage is to separate the most radiotoxic nuclides, mainly the actinides, from the spent nuclear fuel and transmute them with neutron-irradiation to more short-lived or stable nuclides. This will reduce the radiotoxicity and decrease the time needed for the waste to decay to the background level.

The spent nuclear fuel consist of about 96 % uranium, 1 % plutonium and 0.1 % minor actinides, mainly Np, Am and Cm. They are all formed by neutron capture in uranium. The last 2.9 % is fission products formed in the reactor by fission of uranium and plutonium. It is mainly the actinides and plutonium which contribute to the long-term radiotoxicity of the spent nuclear fuel [Spj99]. The hazard of spent fuel relative to natural uranium versus time is shown in Figure 1.1. The hazard decreases with time owing to decay of the nuclides and reach the same level as natural uranium after 10 millions years. The curve, (All An:s) in Figure 1.1, shows that the relative hazard index after some hundred years mainly is due to the relative hazard index of the actinides. After about 1000 years the hazard index from the fission products, (All Fp:s), is 1 % of the hazard index of 1 ton natural uranium. The fission products which contribute most to the relative hazard index during the first 1000 years are  $^{137}\text{Cs}$  and  $^{90}\text{Sr}$  [Cho95]. This means that if the actinides are separated and transmuted to fission products the time needed for the spent fuel to reach the relative hazard index for natural uranium is decreased from 10 millions years to about 300 years.

In England, France, Russia, India and Japan irradiated fuel is reprocessed by the PUREX process (Plutonium Uranium Redox EXtraction) to recover uranium and plutonium. The waste from the PUREX process are fission products, minor actinides and other activation products. The actinides represent a radiotoxicity about 10 000 times higher than that of the fission products, [Bau93], and it would be useful to separate and convert the actinides to less harmful species. This is the reason for the partitioning and transmutation (P&T) projects around the world.

Isotope separation is necessary if some of the long-lived fission products are to be transmuted, e.g. Cs. The reason in this case is that Cs has both short-lived, long-lived and stable isotopes present in the waste and if the short-lived and stable isotopes are irradiated they will be transmuted to long-lived isotopes and increase the radiotoxicity instead of decrease it.

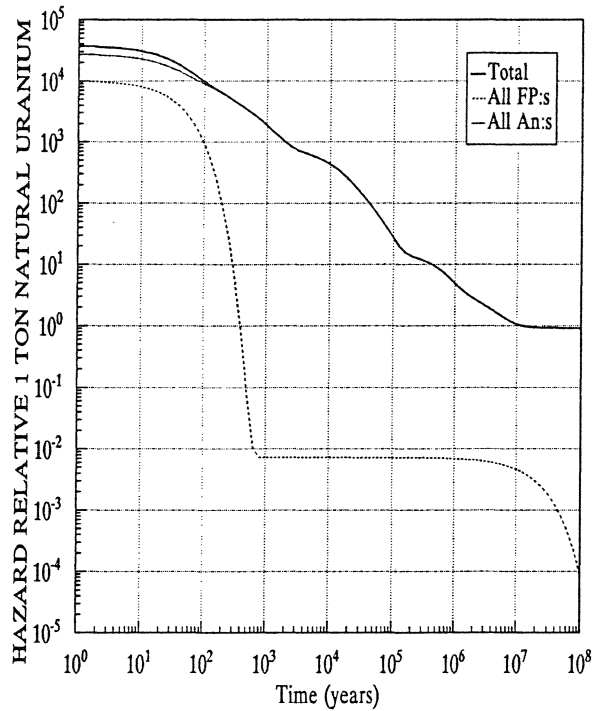


Figure 1.2 Relative hazard of spent nuclear fuel versus time [Skå95].

### 1.2 The separation and transmutation concept

The concept of separation and transmutation is to transmute long-lived radionuclides to short-lived or stable nuclides by neutron irradiation using the same nuclear processes as in a conventional reactor. But a higher neutron flux is necessary than in a conventional reactor to reach a significant transmutation rate. During the transmutation process, energy will be produced which will partly finance the costs of a transmutation process. A schematic overview of the partitioning and transmutation process can be seen in Figure 1.2.

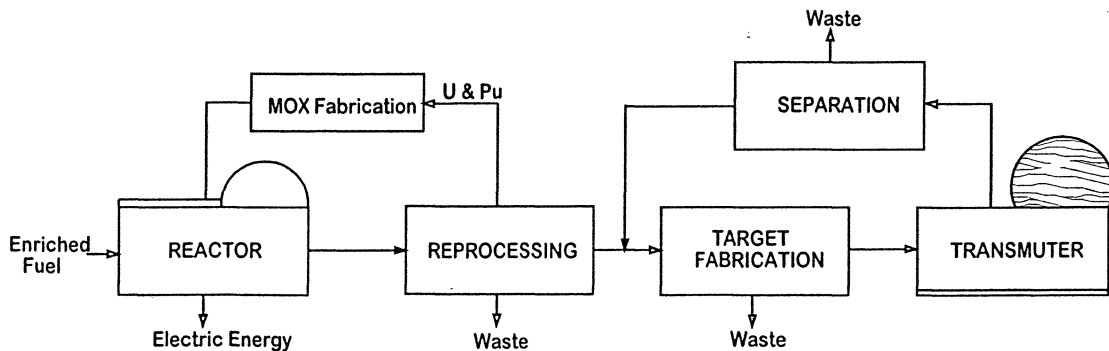


Figure 1.2. Schematic overview of a separation and transmutation concept [Spj99].

### 1.3 Separation process

Before a transmutation process there has to be a separation of the transmutable nuclides from the rest of the waste. Two important steps in this process are the separation of trivalent actinides and lanthanides from the rest of the fission products and the separation of trivalent actinides and lanthanides from each other. The reason for these separation processes is to prevent lanthanides and other fission products from reaching the transmutation process since they are present in much larger amount in the waste than the minor actinides and have higher neutron capture cross-sections, which would lead to an inefficient transmutation process [Skå95]. One technique considered for this separation is solvent extraction. In solvent extraction there are some difficulties in the separation of trivalent actinides and lanthanides due to their similar extraction behavior because of the same valence state and similar ionic radii.

There is a proposed separation process for long-lived radionuclides, see Figure 2.2 for flow sheet, which describe the separation of actinides and lanthanides from other fission products and the separation of actinides from lanthanides. It has been suggested that malonamides may be extractants for trivalent actinides and lanthanides. A great deal of research has been carried out on the extractant in the DIAMEX process, (DIAMide EXtraction), where trivalent actinides and lanthanides will be separated from other fission products.

In the next step, the SANEX process, (Selective ActiNide EXtraction) actinides will be separated from lanthanides. This task can be performed by selective extraction of the actinides with extractants that have one or more nitrogen donor atoms, which show greater affinity to trivalent actinides than lanthanides. To be effective, the nitrogen containing extractants studied today, need to be in a synergistic combination with a lipophilic acid with low  $pK_a$  [Mad94]. However, this research is still in the process of finding an optimal extractant with a preference for trivalent actinides over lanthanides at nitric acid concentration higher than 0.1 M.

To be able to make a process simulation of the SANEX process the behavior of metals which will occur in the feed must be studied. In this work the extraction of some metals, U, Fe, Co, Cs and Ag, with a nitrogen donor extractant has been studied.

The extractant used in this work is 2,2':6',2''-terpyridine (terpyridine), Figure 1.3, in a synergistic combination with 2-bromodecanoic acid (HA), Figure 1.4, dissolved in *tert*-butylbenzene (TBB). The extraction with only HA was also studied, to see the synergistic effect which appear when terpyridine and HA is mixed.

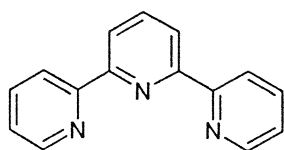


Figure 1.3 2,2':6',2''-terpyridine

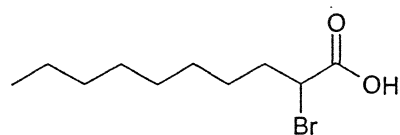


Figure 1.4 2-bromodecanoic acid

## 2. Theory

### 2.1 Separation process

It is mainly the actinides and plutonium which contributes to the long-term radiotoxicity of spent nuclear fuel. With neutron irradiation the actinides can be transmuted to short-lived or stable isotopes. To reach a good transmutation efficiency most lanthanides and other fission products have to be separated from the actinides, since they are neutron absorbing species with relatively short half-lives. The separation can be performed in different ways. One way is to extract U, Pu and Np (and possibly some other isotopes) in a modified PUREX process and then selectively extract the trivalent actinides from the raffinate. Another way is to extract, from the raffinate of the modified PUREX process, the trivalent actinides together with the lanthanides and then separate them from each other in a second step. For a flow-sheet of the PUREX process, see Figure 2.1.

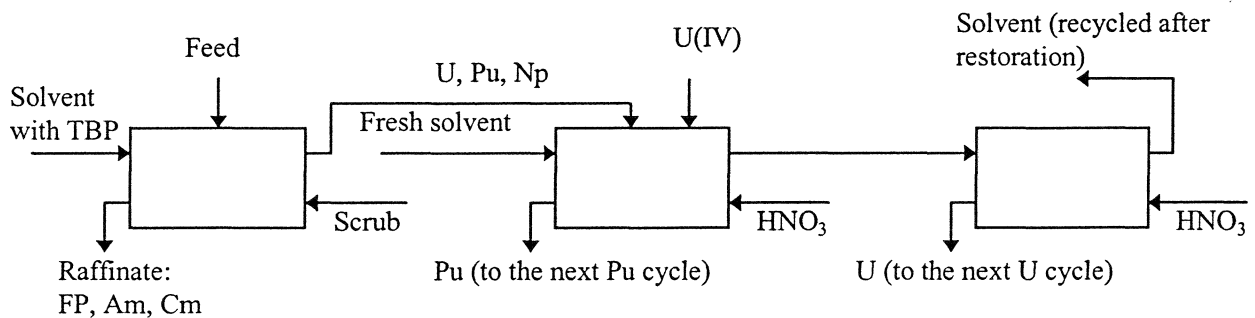


Figure 2.1 Flow-sheet of the PUREX process [Mus92].

One requirement of new extractants is that they should contain only carbon (C), hydrogen (H), oxygen (O), and nitrogen (N), the CHON-principle. The reason for this is that they should not contribute to the secondary waste which will be produced in the process. The CHON-principle makes the extractants totally incinerable and the secondary waste can be transformed by wet or dry incineration into gaseous products and the radionuclides trapped in the wastes can be recovered and recycled.

In Figure 2.2 a proposed flow sheet of a separation process for long-lived radionuclides can be seen. In the DIAMEX process the lanthanides and the trivalent actinides will be extracted together from the HLLW (High Level Liquid Waste) from the modified PUREX process. The extractant has been suggested to be a malonamide [Spj99]. In the next stage, the SANEX process, the trivalent actinides are separated from the lanthanides. The extractant proposed for this stage is a nitrogen donor extractant in synergy with a carboxylic acid. The optimal extractant would be a nitrogen donor which could be used without addition of a second reagent. One nitrogen donor extractant studied today is 2,2':6',2''-terpyridine in combination with 2-bromodecanoic acid. The 2-bromodecanoic acid does not fulfill the CHON-principle, but has been used in studies anyway because of

its low  $pK_a$  and because it is commercially available. A cyano acid would be a better choice in a real process to follow the CHON-principle.

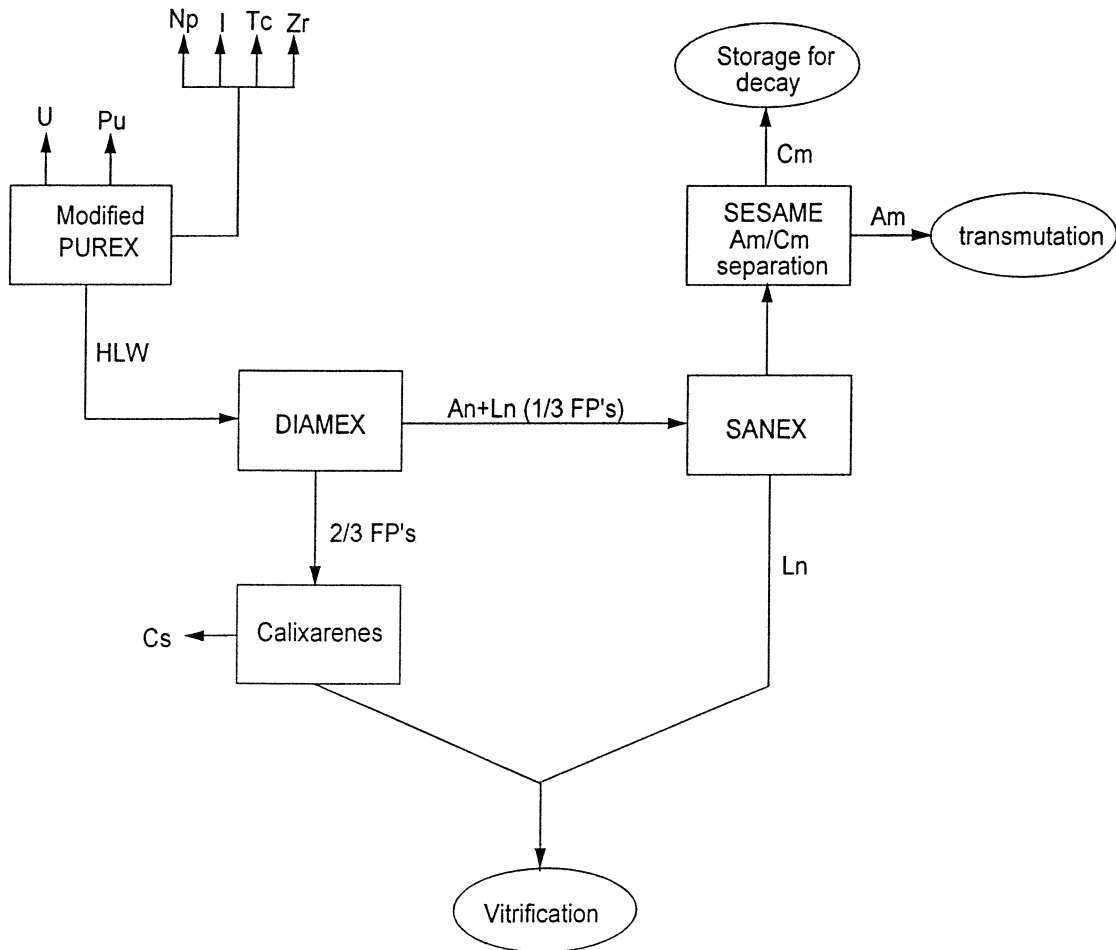


Figure 2.2 Proposed flow sheet of a separation process for long-lived radionuclides [Mad98].

## 2.2 Distribution ratio

The distribution of a certain element  $M$  between two phases can be expressed as either the distribution ratio for element  $M$ ,  $D_M$ , or as the percentage extraction of element  $M$ ,  $\%E_M$ . The distribution ratio  $D_M$  is defined by equation 2.1;

$$D_M = \frac{[M]_{tot,org}}{[M]_{tot,aq}} = \frac{\text{Concentration of all species containing } M \text{ in the organic phase}}{\text{Concentration of all species containing } M \text{ in the aqueous phase}} \quad 2.1$$

The distribution ratio of a metal can be determined by radiometric analysis when radionuclides are used according to;

$$D_M = \frac{\psi_{org} \cdot \frac{R_{org}}{V_{org}}}{\psi_{aq} \cdot \frac{R_{aq}}{V_{aq}}} \quad 2.2$$

where  $R_{org}$  is the measured counting rate in the organic phase  
 $R_{aq}$  is the measured counting rate in the aqueous phase  
 $V_{org}$  is the volume of the sample of the organic phase  
 $V_{aq}$  is the volume of the sample of the aqueous phase  
 $\psi_{org}$  is the detector efficiency for the organic phase  
 $\psi_{aq}$  is the detector efficiency for the aqueous phase

By using  $\gamma$ -emitters or liquid scintillation counting for  $\alpha$ -emitters the same detector and the same volume for the two samples, the detector efficiencies are equal and can be discarded in the formula above.

The percentage extraction,  $\%E_M$ , can be calculated according to;

$$\%E_M = 100 \cdot \frac{D_M \Theta}{1 + D_M \Theta} \quad 2.3$$

where  $\Theta$  is the volume ratio between the organic phase and the aqueous phase.

There will be some statistical fluctuations in the distribution ratio,  $D_M$ , from the measuring since the radioactive decay is a random process. The standard deviation,  $\sigma_D$ , from measuring can be written as;

$$\sigma_D = D_M \cdot \sqrt{\frac{R_{aq} / t_{aq} + R_{0,aq} / t_{0,aq}}{(R_{aq} + R_{0,aq})^2} + \frac{R_{org} / t_{org} + R_{0,org} / t_{0,org}}{(R_{org} + R_{0,org})^2}} \quad 2.4$$

where  $D_M$  is the distribution ratio  
 $R_{aq}$  is the measured counting rate in the aqueous phase  
 $R_{org}$  is the measured counting rate in the organic phase  
 $R_{0,i}$  is the measured counting rate in the background sample  $i$  (aqueous or organic)  
 $t_i$  is the measuring time for the phase  $i$  (aqueous or organic)  
 $t_{0,i}$  is the measuring time for the background sample  $i$  (aqueous or organic)

If the background and the sample is measured at the same time and if the total number of counts is used instead of the count rates, R, equation 2.4 can be rewritten according to equation 2.5, where GROSS and NET are peak areas with the background subtracted for the latter.

$$\sigma_D = D_M \cdot \sqrt{\frac{(2 \cdot GROSS_{aq} - NET_{aq})}{(NET_{aq})^2} + \frac{(2 \cdot GROSS_{org} - NET_{org})}{(NET_{org})^2}} \quad 2.5$$

### 2.3 Extraction mechanism for the 2,2':6',2''-terpyridine and 2-bromodecanoic acid system

The extraction mechanism by which the metal ions are extracted from the aqueous phase to the organic phase depends on the molecular structure of the extractant and also on the binding properties of the extractant to the metals. All metal ions have different extraction behavior, which depends on e.g. different electronic structure, charge and size.

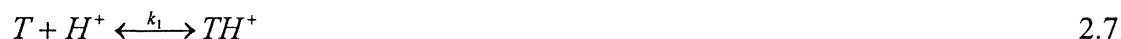
When two extractants are mixed and used, an increase in extraction can appear. This increase in extraction is called synergism. Three different mechanisms have been suggested to account for synergistic metal extraction with a chelating ligand and adduct.

- I) Opening of the chelating rings and occupation of the adduct molecule on the binding site of the metal.
- II) The chelating molecule and water molecules occupy the coordination sphere of the metal and adducts replace the water and increase the lipophilicity of the complex.
- III) The coordination sphere expands when adduct molecules interact with the metal ion. No water has to be replaced to accommodate the adduct molecules [Ryd92].

When 2-bromodecanoic acid is mixed with terpyridine a synergistic effect appears probably owing to the exchange of water or undissociated 2-bromodecanoic acid in the metal complexes by the solvating neutral ligands, or expansion of the coordination sphere of the metal ion.

### 2.3.1 Protonation of terpyridine

It has been shown by two-phase titration of terpyridine - 2-bromodecanoic acid in *tert*-butylbenzene, with nitric acid as the aqueous phase, that terpyridine can be diprotonated. The protonated species are present in the aqueous phase and the terpyridine protonation mechanism can be described according to 2.6-2.9 [Hag99].



T is terpyridine and overlined species denotes species in the organic phase.  $\lambda_T=360\pm 5$  is the distribution constant for terpyridine [Hag99]. The association constant for nitric acid,  $k_a=10^{-1.35}$  [Hägg63], and protonation constants for terpyridine,  $k_1=5.13\cdot 10^4$  and  $k_2=12.6\cdot 10^6$  (23 C and 0.1 M ionic strength) [Sch84].

### 2.3.2 Adduct formation between terpyridine and 2-bromodecanoic acid

When 2-bromodecanoic acid is present in the organic phase the protonation of terpyridine is decreased. One reason could be the adduct formation between terpyridine and 2-bromodecanoic acid in the organic phase. The adduct formation can be described by equation 2.10 [Hag99].



where HA denotes 2-bromodecanoic acid.

### 2.3.3 Distribution of 2-bromodecanoic acid

2-bromodecanoic acid is dimerised according to equation 2.11 when it is dissolved in non-polar solvents, i.e. *tert*-butylbenzene [Vit84].



In contact with an aqueous phase 2-bromodecanoic acid will be slightly transferred from the organic phase to the aqueous phase, where it will dissociate;



where  $K_a = 10^{3.7}$  at 0.001 M ionic strength [Hag99].

Complexation in the aqueous phase was assumed to occur between the dissociated 2-bromodecanoic acid and the free metal ion, in this example a  $M^{3+}$ -ion. Due to the low concentration of nitric acid, complexation of  $M^{3+}$ -ion with nitrate ions is neglected.



Neutral complexes, such as  $MA_3$ , are soluble in the organic phase and will be distributed between the aqueous and organic phases;



In the organic phase mixed complexes will be formed, with both dissociated 2-bromodecanoic acid, undissociated 2-bromodecanoic acid and terpyridine (T).



The distribution ratio  $D_M$  could be calculated from equation 2.14 and 2.16, yielding;

$$D_M = \frac{\sum_{m=0}^M \sum_{n=0}^N [\overline{MA_3(HA)_m T_n}]}{\sum_{x=0}^3 [MA_x^{3-x}]} \quad 2.17$$

If equilibria 2.11 - 2.16 are inserted in equation 2.17;

$$D_M = \frac{\sum_{m=0}^M \sum_{n=0}^N Q_{mn} \lambda_L^m \lambda_{HA}^m \lambda_T^n \alpha_3 K_a^m [A^-]^{3+m} [H^+]^m [T]^n}{\sum_{x=0}^3 \alpha_x [A]^x} \quad 2.18$$

## 2.4 Correction for decay

Due to the high extraction of Fe and Ag, the activity in the aqueous phase is low and the measuring time has been long. Therefore, a correction has been done for decay during the time of measurement in order to compare the activity in the aqueous and organic phase of the same sample. Each correction can be made with a correction factor,  $f$ , which is defined as the ratio between the measured activity,  $A_m$ , to the corrected activity,  $A_0$ . The correction factor is defined as;

$$f_1 = \frac{1 - e^{-\lambda_i t_m}}{\lambda_i t_m} \quad 2.19$$

The two phases was not measured at the same time and a correction has also been done for decay between the start of the two measurements. The correction factor is defined as;

$$f_2 = e^{-\lambda_i t_s} \quad 2.20$$

Both corrections has been taken into account yielding equation 2.21.

$$A_0 = \frac{A_m}{f_1 \cdot f_2} = A_m \cdot \frac{\lambda_i t_m}{1 - e^{-\lambda_i t_m}} e^{\lambda_i t_s} \quad 2.21$$

$$\lambda_i = \frac{\ln 2}{t_{1/2}} \quad 2.22$$

where  $A_m$  is the measured activity (Bq)  
 $A_0$  is the corrected activity (Bq)  
 $\lambda_i$  is the decay constant for measured nuclide ( $s^{-1}$ )  
 $t_s$  is the time between the start of the two measurements (s)  
 $t_m$  is the measuring time (s)  
 $t_{1/2}$  is the half-life for the nuclide (s)

### 3. Experimental

#### 3.1 Materials

Aldrich provided 2,2':6',2''-terpyridine (terpyridine), 98 % purity, and *tert*-butylbenzene (TBB), 99 % purity. 2-bromodecanoic acid (HA), 98 % purity, and nitric acid, p.a. grade, was purchased from Fluka.

#### 3.2 Radionuclides

The radionuclides used in the experiments were either available at the department ( $^{60}\text{Co}$ ,  $^{137}\text{Cs}$ ,  $^{233}\text{U}$ ) or bought ( $^{110\text{m}}\text{Ag}$  and  $^{59}\text{Fe}$ ).  $^{110\text{m}}\text{Ag}$  was provided by Isotoplaboratoriet, Forskningscenter Risø and  $^{59}\text{Fe}$  was bought from Amersham Pharmacia Biotech.

#### 3.3 Preparation of $^{233}\text{U}$ , $^{59}\text{Fe}$ , $^{60}\text{Co}$ , and $^{137}\text{Cs}$ tracer solutions

The stock solutions of  $^{233}\text{U}$ ,  $^{59}\text{Fe}$ ,  $^{60}\text{Co}$  and  $^{137}\text{Cs}$  were converted to nitric acid solution from hydrochloric acid solution. Stock solution, 0.1 ml, of radionuclide solution, and 2 ml 3 M nitric acid was added to a small beaker on a heating plate and the solution was evaporated. The procedure was performed two more times and the last time the solution was evaporated until dryness. The beaker was removed from the heater and allowed to cool down. Thereafter, the residue was dissolved in 0.5 ml 0.1 M nitric acid.

#### 3.4 Titration of radioactive tracers

To determine the nitric acid concentration of the converted  $^{233}\text{U}$ ,  $^{59}\text{Fe}$ ,  $^{60}\text{Co}$  and  $^{137}\text{Cs}$  tracer solutions, the tracer solutions were titrated with an ABU 91 Auto Burette connected to a PC. A titration solution of 0.01 M sodium hydroxide was prepared. At each titration 25  $\mu\text{l}$  tracer solution ( $V_{\text{rad}}$ ) and 40 ml MilliQ-water ( $V_{\text{aq}}$ ) was added to a beaker and was titrated with the titration solutions. The potential (E) in mV was measured and the Gran-function, [Ros65], equation 3.1, was used to calculate  $F_1$ .

$$F_1 = (V_{\text{aq}} + V_{\text{rad}}) \cdot 10^{E/59.16} \quad 3.1$$

With the calculated values of  $F_1$ , a linear regression was performed and  $F_{1,\text{calc}}$  was calculated according to;

$$F_{1,\text{calc}} = kV + m \quad 3.2$$

where  $k$  and  $m$  are the fitted constants and  $V$  is the volume of added sodium hydroxide in ml. For,  $F_{1,\text{calc}} = 0$ , the added volume,  $V$ , of 0.01 M sodium hydroxide at pH 7 can be calculated with equation 3.2.

Thus, the nitric acid concentration of the stock solution ( $c_{rad}$ ) could be calculated according to 3.3.

$$c_{rad} = \frac{c_{NaOH} \cdot V_{NaOH}}{V_{rad}} \quad 3.3$$

### **3.5 Determination of extraction curves for different nitric acid concentrations with constant concentrations of 2,2':6',2''-terpyridine and 2-bromodecanoic acid in *tert*-butylbenzene**

The nitric acid concentration range under study was 0.01 - 0.4 M. Aqueous phase, 0.99 ml, of different nitric acid concentration, 1 ml of the organic phase, 0.02 M terpyridine, 1 M HA in TBB and 10  $\mu$ l radioactive tracer solution was added to a 3 ml test tube. The test tubes were shaken vigorously for five minutes with Ag, Co, Cs and U, and for 2 hours with Fe at room temperature. The longer time of shaking for Fe is due to slower rate to reach equilibrium. During this time equilibrium is reached between the two phases. Thereafter, the test tubes were centrifuged at 4500 rpm for five minutes. Depending on the radionuclide under study different volumes of samples, 0.05-0.8 ml, of the aqueous phase and the organic phase were taken and measured radiometrically. For the preparation of the samples before measuring see section 3.10.1.

### **3.6 Determination of extraction curves for constant nitric acid concentration with different concentrations of 2,2':6',2''-terpyridine and constant 2-bromodecanoic acid concentration in *tert*-butylbenzene**

The terpyridine concentration range under study was 0.0001 - 0.04 M and the nitric acid concentration in all experiment was 0.02 M. Aqueous phase, 0.99 ml, of suitable nitric acid concentration, 1 ml of the organic phase with different concentration of terpyridine and 1.0 M HA in TBB and 10  $\mu$ l radioactive tracer solution was added to a 3 ml test tube. The test tubes were shaken vigorously for 5 minutes with Ag, Co, Cs and U and 2 hours with Fe, a time which enables equilibrium between the two phases to be reached in room temperature. The test tubes were centrifuged at 4500 rpm for five minutes. Depending on the radionuclide under study different volumes of samples, 0.05-0.8 ml, of the aqueous phase and the organic phase were taken and measured radiometrically. For the preparation of the samples before measuring see section 3.10.1.

### **3.7 Determination of extraction curves for constant nitric acid concentration with different 2-bromodecanoic acid concentrations and constant 2,2':6',2''- terpyridine concentration in *tert*-butylbenzene**

The 2-bromodecanoic acid concentration range under study was 0.05 - 2.0 M and the nitric acid concentration in all experiment was 0.02 M. Nitric acid, 0.99 ml, 0.02M, 1 ml organic phase of suitable HA concentration in TBB, 0.02 M terpyridine and 10  $\mu$ l stock

solution was added to a 3 ml test tube. The tube was sealed and shaken vigorously in room temperature until equilibrium was reached, 5 min with Ag, Co, Cs and U and 2 hours with Fe. The test tubes were centrifuged at 4500 rpm for five minutes. Depending on the radionuclide under study different volumes of samples, 0.05-0.8 ml of the aqueous phase and the organic phase, were taken and added to measuring vials. For the preparation of the samples before measuring see section 3.10.1.

### **3.8 Determination of extraction curves for different nitric acid concentrations with constant concentration of 2-bromodecanoic acid in *tert*-butylbenzene**

The nitric acid concentration range under study was 0.01 - 0.4 M. Aqueous phase, 0.99 ml, of different nitric acid concentration, 1 ml of the organic phase, 1 M HA in TBB and 10 µl radioactive tracer solution was added to 3 ml test tubes. The test tubes were sealed and shaken at room temperature until equilibrium was reached, 5 min with Ag, Co, Cs and U and 2 hours with Fe. The test tubes were centrifuged at 4500 rpm for five minutes. Depending on the radionuclide under study different volumes, 0.05-0.8 ml, of the two phases were withdrawn and added to measuring vials and measured radiometrically. For the preparation of the samples before measuring see section 3.10.1.

### **3.9 Determination of extraction curve for $^{137}\text{Cs}$ for constant nitric acid concentration with different concentration of 2-bromodecanoic acid in *tert*-butylbenzene**

The HA concentration range in the experiments were 0.05 - 2.0 M and the nitric acid concentration was 0.02 M. Nitric acid, 0.99 ml, 0.02 M, 1 ml organic phase of suitable 2-bromodecanoic acid concentration in TBB and 10 µl stock solution of  $^{137}\text{Cs}$  was added to a 3 ml test tube. The tubes were shaken vigorously for 5 minutes, a time which enables equilibrium to be reached in room temperature. The test tubes were centrifuged for five minutes at 4500 rpm. Samples of 0.5-0.8 ml of the organic phase and 0.05 ml of the aqueous phase were added to measuring vials and measured radiometrically. For the preparation of the samples before measuring see section 3.10.1.

## **3.10 Measuring conditions**

### **3.10.1 Preparation of sample before measuring**

To achieve equal detector geometry, aqueous and organic liquid was added to yield a total volume of 2 ml in all samples, except for the uranium samples where 10 ml Hionic-fluor scintillation liquid was added. Depending on the radionuclide under study different detectors were used, see section 3.10.2-3.10.6, to determine the distribution ratio.

### 3.10.2 Uranium

The radionuclide  $^{233}\text{U}$  disintegrates by emitting  $\alpha$ -particles with energies of 4729.2 keV (1.6 %), 4783.0 keV (13.2 %) and 4824.7 keV (84.4 %). The half-life is  $1.592 \cdot 10^5$  year. Measurement was made by a LKB Wallac 1219 Rackbeta Liquid Scintillation Counter. The measuring times varied between 5 minutes and 1 hour.

### 3.10.3 Iron

$^{59}\text{Fe}$  has  $\gamma$ -energies at 142.652 keV (1.02 %), 192.349 (3.08 %), 1099.251 keV (56.5 %) and 1291.596 keV (43.2 %). The  $\gamma$ -energy at 1099.251 keV was used and measured by a high purity germanium (HPGe) detector. The half-life is 44.496 days. A compensation has been done for disintegration during measurement and for the different times of measurement, see section 2.4.

### 3.10.4 Cobalt

The radionuclide  $^{60}\text{Co}$  has  $\gamma$ -energies at 1173.237 keV (99.90 %) and 1332.501 keV (99.9824 %). The  $\gamma$ -energy at 1173.237 keV was used and measured by a high purity germanium (HPGe) detector. The measuring times varied between 6 minutes and 72 hours. The half-life for  $^{60}\text{Co}$  is 5.272 years.

### 3.10.5 Cesium

The radionuclide  $^{137}\text{Cs}$  has  $\gamma$ -energies at 31.817 keV (2.05 %), 32.194 keV (3.77 %), 36.357 keV (1.04 %) and 661.660 keV (85.21 %). The half-life is 30.17 year. The  $\gamma$ -energy at 661.660 keV was measured by a high purity germanium (HPGe) detector. The measuring times varied between 2.5 minutes and 3 hours.

### 3.10.6 Silver

The radionuclide  $^{110\text{m}}\text{Ag}$  has a half-life of 249.76 days. Compensation for both disintegration during measurement and for the different times of measurement were made, see section 2.4.  $^{110\text{m}}\text{Ag}$  has  $\gamma$ -energies at 657.7617 keV (94.6 %), 677.6218 keV (10.36 %), 687.013 keV (6.44 %), 706.6808 keV (16.4 %), 744.276 keV (4.7 %), 763.943 keV (22.3 %), 818.030 keV (7.31 %), 884.684 keV (72.7 %), 937.492 keV (34.4 %) 1384.2979 keV (24.3 %), 1475.786 keV (4.02 %), 1505.038 keV (13.0 %), 1562.300 keV (1.003 %). The  $\gamma$ -energy at 657.7617 keV was used and measured by a HPGe-detector. The measuring times varied between 8 minutes and 73 hours.

## 4. Results and discussion

### 4.1 Uranium

#### 4.1.1 Uranium extraction with 2-bromodecanoic acid

The aqueous solution contains uranium on the form  $UO_2^{2+}$  which is extracted by 2-bromodecanoic acid, (HA), into the organic phase. As can be seen in Appendix 3 the slope of the curve in the figure is 2 which tells us that two HA molecules will participate in the reaction. The slope of the curve in the figure in Appendix 4 where the nitric acid concentration is changed is -2 and the extracted specie is probably  $UO_2A_2$ .



The extraction coefficient,  $k_{ex,U,HA}$ , can be calculated according to equation 4.2.

$$k_{ex,U,HA} = \frac{[\overline{UO_2A_2}] \cdot [H^+]^2}{[UO_2^{2+}] \cdot [(\overline{HA})_2]} \quad 4.2$$

which can be reformulated;

$$k_{ex,U,HA}'' = \frac{\sum_{i=1}^N D_{U,HA,i} \cdot \frac{[H^+]_i^2}{[\overline{HA}]_i^2}}{N} \quad 4.3$$

where  $D_{U,HA,i}$  is the distribution ratio for uranium extracted with 2-bromodecanoic acid

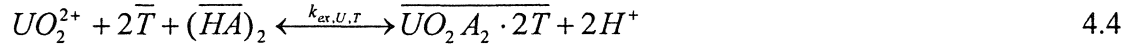
$[H^+]_i$  is the concentration of  $H^+$  in the aqueous phase (M)

$[\overline{HA}]_i$  is the concentration of 2-bromodecanoic acid in the organic phase (M)

#### 4.1.2 Uranium extraction with 2,2':6',2''-terpyridine and 2-bromodecanoic acid

The  $UO_2^{2+}$ -ion can form different complexes with terpyridine. In the figure with increasing terpyridine concentrations, Appendix 2, the distribution ratio increase exponentially with a maximum slope of 2. The conclusions from this figure is that  $UO_2^{2+}$  can form a complex with 0, 1 and 2 terpyridine molecules. In the figure with different nitric acid concentrations and constant terpyridine and HA concentration, Appendix 1, two different slopes of the curve can be seen. The slope -2 will appear when  $UO_2^{2+}$  form a complex with two terpyridine molecules and two  $A^-$ . The  $A^-$  could bound directly to the uranium ion or they could form an outer sphere complex.

When the nitric acid concentration increase the number of terpyridine decrease and the extracted specie is probably  $UO_2A_2 \cdot T$ . At 0.4 M nitric acid concentration the distribution ratio for extraction with a terpyridine and HA mixtures is approximately the same as the distribution ratio for extraction with only HA and the extracted specie is  $UO_2A_2$ . For the complex with 2 terpyridine molecules the reaction can be written as;



The extraction coefficient,  $k_{ex,U,T}$ , can be calculated according to equation 4.5;

$$k_{ex,U,T} = \frac{[\overline{UO_2A_2 \cdot 2T}] \cdot [H^+]^2}{[UO_2^{2+}] \cdot [\bar{T}]^2 \cdot [(\overline{HA})_2]} \quad 4.5$$

which can be reformulated;

$$k_{ex,U,T}'' = \frac{\sum_{i=1}^N D_{U,T,i} \cdot \frac{[H^+]_i^2}{[\bar{T}]_i^2 \cdot [\overline{HA}]_i^2}}{N} \quad 4.6$$

where  $D_{U,T,i}$  is the distribution ratio for uranium extracted with terpyridine and 2-bromodecanoic acid

$[H^+]_i$  is the concentration of  $H^+$  in the aqueous phase (M)

$[\overline{HA}]_i$  is the concentration of 2-bromodecanoic acid in the organic phase (M)

$[\bar{T}]_i$  is the concentration of terpyridine in the organic phase (M)

The increase in extraction when terpyridine is added can be seen in Figure 4.1. The distribution ratio from 0.01 M nitric acid is approximately 500 times higher when terpyridine is present.

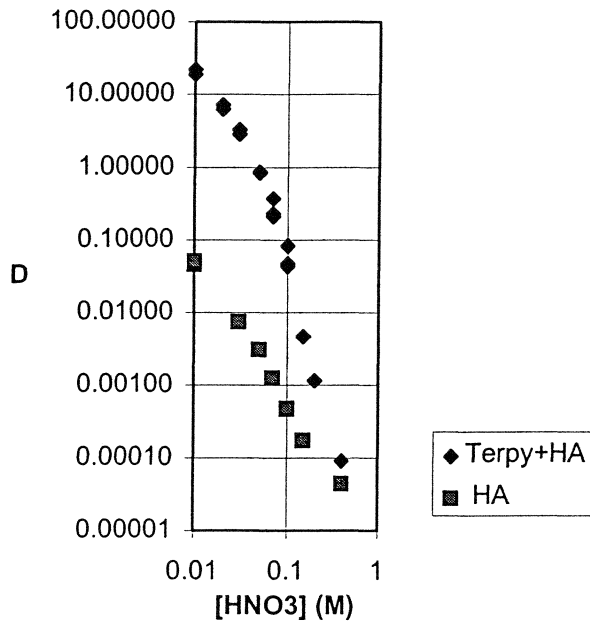


Figure 4.1 Distribution ratio for uranium with terpyridine and HA compared with HA from different nitric acid concentrations.

## 4.2 Iron

### 4.2.1 Iron extraction with 2-bromodecanoic acid

The time to reach equilibrium is longer for iron than for the other studied metals. In Appendix 8 it can be seen that the slope in the figure is -3 and probably three HA will participate in the reaction.



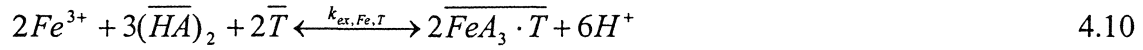
The extraction coefficient,  $k_{ex,Fe,HA}$ , can be calculated according to equation 4.8 where the ratio between the iron complex in the organic phase and the iron ion in the aqueous phase determine the distribution ratio,  $D_{Fe,HA,i}$ . If this is used equation 4.8 can be reformulated to equation 4.9.

$$k_{ex,Fe,HA} = \frac{[\overline{FeA}_3]^2 \cdot [H^+]^6}{[Fe^{3+}]^2 \cdot [(\overline{HA})_2]^3} \quad 4.8$$

$$k_{ex,Fe,HA}'' = \frac{\sum_{i=1}^N D_{Fe,HA,i}^2 \cdot \frac{[H^+]_i^6}{[\overline{HA}]_i^6}}{N} \quad 4.9$$

#### 4.2.2 Iron extraction with 2,2':6',2''-terpyridine and 2-bromodecanoic acid

The extraction of iron with a terpyridine - HA mixture is very high. As said earlier in section 4.2.1 three HA will participate in the reaction between  $Fe^{3+}$  and HA. From Appendix 6 it can be seen that there will probably be one terpyridine molecule in the extracted complex,  $FeA_3T$ . The distribution ratio is not so much influenced by the terpyridine concentration but more by the HA concentration when the nitric acid concentration is about 0.4 M.



The extraction coefficient,  $k_{ex,Fe,T}$ , can be calculated according to equation 4.11

$$k_{ex,Fe,T} = \frac{[\overline{FeA_3 \cdot T}]^2 \cdot [H^+]^6}{[Fe^{3+}]^2 \cdot [(\overline{HA})_2]^3 \cdot [\overline{T}]^2} \quad 4.11$$

This expression can be reformulated with help of the distribution ratio,  $D_{Fe,T,i}$ , for iron extracted with terpyridine and 2-bromodecanoic acid;

$$k_{ex,Fe,T}'' = \frac{\sum_{i=1}^N D_{Fe,T,i}^2 \cdot \frac{[H^+]_i^6}{[\overline{HA}]_i^6 \cdot [\overline{T}]_i^2}}{N} \quad 4.12$$

In Figure 4.2 the difference in distribution ratio when terpyridine is added to the organic phase can be seen. The distribution ratio for 0.01 M nitric acid is increased by a factor of 1000, the second largest increase for the studied metals.

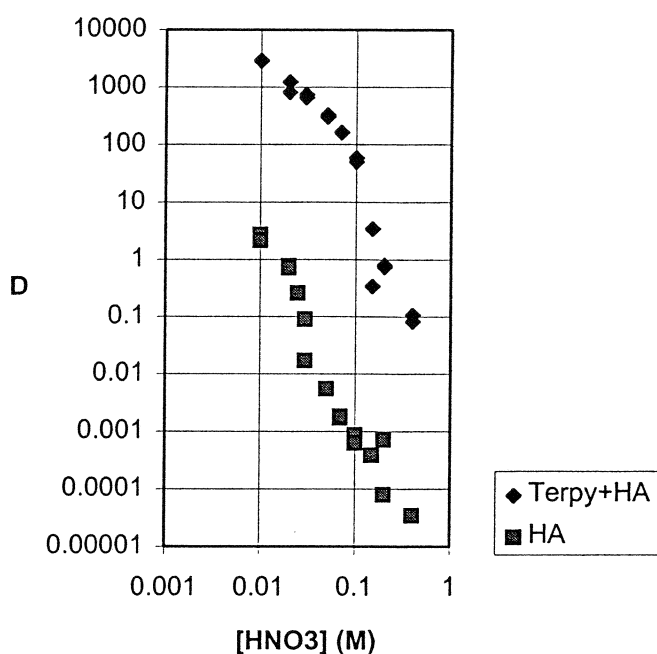
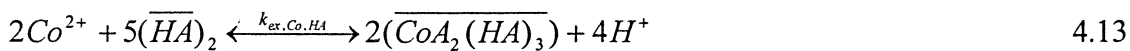


**Figure 4.2** Distribution ratio for iron with terpyridine and HA compared with HA from different nitric acid concentrations.

### 4.3 Cobalt

#### 4.3.1 Cobalt extraction with 2-bromodecanoic acid

To determine the extracted complex of cobalt is more complicated. The result in Appendix 9 implicates that the charge of the studied ion is +2 but it can also be +3. In the following discussion we suppose that the charge is +2. The dependency in the distribution ratio on the HA concentration is large, which can be seen in Appendix 11. However, the extracted specie could possibly be  $\text{CoA}_2(\text{HA})_3$ . The reaction of this specie can be written as;



and the extraction coefficient,  $k_{\text{ex,Co,HA}}$ , can be written as equation 4.14.

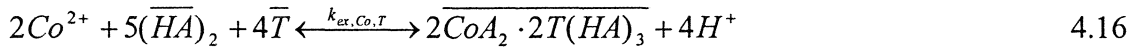
$$k_{\text{ex,Co,HA}} = \frac{[\overline{\text{CoA}_2(\text{HA})_3}]^2 \cdot [\text{H}^+]^4}{[\text{Co}^{2+}]^2 \cdot [(\overline{\text{HA}})_2]^5} \quad 4.14$$

The distribution ratio,  $D_{Co,HA,i}$ , for cobalt extracted with terpyridine and 2-bromodecanoic acid can be used in equation 4.14 and the new equation for the extraction coefficient is;

$$k_{ex,Co,HA}'' = \frac{\sum_{i=1}^N D_{Co,HA,i}^2 \cdot \frac{[H^+]_i^4}{[HA]_i^{10}}}{N} \quad 4.15$$

#### 4.3.2 Cobalt extraction with 2,2':6',2''-terpyridine and 2-bromodecanoic acid

As said earlier in section 4.3.1 there are some problem to determine the extracted specie of cobalt. There are both problem to determine the number of HA molecules and terpyridine molecules. It is probably two terpyridine molecules in the extracted specie, the uncertainty depends on that we are close to the plateau for the distribution ratio in the studied terpyridine interval, which can be seen in the figure in Appendix 10.



The extraction coefficient,  $k_{ex,Co,HA}$ , can be written as;

$$k_{ex,Co,T} = \frac{[\overline{CoA_2} \cdot 2\overline{T(HA)_3}]^2 \cdot [H^+]^4}{[Co^{2+}]^2 \cdot [(\overline{HA})_2]^5 \cdot [\overline{T}]^4} \quad 4.17$$

This equation can be reformulated to equation 4.18.

$$k_{ex,Co,T}'' = \frac{\sum_{i=1}^N D_{Co,T,i}^2 \cdot \frac{[H^+]_i^4}{[\overline{HA}]_i^{10} \cdot [\overline{T}]_i^4}}{N} \quad 4.18$$

As can be seen in Figure 4.3 the distribution ratio increases with at least a factor of 1000 in the entire studied nitric acid interval. At 0.01 M nitric acid the factor is  $10^5$  and this increase is the highest for the studied metals.

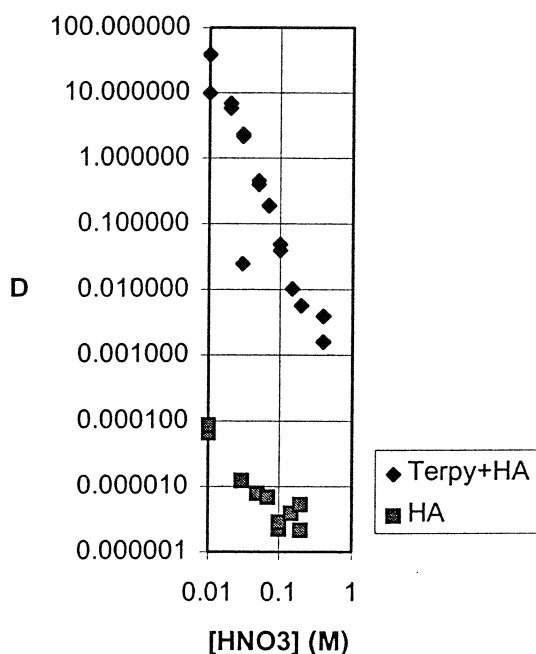
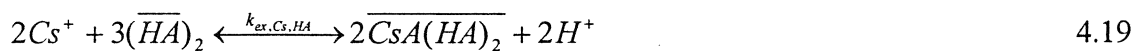


Figure 4.3 Distribution ratio for cobalt with terpyridine and HA compared with HA from different nitric acid concentrations.

## 4.4 Cesium

### 4.4.1 Cesium extraction with 2-bromodecanoic acid

Cs is extracted with 2-bromodecanoic acid dissolved in TBB. From Appendix 14 it can be seen that three HA will participate in the reaction but only one of them will appear as  $A^-$  in the extracted complex which can be seen in Appendix 15. The reaction can be written as;



The extraction coefficient,  $k_{ex,Cs,HA}$ , can be calculated according to equation 4.20.

$$k_{ex,Cs,HA} = \frac{[\overline{CsA(HA)_2}]^2 \cdot [H^+]^2}{[Cs^+]^2 \cdot [(\overline{HA})_2]^3} \quad 4.20$$

The equation 4.20 can be converted to equation 4.21, where  $D_{Cs,HA,i}$  is the distribution ratio for cesium extracted with 2-bromodecanoic acid.

$$k''_{ex,Cs,HA} = \frac{\sum_{i=1}^N D_{Cs,HA,i}^2 \cdot \frac{[H^+]_i^2}{[HA]_i^6}}{N} \quad 4.21$$

#### 4.4.2 Cesium extraction with 2,2':6',2''-terpyridine and 2-bromodecanoic acid

The distribution ratio for each nitric acid concentration in Appendix 13 and Appendix 15 are equal, also shown in Figure 4.4, and the conclusion is that cesium is not extracted with terpyridine. The reason to this can be the larger ionic-radius for  $Cs^+$  than for the other studied metal ions.

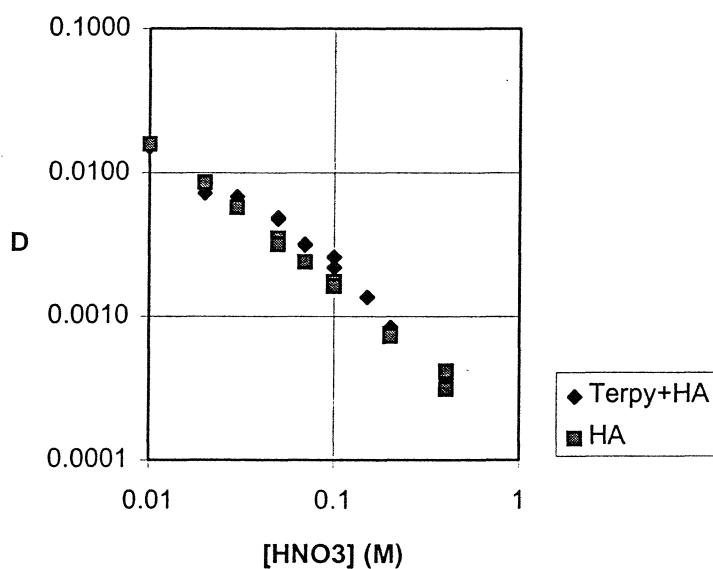


Figure 4.4 Distribution ratio for cesium with terpyridine and HA compared with HA from different nitric acid concentrations.

## 4.5 Silver

### 4.5.1 Silver extraction with 2-bromodecanoic acid

The slope of the curve in Appendix 18 is two, which tells us that two HA molecules will participate in the reaction between silver and HA. From the figure in Appendix 19 it can be seen that one of the HA will appear as  $A^-$  in the extracted complex. The reaction can be written as;



The extraction coefficient,  $k_{ex,Ag,HA}$ , can be calculated according to equation 4.23 which can be reformulated to equation 4.24;

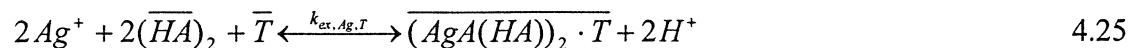
$$k_{ex,Ag,HA} = \frac{[\overline{AgA(HA)}] \cdot [H^+]}{[Ag^+] \cdot [(\overline{HA})_2]} \quad 4.23$$

$$k_{ex,Ag,HA}'' = \frac{\sum_{i=1}^N D_{Ag,HA,i} \frac{[H^+]_i}{[\overline{HA}]_i^2}}{N} \quad 4.24$$

where  $D_{Ag,HA,i}$  is the distribution coefficient for silver extracted with terpyridine and 2-bromodecanoic acid.

### 4.5.2 Silver extraction with 2,2':6',2''-terpyridine and 2-bromodecanoic acid

As said earlier in section 4.5.1, two HA will participate in the reaction between silver and HA. The curve in the figure in Appendix 17 shows that one terpyridine molecule will bound two silver, due to the slope of 0.5.



the extraction coefficient,  $k_{ex,Ag,T}$ , can be calculated according to equation 4.26;

$$k_{ex,Ag,T} = \frac{[\overline{(AgA(HA))_2 \cdot T}] \cdot [H^+]^2}{[Ag^+]^2 \cdot [\overline{T}] \cdot [(\overline{HA})_2]^2} \quad 4.26$$

which can be reformulated;

$$k_{ex,Ag,T}'' = \frac{\sum_{i=1}^N D_{Ag,T,i} \frac{[H^+]_i^2}{[HA]_i^4 [T]_i}}{N} \quad 4.27$$

where  $D_{Ag,T,i}$  is the distribution coefficient for silver extracted with terpyridine and 2-bromodecanoic acid.

The distribution ratio for silver is higher when terpyridine is present, see Figure 4.5, at lower nitric acid concentrations. However, the distribution ratio is only a factor 10-100 times higher compared to extraction with HA. This is the smallest increase, apart from cesium where no increase at all can be seen, for the studied metals.

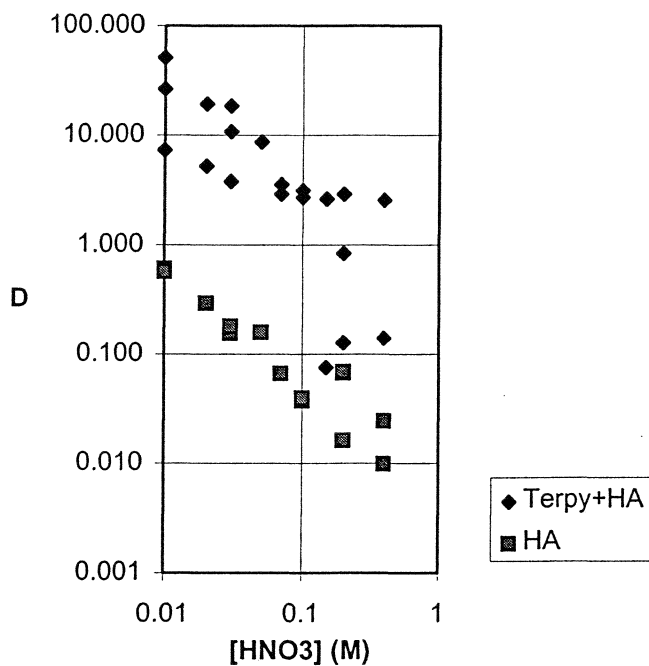
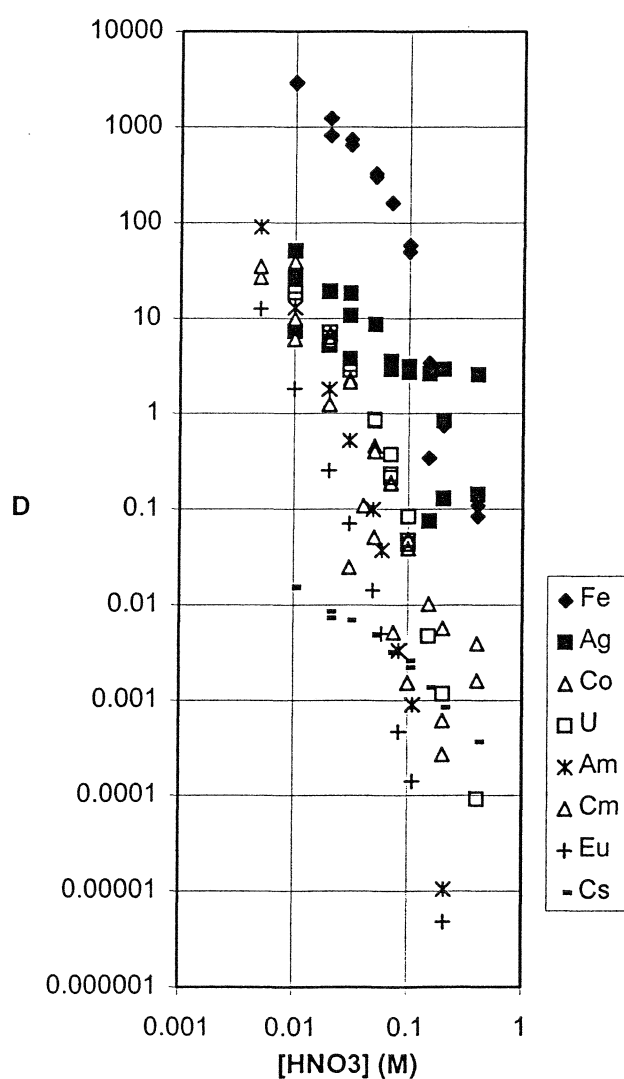


Figure 4.5 Distribution ratio for silver with terpyridine and HA compared with HA from different nitric acid concentrations.

#### 4.6 Separation process possibilities

In Figure 4.6, the distribution ratio for a number of metals are shown with the terpyridine and HA mixture. Iron is extracted to the largest extent followed by silver, cobalt, uranium, americium, curium, europium and cesium at 0.01 M nitric acid. For the SANEX process, separation of trivalent actinides from lanthanides, to function then iron, silver, cobalt and uranium has to be removed first, alternatively not be present in the feed. The separation factor between iron, silver, uranium and cobalt from americium are 54 000, 1 100, 90 and 63 respectively at 0.07 M nitric acid. These separation factors are larger or much larger than the separation factor between curium and europium which is 7 [Spj99]. Furthermore, for nitric acid concentrations lower than 0.07 M cesium will follow the lanthanides and thus, causes no trouble in a separation process.



**Figure 4.6** Distribution ratios for Fe, Ag, Co, U, Am, Cm, Eu and Cs extracted with terpyridine and HA from different nitric acid concentrations. Data for Am, Cm and Eu from [Spj].

In Figure 4.7 the distribution ratios for extraction with HA is shown. These are all lower, except for Cs, compared to when terpyridine is present. At 0.01 M nitric acid the order of extraction are iron, silver, uranium, americium, cesium, europium and cobalt. The differences in order compared to for extraction with terpyridine and HA are that cobalt is now the less extracted metal and cesium is more extracted than europium. The order at 0.1 M nitric acid is on the other hand a bit different compared to 0.01 M nitric acid with silver being extracted the most and then follows cesium > iron > uranium > americium and europium > cobalt.

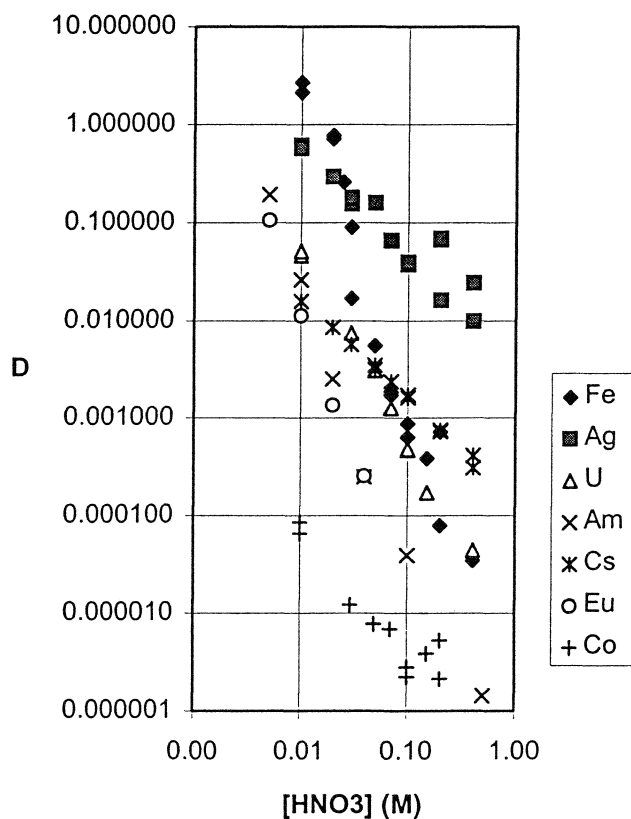


Figure 4.7 Distribution ratios for Fe, Ag, Co, U, Am, Eu and Cs extracted with HA from different nitric acid concentrations. Data for Am, Cm and Eu from [Spj].

## 5. Conclusions

### 5.1 Determined extracted complexes

For uranium the extracted species are  $\text{UO}_2\text{A}_2 \cdot 2\text{T}$ ,  $\text{UO}_2\text{A}_2 \cdot \text{T}$  and  $\text{UO}_2\text{A}_2$ . When the nitric acid concentration increase the number of terpyridine ligands decreases. For the extraction without terpyridine the extracted specie is  $\text{UO}_2\text{A}_2$ .

The extraction of iron with the terpyridine and 2-bromodecanoic acid mixture is very high, but the time to reach equilibrium is longer than for uranium, cobalt, cesium and silver. The extracted species are  $\text{FeA}_3 \cdot \text{T}$ , when terpyridine is present, and otherwise  $\text{FeA}_3$ .

There are some problem to determine the extracted specie of cobalt but they could possible be  $\text{CoA}_2(\text{HA})_3$ , no terpyridine present, and  $\text{CoA}_2(\text{HA})_3 \cdot 2\text{T}$ , when terpyridine is added.

The distribution ratio for each nitric acid concentration when cesium is extracted from a mixture of terpyridine and 2-bromodecanoic acid or with only 2-bromodecanoic acid is approximately the same. The extracted complex is  $\text{CsA}(\text{HA})_2$ .

The extracted specie for silver is  $(\text{AgA}(\text{HA}))_2 \cdot \text{T}$  but when the nitric acid concentration increases the extracted specie may be of the type  $\text{AgAHA}$ . The complex  $\text{AgAHA}$  is the extracted complex when no terpyridine is added.

### 5.2 Possibilities for separation

Iron and silver could be separated from the other studied metals at 0.1 M nitric acid. After this cobalt and uranium can be separated from americium, curium, europium and cesium at approximately 0.03 M nitric acid. Cobalt and uranium can be separated from each other if extraction without terpyridine is used. At nitric acid concentrations lower than 0.07 M cesium will follow the lanthanides in the separation and does not interfere in the separation between trivalent actinides and lanthanides.

## 6. Future work

Determination of the distribution ratio for more metals which is present in the feed to the SANEX process.

Solve the problem with the recovery of terpyridine due to the transfer of terpyridine to the aqueous phase when the pH-value is low.

A process modeling of the SANEX process.

To follow the CHON-principle another acid than 2-bromodecanoic acid has to be found.

Extractants other than terpyridine has to be used which have higher separation factors between trivalent actinides and lanthanides.

## 7. Acknowledgements

*I would like to thank Prof. Jan-Olov Liljenzin for his help with all sorts of problems this work has caused me.*

*I would also like to thank Dr. Lena Spjuth with all help in the beginning of this work, without you the experimental work would not have been started yet.*

*Finally, I would like to thank all other people at the Department of Nuclear Chemistry for all help and all cakes during my time as diploma worker.*

*Charlotta Gustafsson*  
Charlotta Gustafsson

## 8. References

- [Bau93] BAUDIN G., LEFEVRE J., PRUNIER C., SALVATORES M., *IAEA REPORT; Vienna* 29 November to 2 December 1993
- [Cho95] CHOPPIN G., RYDBERG J., LILJENZIN J.O., *RADIOCHEMISTRY and NUCLEAR CHEMISTRY, 2nd Edition of Nuclear Chemistry Theory and Applications* 1995
- [[Eva64] EVANS R.C., *Crystal chemistry, ed. 2* The University Press, Cambridge, 1964
- [Gre59] GREEN JACK, *Geochemical table of the elements for 1959*, Bull. Geol. Soc. Am. 70:1127-1184, 1959
- [Hag99] HAGSTRÖM I., SPJUTH L., ENARSSON Å., LILJENZIN J.O., SKÅLBERG M., HUDSON M.J., IVESON P.B., MADIC C., CORDIER P.Y., HILL C., FRANCOIS N., *Synergistic solvent extraction of trivalent americium and europium by 2-bromodecanoic acid and neutral nitrogen-containing reagents*, Solvent extraction and ion exchange, 17(2), 221-242, 1999
- [Häg63] HÄGG G., *Allmän och oorganisk kemi*, 1963
- [Mad94] MADIC C., BOURGES J., DOZOL J-F., *International Conference on Accelerator-Driven Transmutation Technologies and Applications*, Las Vegas 1994
- [Mad98] MADIC C., HUDSON M.J. *EUR 18038*, 1998
- [Mus92] MUSIKAS C., SHULZ W., Chapter 11 in *Principles and Practices of Solvent Extraction*, editors RYDBERG J., MUSIKAS C., CHOPPIN G.R., Marcel Dekker Inc., 1992
- [Pau60] PAULING LINUS, *The nature of Chemical Bond, ed. 3* Cornell University Press, Ithaca, N.Y., 1960
- [Ros65] ROSSOTTI F.J.C., ROSSOTTI H., *J. Chem. Education*, 42(7), 375-378, 1965
- [Ryd92] RYDBERG J., MUSIKAS C., CHOPPIN G.R., *Principles and Practices of Solvent Extraction*, Marcel Dekker Inc., 1992
- [Sch84] SCHILT A.A., WONG S.W., *J. Coord. Chem.* 13, 33, 1990
- [Skå95] SKÅLBERG M., LANDGREN A., SPJUTH L., LILJENZIN J.O., GUDOWSKI W., *Swedish Nuclear Fuel and Waste Management Co., SKB Technical Report TR-95-32*, 1995
- [Spj] Personal communications with Spjuth L.
- [Spj99] SPJUTH L., *Solvent Extraction Studies with Substituted Malonamides and Oligopyridines*, Department of Nuclear Chemistry, Chalmers University of Technology, 1999
- [Sto50] STOCKAR KLAUS, *Zur Kenntnis der Radien positiver Atomionen*, Helvetica Chimica Acta 33:1409-1420, 1950

[Vit84] VITORGE P., *Thesis*, Université Pierre et Marie Curie, CEA-R-5270, 1984

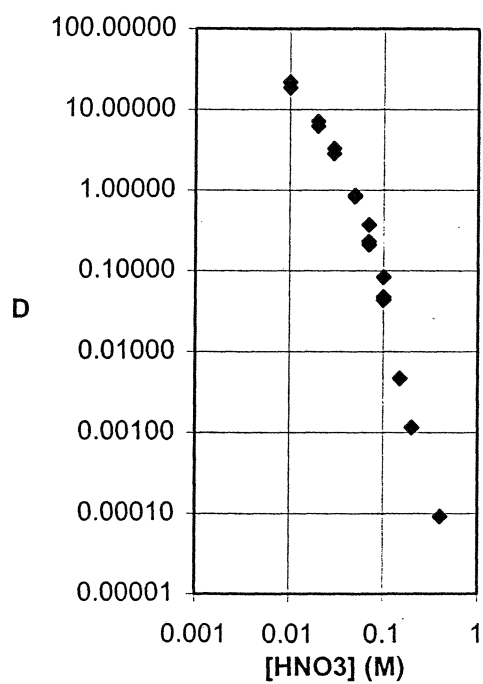
[Wyc31] WYCKOFF R.W.G., *The structure of crystals*, American Chemical Society Monograph, ed. 2, Chemical Catalog Co., Inc., New York, 1931

## Appendix 1

### Experimental distribution ratio for uranium

Experimental distribution ratio for uranium at some different nitric acid concentrations with 0.02 M 2,2':6',2''-terpyridine and 1.0 M 2-bromodecanoic acid in *tert*-butylbenzene.

[HNO <sub>3</sub> ] (M)	D
0.01	18.76
0.01	21.96
0.02	6.31
0.02	7.19
0.03	2.85
0.03	3.29
0.05	0.83
0.05	0.86
0.07	0.21
0.07	0.37
0.07	0.23
0.10	0.0831
0.10	0.0470
0.10	0.0432
0.15	0.004688
0.20	0.001162
0.40	0.000091

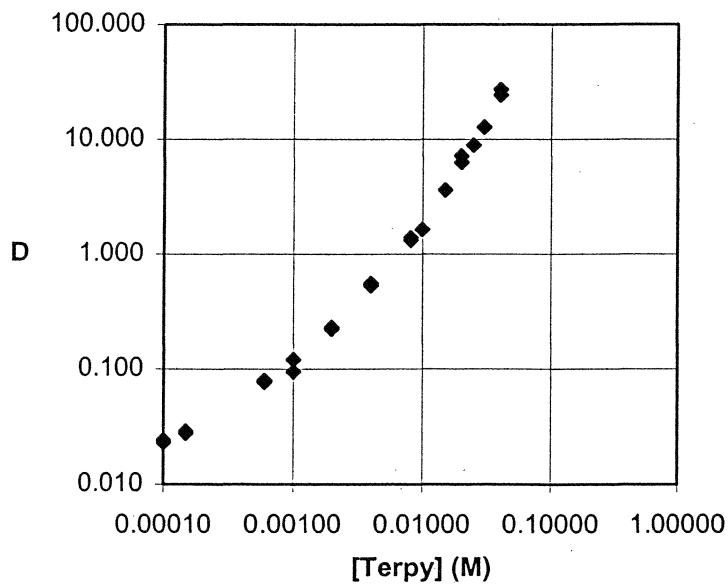


## Appendix 2

### Experimental distribution ratio for uranium

Experimental distribution ratio for uranium with different concentrations of 2,2':6',2''-terpyridine (Terpy) and 1 M 2-bromodecanoic acid in *tert*-butylbenzene from 0.02 M nitric acid.

[Terpy] (M)	D
0.00010	0.024
0.00010	0.023
0.00015	0.029
0.00015	0.028
0.0006	0.080
0.0006	0.077
0.0010	0.095
0.0010	0.121
0.0020	0.230
0.0020	0.222
0.0040	0.556
0.0040	0.530
0.0081	1.397
0.0081	1.327
0.0099	1.642
0.0150	3.615
0.0150	3.619
0.0200	6.309
0.0200	7.193
0.0249	8.874
0.0300	12.787
0.0401	24.391
0.0401	27.208

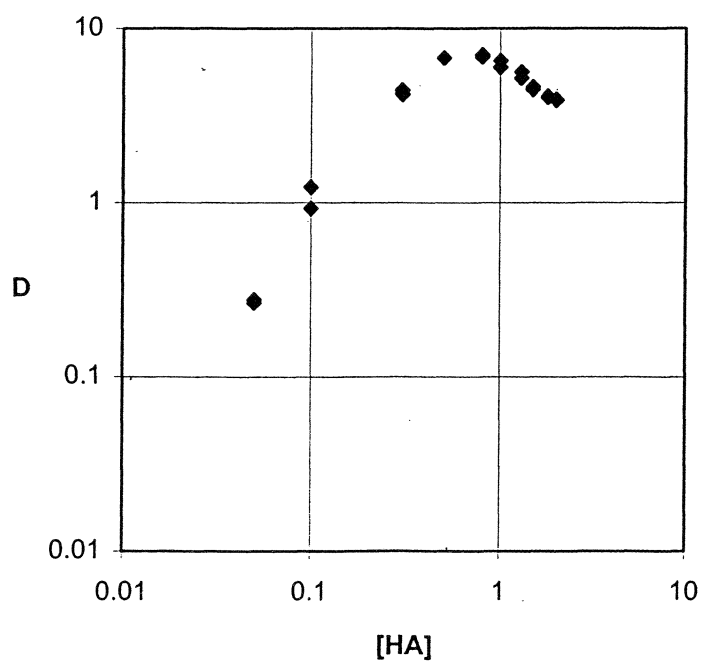


## Appendix 3

### Experimental distribution ratio for uranium

Experimental distribution ratio for uranium at some different 2-bromodecanoic acid, (HA), concentrations and 0.02 M 2,2':6',2''-terpyridine in *tert*-butylbenzene from 0.02 M nitric acid.

[HA] (M)	D
0.1	0.27
0.1	0.28
0.1	0.93
0.1	1.23
0.3	4.43
0.3	4.22
0.5	6.79
0.5	6.79
0.8	7.06
0.8	6.87
1.0	6.01
1.0	6.54
1.3	5.19
1.3	5.63
1.5	4.63
1.5	4.48
1.8	4.08
1.8	4.03
2.0	3.88
2.0	3.92

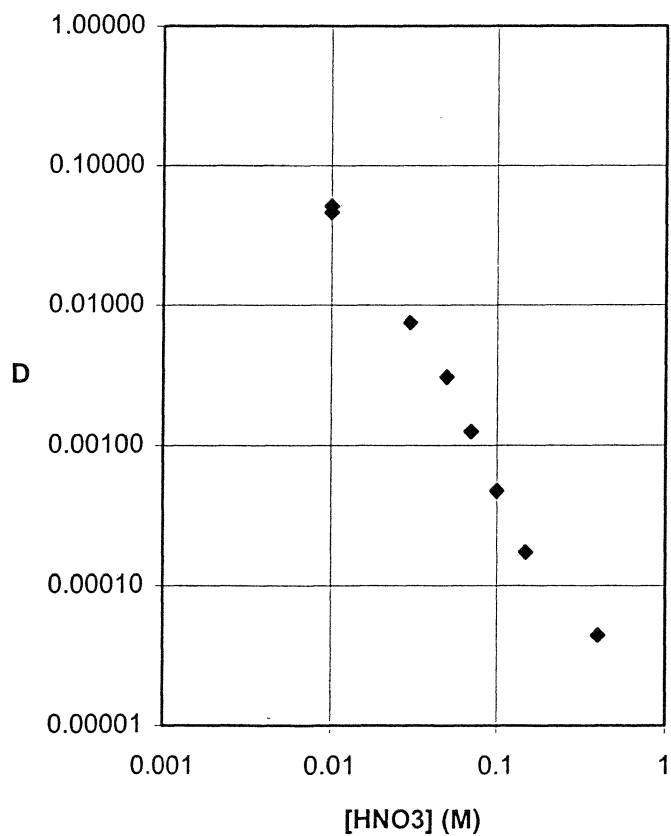


## Appendix 4

### Experimental distribution ratio for uranium

Experimental distribution ratio for uranium at some different nitric acid concentrations with 1.0 M 2-bromodecanoic acid in *tert*-butylbenzene.

[HNO <sub>3</sub> ] (M)	D
0.01	0.0462
0.01	0.0512
0.03	0.0075
0.05	0.003070
0.07	0.001255
0.10	0.000469
0.10	0.000476
0.15	0.000172
0.40	4.43E-05

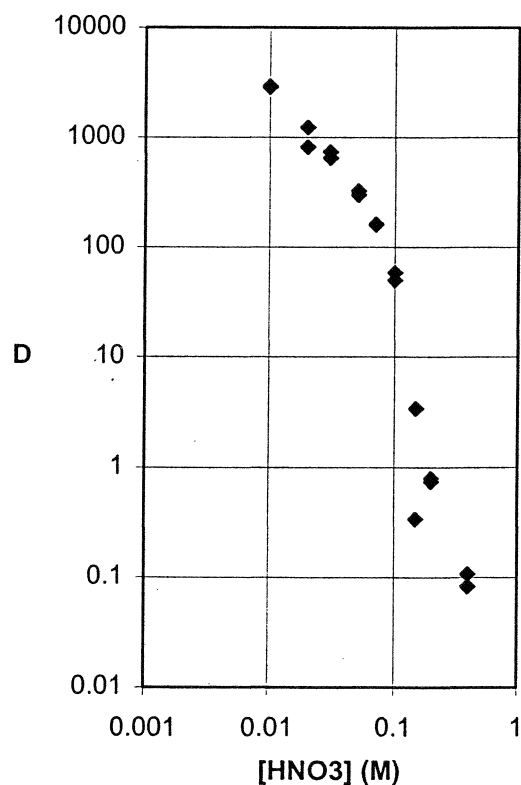


## Appendix 5

### Experimental distribution ratio for iron

Experimental distribution ratio for iron at some different nitric acid concentrations with 0.02 M 2,2':6',2''-terpyridine and 1.0 M 2-bromodecanoic acid in *tert*-butylbenzene.

[HNO <sub>3</sub> ] (M)	D	D <sub>min</sub>	D <sub>max</sub>	Error in D %	SigmaD %
0.01	2861.49	2799.21	2925.74	2.21	1.69
0.01	2918.33	2867.17	2970.69	1.77	1.31
0.02	1232.34	1215.22	1249.69	1.40	0.99
0.02	816.19	803.08	829.55	1.62	1.16
0.03	738.58	727.75	749.61	1.48	1.06
0.03	650.54	642.72	658.49	1.21	0.92
0.05	326.44	323.10	329.83	1.03	0.73
0.05	299.95	295.85	304.10	1.37	0.99
0.07	160.97	159.08	162.88	1.18	0.88
0.07	162.08	159.32	164.90	1.72	1.27
0.10	49.86	49.32	50.39	1.07	0.84
0.10	58.38	57.77	59.01	1.06	0.83
0.15	0.340	0.335	0.345	1.52	1.09
0.15	3.42	3.40	3.43	0.49	0.39
0.20	0.743	0.734	0.753	1.29	0.93
0.20	0.795	0.786	0.804	1.10	0.78
0.40	0.107	0.106	0.109	1.01	0.71
0.40	0.083	0.083	0.084	0.90	0.66

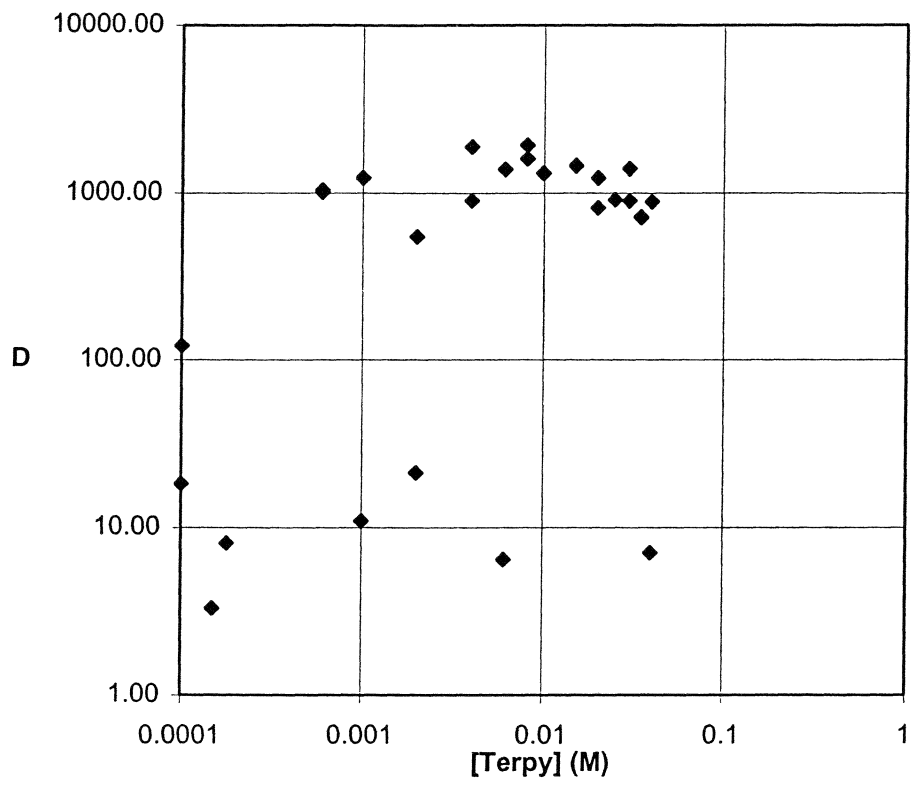


## Appendix 6

### Experimental distribution ratio for iron

Experimental distribution ratio for iron with different concentrations of 2,2':6',2''-terpyridine (Terpy) and 1 M 2-bromodecanoic acid in *tert*-butylbenzene from 0.02 M nitric acid.

[Terpy] (M)	D	D <sub>min</sub>	D <sub>max</sub>	Error in D %	SigmaD %
0.0001	18.33	18.09	18.56	1.27	0.91
0.0001	121.37	118.74	124.08	2.20	1.61
0.00015	3.32	3.28	3.36	1.21	0.87
0.00018	8.09	7.99	8.19	1.22	0.88
0.0006	1044.42	1024.88	1064.46	1.89	1.42
0.0006	1010.87	988.56	1033.86	2.24	1.68
0.001	10.98	10.87	11.08	0.97	0.71
0.001	1228.62	1193.88	1264.97	2.89	2.34
0.002	21.33	21.10	21.57	1.10	0.78
0.002	546.77	534.73	559.22	2.24	1.75
0.004	1892.35	1845.49	1941.06	2.53	2.02
0.004	903.24	886.36	920.52	1.89	1.38
0.0061	1386.43	1347.52	1427.04	2.87	2.25
0.0061	6.46	6.38	6.54	1.29	0.92
0.0081	1933.39	1894.67	1973.13	2.03	1.49
0.0081	1602.54	1555.42	1651.86	3.01	2.39
0.0099	1316.49	1292.03	1341.63	1.88	1.45
0.0099	1316.49	1292.03	1341.63	1.88	1.45
0.015	1460.32	1425.94	1495.91	2.40	1.85
0.015	1445.28	1421.00	1470.36	1.71	1.63
0.02	1232.34	1215.22	1249.69	1.40	0.99
0.02	816.19	803.08	829.55	1.62	1.16
0.0249	911.77	901.46	922.19	1.14	0.80
0.0249	910.59	900.30	920.99	1.14	0.80
0.03	1397.06	1368.71	1426.26	2.06	1.59
0.03	899.58	877.79	922.13	2.46	1.88
0.0349	710.49	698.21	723.05	1.75	1.30
0.0349	721.53	710.26	732.97	1.57	1.11
0.0401	887.42	870.24	905.06	1.96	1.47
0.0401	7.09	6.58	7.62	7.37	6.23

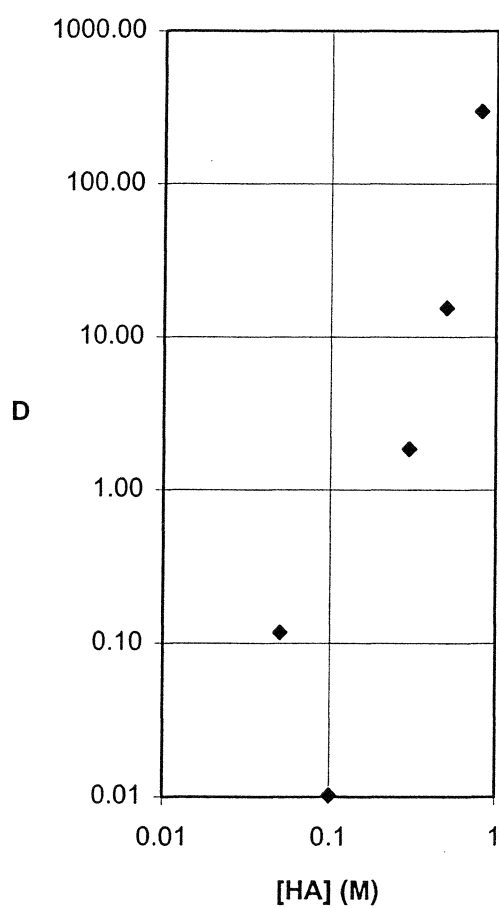


## Appendix 7

### Experimental distribution ratio for iron

Experimental distribution ratio for iron at some different 2-bromodecanoic acid (HA) concentrations and 0.02 M 2,2':6',2''-terpyridine in *tert*-butylbenzene from 0.02 M nitric acid.

[HA] (M)	D	D <sub>min</sub>	D <sub>max</sub>	Error in D %	SigmaD %
0.05	0.12	0.12	0.120	1.75	1.27
0.1	0.010	0.010	0.010	1.38	0.97
0.3	1.86	1.84	1.879	1.02	0.79
0.5	15.43	15.28	15.573	0.94	0.86
0.8	298.45	293.26	303.769	1.76	1.31

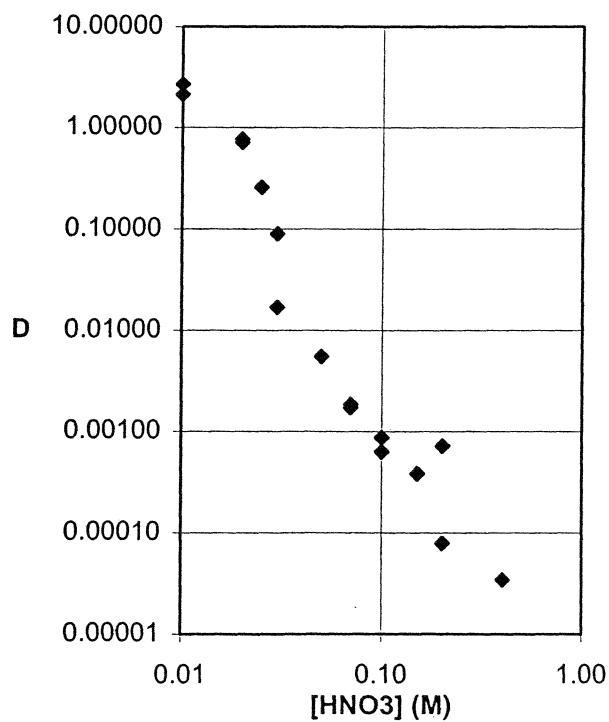


## Appendix 8

### Experimental distribution ratio for iron

Experimental distribution ratio for iron at some different nitric acid concentrations with 1.0 M 2-bromodecanoic acid in *tert*-butylbenzene.

[HNO <sub>3</sub> ] (M)	D	D <sub>min</sub>	D <sub>max</sub>	Error in D %	SigmaD %
0.01	2.69	2.649	2.741	1.70	1.21
0.01	2.13	2.107	2.149	0.99	0.70
0.02	0.77	0.76	0.78	1.55	1.10
0.02	0.71	0.708	0.72	0.91	0.65
0.03	0.26	0.26	0.26	1.12	0.86
0.03	0.0170	0.0169	0.0171	0.62	0.54
0.03	0.0896	0.0885	0.0906	1.16	0.82
0.05	0.0055	0.0055	0.0056	1.42	1.16
0.07	0.0017	0.0016	0.0018	6.24	5.67
0.07	0.001848	0.0018	0.0019	1.54	1.16
0.10	0.000872	0.0008	0.0010	10.12	9.70
0.10	0.000630	0.0006	0.0006	1.34	1.02
0.15	0.000385	0.0003	0.0005	22.75	22.28
0.20	0.000717	2.50E-04	0.0012	69.05	63.36
0.20	0.000079	7.66E-05	8.15E-05	3.10	2.75
0.40	0.000035	0	0.000119	2.75	241.43

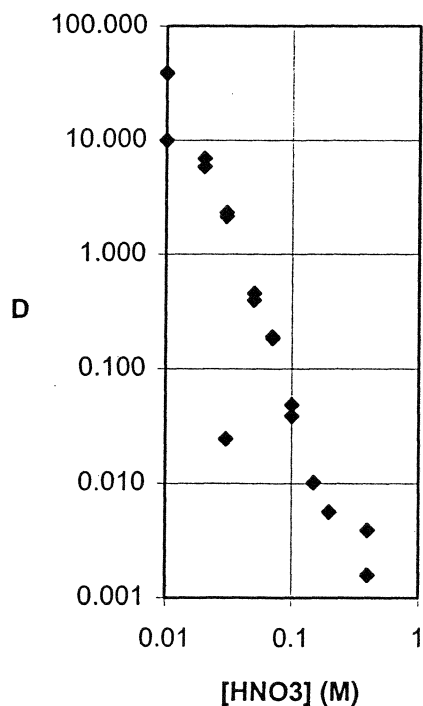


## Appendix 9

### Experimental distribution ratio for cobalt

Experimental distribution ratio for cobalt at some different nitric acid concentrations with 0.02 M 2,2':6',2''-terpyridine and 1.0 M 2-bromodecanoic acid in *tert*-butylbenzene.

[HNO <sub>3</sub> ] (M)	D	D <sub>min</sub>	D <sub>max</sub>	Error in D %	SigmaD %
0.01	9.96	9.85	10.08	1.19	0.85
0.01	38.55	38.00	39.11	1.43	1.02
0.01	39.23	38.85	39.61	0.97	0.70
0.02	6.91	6.85	6.98	0.97	0.72
0.02	5.85	5.80	5.91	0.93	0.70
0.03	0.025	0.0243	0.0250	1.47	1.05
0.03	2.32	2.29	2.35	1.39	1.05
0.03	2.15	2.14	2.16	0.49	0.41
0.05	0.45	0.449	0.458	1.05	0.76
0.05	0.40	0.391	0.400	1.21	0.86
0.07	0.19	0.189	0.191	0.62	0.49
0.07	0.18	0.181	0.187	1.62	1.17
0.1	0.049	0.048	0.049	0.83	0.60
0.1	0.039	0.039	0.039	0.77	0.54
0.15	0.010	0.010	0.010	1.27	0.93
0.2	0.0057	0.0056	0.00571	0.92	0.70
0.4	0.0039	0.0039	0.0040	1.21	0.86
0.4	0.0016	0.0016	0.0016	1.36	1.29

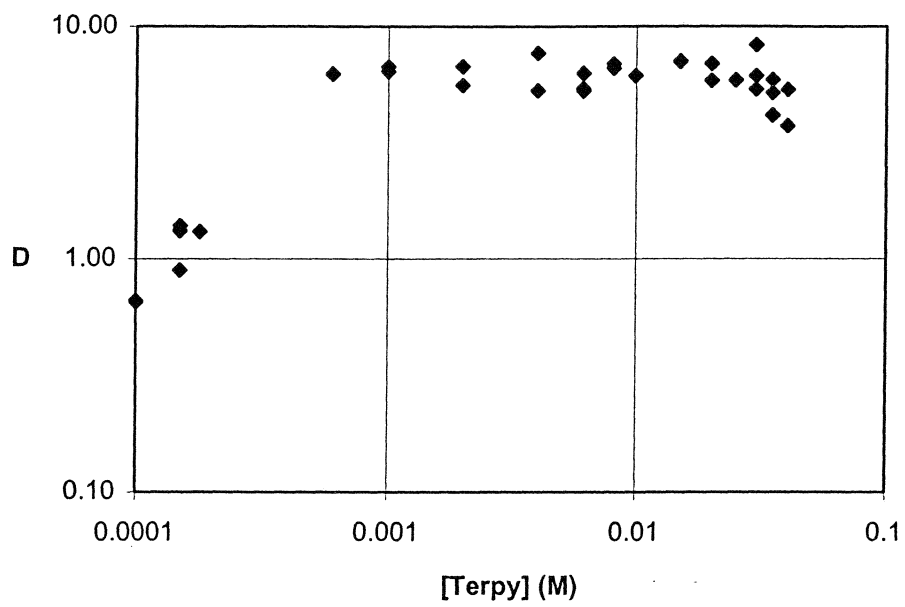


## Appendix 10

### Experimental distribution ratio for cobalt

Experimental distribution ratio for cobalt with different concentrations of 2,2':6',2''-terpyridine (Terpy) and 1 M 2-bromodecanoic acid in *tert*-butylbenzene from 0.02 M nitric acid.

[Terpy] (M)	D	D <sub>min</sub>	D <sub>max</sub>	Error in D %	SigmaD %
0.0001	0.66	0.66	0.67	1.26	0.90
0.0001	0.66	0.65	0.67	1.22	0.86
0.0001	0.65	0.65	0.66	1.03	0.75
0.0001	0.65	0.65	0.66	1.16	0.83
0.00015	1.39	1.38	1.40	0.56	0.48
0.00015	0.90	0.89	0.90	0.78	0.70
0.00015	1.32	1.30	1.34	1.35	0.95
0.00015	1.33	1.31	1.35	1.42	1.01
0.00018	1.31	1.30	1.33	1.21	0.87
0.0006	6.23	6.18	6.29	0.85	0.94
0.0006	6.26	6.19	6.33	1.13	0.80
0.001	6.41	6.34	6.49	1.17	0.85
0.001	6.70	6.61	6.79	1.31	0.94
0.002	5.58	5.49	5.67	1.66	1.18
0.002	6.73	6.66	6.80	1.02	0.74
0.004	5.29	5.24	5.34	0.94	0.68
0.004	7.67	7.57	7.78	1.34	0.99
0.0061	6.29	6.24	6.34	0.82	0.68
0.0061	6.28	6.19	6.36	1.38	0.99
0.0061	5.40	5.34	5.45	0.98	0.73
0.0061	5.27	5.23	5.31	0.68	0.49
0.0081	6.91	6.83	6.99	1.12	0.82
0.0081	6.63	6.57	6.69	0.87	0.63
0.0099	6.14	6.09	6.20	0.90	0.64
0.015	7.10	7.01	7.19	1.27	0.91
0.015	7.04	6.96	7.13	1.23	0.88
0.02	6.91	6.85	6.98	0.97	0.72
0.02	5.85	5.80	5.91	0.93	0.70
0.0249	5.88	5.81	5.95	1.21	0.89
0.0249	5.89	5.83	5.96	1.09	0.87
0.0249	5.89	5.83	5.96	1.09	0.87
0.03	8.35	8.30	8.39	0.53	0.46
0.03	6.13	6.06	6.21	1.19	0.85
0.03	5.37	5.29	5.45	1.46	1.03
0.0349	5.90	5.86	5.93	0.59	0.47
0.0349	5.19	5.13	5.25	1.11	0.79
0.0349	4.16	4.10	4.22	1.48	1.05
0.0349	4.16	4.10	4.22	1.48	1.05
0.0401	5.35	5.30	5.41	1.05	0.80
0.0401	3.74	3.69	3.78	1.20	0.85

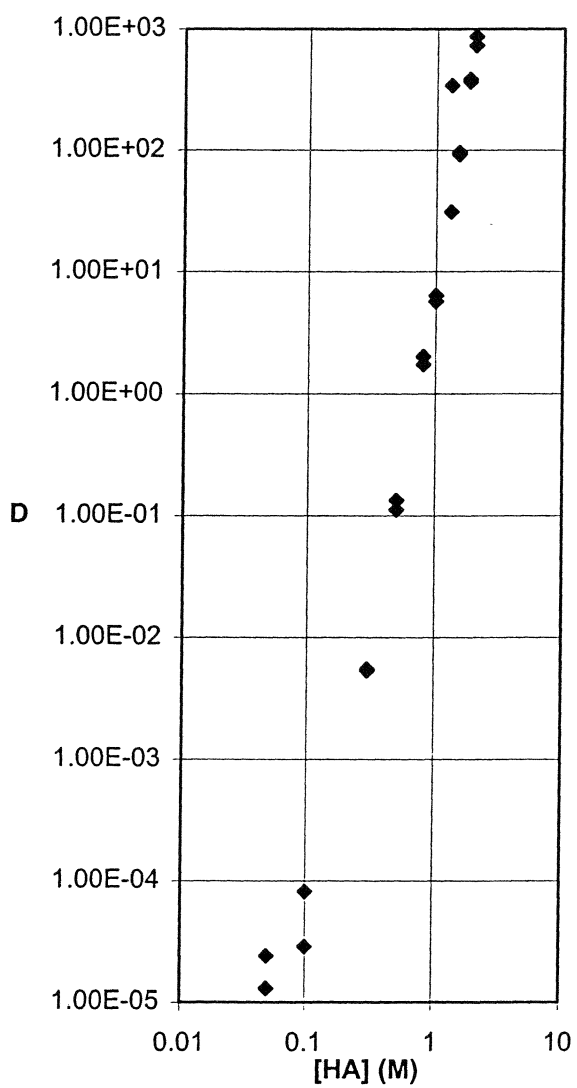


## Appendix 11

### Experimental distribution ratio for cobalt

Experimental distribution ratio for cobalt at some different 2-bromodecanoic acid, (HA) concentrations and 0.02 M 2,2':6',2''-terpyridine in *tert*-butylbenzene from 0.02 M nitric acid.

[HA] (M)	D	D <sub>min</sub>	D <sub>max</sub>	Error in D %	SigmaD %
0.05	2.40E-05	0	5.14E-05	113.90	113.80
0.05	1.30E-05	1.15E-05	1.46E-05	11.57	10.95
0.1	8.17E-05	5.05E-05	1.13E-04	38.38	37.84
0.1	2.86E-05	2.57E-05	3.15E-05	10.26	9.64
0.3	0.0053	0.0052	0.0055	3.19	2.53
0.3	0.0055	0.0054	0.0056	1.47	1.28
0.5	0.112	0.110	0.113	1.39	1.02
0.5	0.134	0.132	0.135	14.25	0.80
0.8	1.74	1.72	1.77	1.33	0.94
0.8	2.01	2.00	2.03	0.78	0.55
1	6.35	6.33	6.37	0.01	0.28
1	5.69	5.64	5.74	0.74	0.88
1.3	31.23	30.68	31.80	1.81	1.37
1.3	342.47	330.00	355.76	3.23	3.76
1.5	95.96	94.60	97.36	1.44	1.34
1.5	92.39	91.00	93.80	1.12	1.52
1.8	384.62	374.40	395.25	2.71	2.08
1.8	366.20	360.10	372.44	1.21	1.68
2	733.19	712.82	754.35	2.83	2.13
2	868.06	849.15	887.54	1.66	2.21

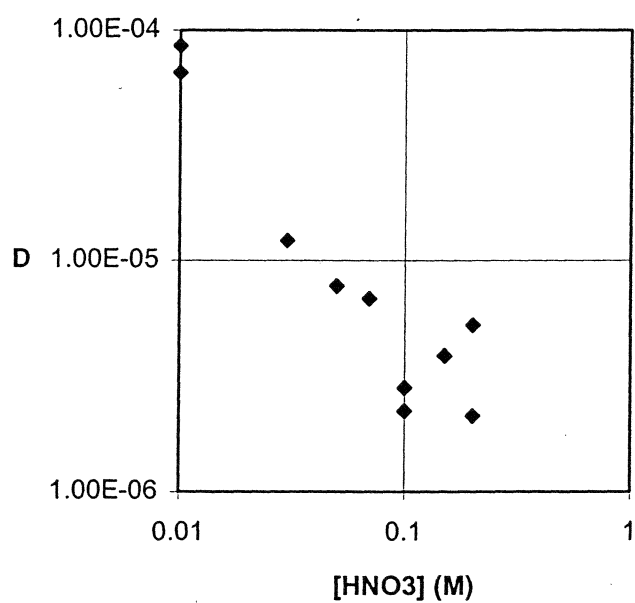


## Appendix 12

### Experimental distribution ratio for cobalt

Experimental distribution ratio for cobalt at some different nitric acid concentrations with 1.0 M 2-bromodecanoic acid in *tert*-butylbenzene.

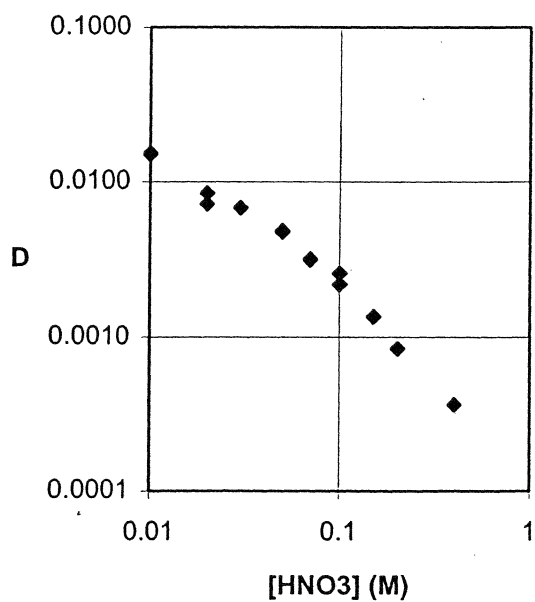
[HNO <sub>3</sub> ] (M)	D	D <sub>min</sub>	D <sub>max</sub>	Error in D %	SigmaD %
0.01	6.54E-05	6.40E-05	6.68E-05	2.13	1.86
0.01	8.57E-05	8.39E-05	8.74E-05	2.06	1.67
0.03	1.22E-05	1.18E-05	1.26E-05	3.27	3.05
0.05	7.77E-06	7.06E-06	8.49E-06	9.16	8.49
0.05	7.74E-06	7.28E-06	8.21E-06	5.97	5.50
0.07	6.83E-06	5.97E-06	7.70E-06	12.63	11.94
0.1	2.23E-06	1.57E-06	2.91E-06	30.05	29.34
0.1	2.81E-06	2.39E-06	3.24E-06	15.06	14.76
0.15	3.86E-06	3.52E-06	4.21E-06	9.01	8.33
0.2	2.13E-06	1.84E-06	2.43E-06	13.84	13.29
0.2	5.25E-06	4.52E-06	5.99E-06	14.03	13.67



### Experimental distribution ratio for cesium

Experimental distribution ratio for cesium at some different nitric acid concentrations with 0.02 M 2,2':6',2''-terpyridine and 1.0 M 2-bromodecanoic acid in *tert*-butylbenzene.

[HNO <sub>3</sub> ] (M)	D	D <sub>min</sub>	D <sub>max</sub>	Error in D %	SigmaD %
0.01	0.0151	0.0149	0.0152	1.21	0.93
0.01	0.0153	0.0151	0.0156	1.74	1.26
0.02	0.00848	0.00844	0.00852	0.49	0.35
0.02	0.00725	0.00711	0.00738	1.87	1.36
0.03	0.00685	0.00675	0.00694	1.41	1.04
0.05	0.00477	0.00473	0.00481	0.78	0.56
0.05	0.00488	0.00478	0.00497	1.89	1.38
0.07	0.00319	0.00314	0.00324	1.56	1.19
0.07	0.00314	0.00311	0.00318	1.15	0.82
0.1	0.00219	0.00215	0.00223	1.72	1.31
0.1	0.00258	0.00254	0.00262	1.52	1.12
0.15	0.00136	0.00134	0.00137	1.12	0.83
0.2	0.00084	0.000832	0.000849	1.01	0.79
0.4	0.000364	0.00036	0.000369	1.23	0.97

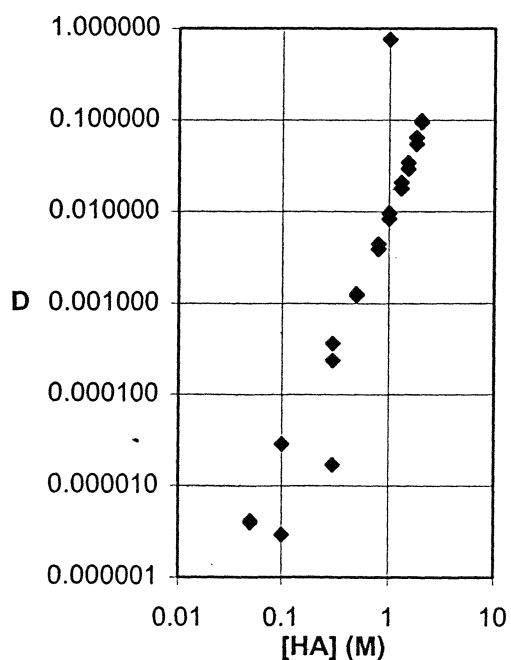


## Appendix 14

### Experimental distribution ratio for cesium

Experimental distribution ratio for cesium at some different 2-bromodecanoic acid (HA) concentrations in *tert*-butylbenzene from 0.02 M nitric acid.

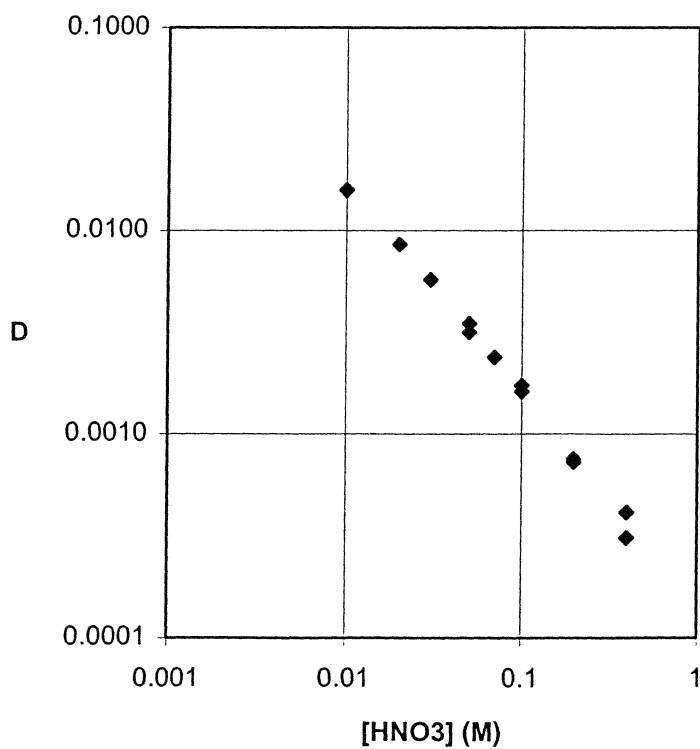
[HA] (M)	D	D <sub>min</sub>	D <sub>max</sub>	Error in D %	SigmaD %
0.05	3.99E-06	3.82E-06	4.16E-06	4.29	3.93
0.05	4.16E-06	3.96E-06	4.36E-06	4.71	4.39
0.1	2.92E-06	2.86E-05	2.98E-05	2.08	1.73
0.1	2.85E-05	2.79E-05	2.90E-05	1.98	1.58
0.3	0.00037	0.00036	0.00037	1.15	0.88
0.3	0.00024	0.00023	0.00024	1.65	1.26
0.3	1.68E-05	1.64E-05	1.72E-05	2.33	1.92
0.5	0.0012	0.0012	0.0012	0.57	0.43
0.5	0.0013	0.0013	0.0013	1.00	0.73
0.8	0.0039	0.0039	0.0039	0.81	0.57
0.8	0.0045	0.0044	0.0045	0.58	0.48
1	0.76	0.75	0.77	0.97	0.70
1	0.0096	0.0096	0.0097	0.87	0.62
1	0.0084	0.0083	0.0084	0.47	0.39
1.3	0.018	0.018	0.018	1.06	0.79
1.3	0.021	0.021	0.021	0.90	0.64
1.5	0.029	0.029	0.030	0.68	0.49
1.5	0.034	0.034	0.035	1.12	0.80
1.8	0.055	0.054	0.055	0.81	0.57
1.8	0.064	0.064	0.065	0.89	0.63
2	0.098	0.097	0.099	0.78	0.55
2	0.094	0.093	0.095	0.84	0.60



### Experimental distribution ratio for cesium

Experimental distribution ratio for cesium at some different nitric acid concentrations with 1.0 M 2-bromodecanoic acid in *tert*-butylbenzene.

[HNO <sub>3</sub> ] (M)	D	D <sub>min</sub>	D <sub>max</sub>	Error in D %	SigmaD %
0.01	0.016	0.016	0.019	0.85	0.63
0.01	0.016	0.016	0.016	0.85	0.60
0.02	0.0086	0.0085	0.0087	1.17	0.84
0.03	0.0057	0.0057	0.0058	0.81	0.60
0.05	0.0035	0.0035	0.0035	0.93	0.69
0.05	0.0032	0.0031	0.0032	1.23	0.89
0.07	0.0024	0.0024	0.0024	0.97	0.66
0.1	0.0017	0.0017	0.0018	1.12	0.82
0.1	0.0016	0.0016	0.0016	1.20	0.87
0.2	0.00075	0.00074	0.000762	1.22	0.89
0.2	0.00073	0.00071	0.000737	1.58	1.20
0.4	0.00041	0.000407	0.000420	1.52	1.12
0.4	0.00031	0.000306	0.000313	1.09	0.77

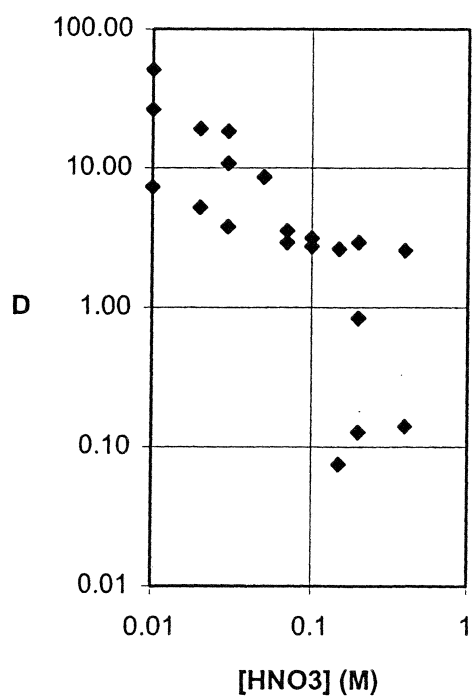


## Appendix 16

### Experimental distribution ratio for silver

Experimental distribution ratio for silver at some different nitric acid concentrations with 0.02 M 2,2':6',2''-terpyridine and 1.0 M 2-bromodecanoic acid in *tert*-butylbenzene.

[HNO <sub>3</sub> ] (M)	D	D <sub>min</sub>	D <sub>max</sub>	Error in D %	SigmaD %
0.01	51.08	50.61	51.55	0.92	0.65
0.01	26.39	25.79	27.01	2.31	1.69
0.01	7.32	7.23	7.42	1.33	0.94
0.02	19.15	19.00	19.30	0.77	0.56
0.02	5.22	5.13	5.31	1.66	1.17
0.03	18.41	18.24	18.58	0.92	0.73
0.03	10.78	10.68	10.88	0.91	0.67
0.03	3.78	3.75	3.81	0.77	0.65
0.05	8.62	8.47	8.78	1.78	1.30
0.07	3.54	3.47	3.62	2.11	1.58
0.07	2.92	2.87	2.97	1.73	1.23
0.1	2.73	2.69	2.77	1.49	1.09
0.1	3.13	3.10	3.16	0.98	0.92
0.15	2.63	2.59	2.68	1.73	1.23
0.15	0.08	0.07	0.08	2.12	1.52
0.2	0.84	0.83	0.85	0.95	0.83
0.2	2.91	2.87	2.96	1.55	1.09
0.2	0.13	0.13	0.13	1.93	1.38
0.4	2.56	2.52	2.59	1.31	0.93
0.4	0.14	0.14	0.14	1.45	1.03



## Appendix 17

### Experimental distribution ratio for silver

Experimental distribution ratio for silver with different concentrations of 2,2':6',2''-terpyridine (Terpy) and 1 M 2-bromodecanoic acid in *tert*-butylbenzene from 0.02 M nitric acid.

[Terpy] (M)	D	D <sub>min</sub>	D <sub>max</sub>	Error in D %	SigmaD %
0.0001	4.45	4.38	4.52	1.56	1.11
0.0001	0.63	0.62	0.64	1.24	1.75
0.00015	4.89	4.83	4.96	1.29	0.93
0.00015	0.95	0.93	0.96	1.03	1.45
0.0006	4.71	4.66	4.77	1.17	0.88
0.0006	1.83	1.81	1.85	1.29	0.94
0.001	8.55	8.42	8.69	1.59	1.13
0.001	5.78	5.69	5.86	1.05	1.48
0.002	10.11	9.95	10.27	1.59	1.12
0.004	10.79	10.64	10.95	1.44	1.02
0.004	17.70	17.30	18.10	2.25	1.76
0.004	2.88	2.83	2.93	1.18	1.67
0.0061	14.34	14.16	14.52	1.28	0.93
0.0061	6.38	6.33	6.43	0.78	0.58
0.0061	2.78	2.73	2.83	1.29	1.82
0.0081	16.45	16.18	16.72	1.64	1.16
0.0081	19.59	19.34	19.84	1.25	0.95
0.0099	19.87	19.55	20.20	1.62	1.15
0.0099	18.79	18.47	19.12	1.72	1.24
0.0099	8.77	8.64	8.90	1.48	1.06
0.015	14.23	13.93	14.53	2.08	1.49
0.015	16.12	15.78	16.47	2.13	1.55
0.02	19.15	19.00	19.30	0.77	0.56
0.0249	18.54	18.19	18.89	1.89	1.35
0.0249	12.84	12.68	13.00	1.27	0.93
0.03	24.52	24.19	24.86	1.37	1.03
0.03	6.87	6.75	6.99	1.29	1.77
0.0349	17.75	17.57	17.94	1.07	0.77
0.0401	36.30	35.90	36.70	1.11	0.88
0.0401	3.29	3.27	3.32	0.68	0.54
0.0401	4.18	4.12	4.23	0.87	1.19

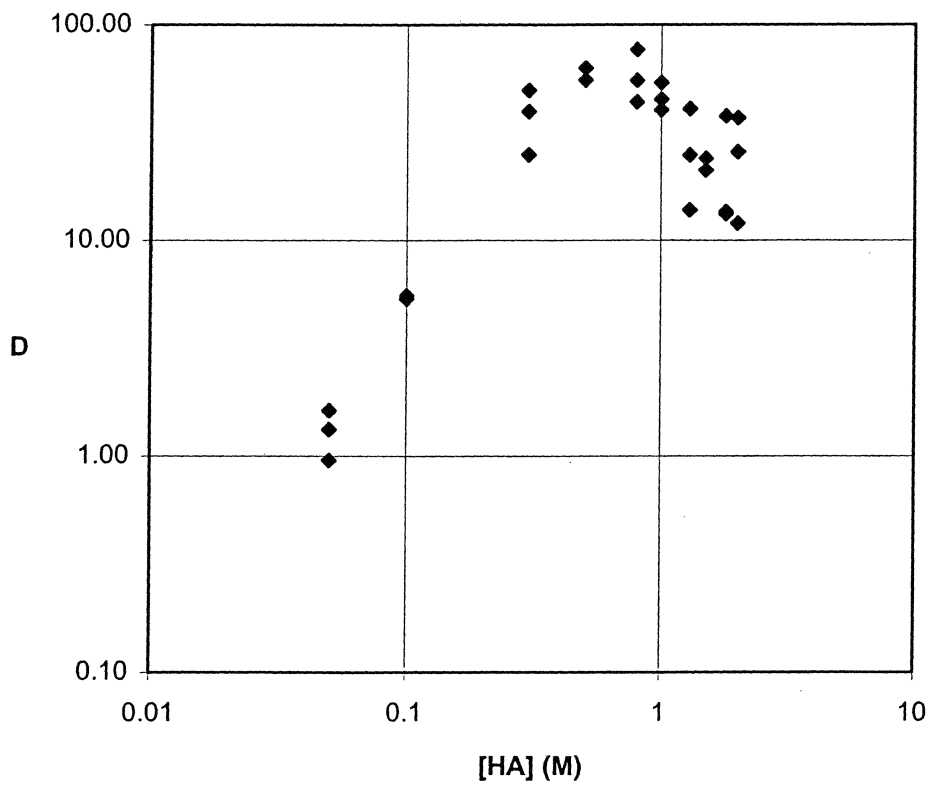


## Appendix 18

### Experimental distribution ratio for silver

Experimental distribution ratio for silver at some different 2-bromodecanoic acid, (HA) concentrations and 0.02 M 2,2':6',2''-terpyridine in *tert*-butylbenzene from 0.02 M nitric acid.

[HA] (M)	D	D <sub>min</sub>	D <sub>max</sub>	Error in D %	SigmaD %
0.05	0.96	0.95	0.97	0.83	0.78
0.05	1.33	1.31	1.35	1.54	1.09
0.05	1.63	1.61	1.65	1.33	0.97
0.1	5.35	5.28	5.43	1.43	1.02
0.1	5.53	5.51	5.56	0.45	0.34
0.3	39.61	39.16	40.06	1.14	0.86
0.3	24.98	24.68	25.29	1.22	0.86
0.3	49.70	48.73	50.70	1.99	1.43
0.5	63.02	62.07	64.00	1.53	1.10
0.5	55.51	54.71	56.33	1.47	1.06
0.8	55.26	54.38	56.15	1.60	1.17
0.8	43.90	43.34	44.46	1.27	0.94
0.8	76.71	75.34	78.11	1.81	1.29
1	54.01	53.35	54.67	1.23	0.92
1	40.36	39.72	41.01	1.60	1.13
1	45.12	44.39	45.86	1.62	1.15
1.3	13.84	13.60	14.08	1.71	1.21
1.3	40.84	40.45	41.24	0.97	0.84
1.3	24.90	24.64	25.16	1.03	0.78
1.5	21.14	20.78	21.52	1.76	1.26
1.5	24.06	23.67	24.44	1.60	1.13
1.8	13.26	13.03	13.49	1.74	1.24
1.8	37.81	37.44	38.18	0.98	0.74
1.8	13.61	13.40	13.82	1.54	1.09
2	12.03	11.88	12.19	1.27	0.93
2	25.71	25.32	26.12	1.56	1.10
2	37.03	36.37	37.70	1.80	1.28

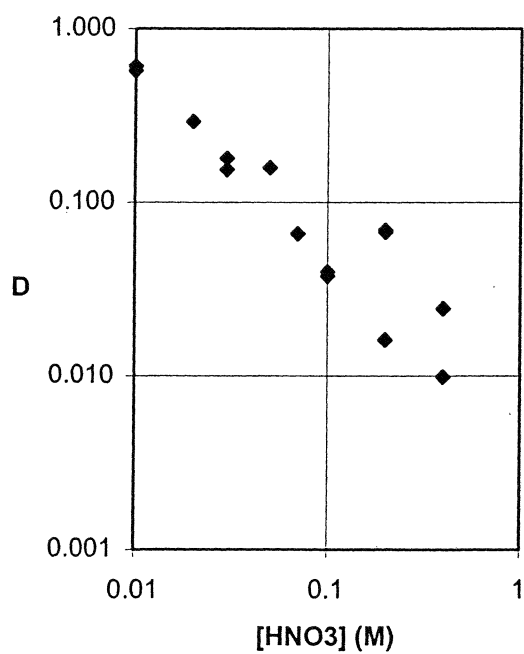


## Appendix 19

### Experimental distribution ratio for silver

Experimental distribution ratio for silver at some different nitric acid concentrations with 1.0 M 2-bromodecanoic acid in *tert*-butylbenzene.

[HNO <sub>3</sub> ] (M)	D	D <sub>min</sub>	D <sub>max</sub>	Error in D %	SigmaD %
0.01	0.61	0.60	0.62	1.30	0.92
0.01	0.57	0.56	0.58	1.40	1.00
0.02	0.29	0.29	0.30	1.39	0.98
0.03	0.15	0.15	0.16	0.68	0.49
0.03	0.18	0.18	0.18	0.92	0.66
0.05	0.16	0.16	0.16	1.26	0.90
0.07	0.066	0.065	0.067	1.55	1.10
0.1	0.038	0.037	0.038	1.17	1.10
0.1	0.040	0.039	0.040	1.43	1.05
0.2	0.016	0.016	0.017	1.82	1.37
0.2	0.067	0.066	0.068	1.62	1.15
0.2	0.069	0.068	0.070	1.43	1.01
0.4	0.024	0.024	0.025	1.59	1.14
0.4	0.0099	0.0096	0.0101	1.72	2.34



# Appendix IV

## COMPARISON OF EXTRACTION BEHAVIOUR AND BASICITY OF SOME SUBSTITUTED MALONAMIDES

L. Spjuth<sup>1</sup>, J.O. Liljenzin<sup>1</sup>, M.J. Hudson<sup>2</sup>, M.G.B. Drew<sup>2</sup>, P.B. Iveson<sup>2</sup> and C. Madic<sup>3</sup>  
1. Department of Nuclear Chemistry, Chalmers University of Technology, S-41296 Göteborg, Sweden. 2. Department of Chemistry, University of Reading, Box 224, Whiteknights, Berkshire, RG6 6AD, UK. 3. CEA-Valrhô, Marcoule, BP171, 30207 Bagnols-sur-Cèze, France

### ABSTRACT

The extraction behaviour for Am(III), Eu(III) and nitric acid is compared for eight different malonamides together with experimentally determined basicities and calculated gas-phase basicities. Water extraction data for two of the malonamides are also presented and shows that the water is co-extracted or solubilised by malonamide-HNO<sub>3</sub> species. The relationship between metal extraction from aqueous nitric acid solution, basicity and the structure of the malonamide was investigated and it was found that the highest metal extraction was achieved with ligands of lowest basicity. The introduction of phenyl substituents on the nitrogens in the malonamide or the replacement of a carbon of the central carbon chain by an ether oxygen decreases the basicity and thus increases the metal extraction. The relative order of calculated gas-phase basicities, using *ab initio* methods, is in good agreement with the experimentally determined basicity scale.

### INTRODUCTION

Malonamides have been established as suitable coextractants for the minor actinides and lanthanides in advanced reprocessing of spent nuclear fuels [1-3]. In this process, the long-lived minor actinides are then separated from the lanthanides

and transmuted to short-lived nuclides in a reactor or a sub-critical accelerator-driven system. The chemistry and extraction behaviour of the malonamides are, therefore, important. The extraction efficiency of the malonamides is considered to be related to both electro-inductive effects and to steric hindrances around the binding site [1]. The influence of the different malonamide structures on metal, water and nitric acid extraction has been studied and the extraction is related to the basicity of the malonamide. Gas-phase basicities have been calculated using *ab initio* methods (Gaussian 94 software).

## EXPERIMENTAL

### Reagents

Eight different malonamides have been investigated in this study. The structures of the different malonamides and abbreviations used in this work are listed in Table 3. Malonamides, which have an oxyalkyl group attached on the central carbon, are denoted with an *x* at the end of the abbreviation. The synthesis of seven of the eight malonamides is described in [2, 4]. Their purities are all over 98% and have been checked by <sup>1</sup>H (400MHz) NMR, elemental analysis and melting point. The synthesis of the 4-chlorophenyl substituted malonamide is described below. *Tert*-butylbenzene, 99% purity (Acros) was used as the diluent in all experiments. Anhydrous pyridine, 99.8%, from Aldrich and imidazole, 99%, from Sigma were used as the reference substances in the basicity titrations and 0.1M HClO<sub>4</sub> in anhydrous acetic acid from Merck was used as the titrant. Acetonitrile from Fischer Scientific was HPLC-grade (99.99%) with a maximum water content of 0.0065% and the acetic anhydride had a purity of ≥99.5% and was bought from Fluka. Hydranal-Titrant 5 with a capacity of 5.00±0.002 mg H<sub>2</sub>O/mL and Hydranal-solvent, from Riedel-de Haën, was used in the Karl Fischer titrations.

### Synthesis of N,N'-dimethyl-N,N'-di(4-chlorophenyl)tetradecyl malonamide

All starting chemicals for the synthesis were obtained from Aldrich and used without further purification. 4-chloro-N-methylaniline (10 g, 0.066 mol) and dimethyl malonate (4.38 g, 0.033 mol) were heated at 200°C for 5 h. A small

TABLE 1.

Elemental analysis data for N,N'-dimethyl-N,N'-di(4-chlorophenyl)tetradecyl malonamide

	C	H	N
Analysis %	68.31	8.03	5.23
Calculated %	67.04	7.76	5.39

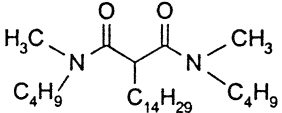
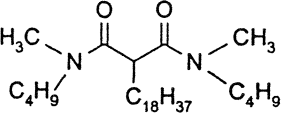
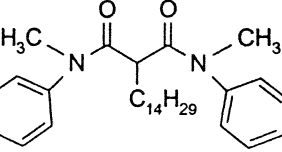
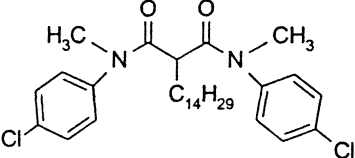
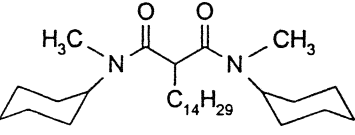
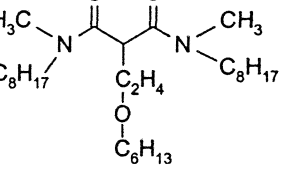
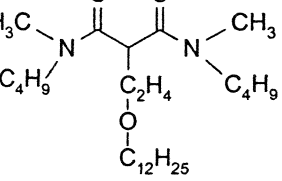
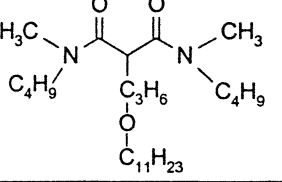
TABLE 2.

Proton NMR assignments for N,N'-dimethyl-N,N'-di(4-chlorophenyl)tetradecyl malonamide

Structure	<sup>1</sup> H NMR (δ)
	0.79-1.41 (27 H, m, a)
	1.69-1.82 (2 H, br, b)
	3.15-3.23 (7 H, m, c)
	6.68-6.71 (4 H, m, d)
	7.31-7.35 (4 H, m, e)

portion of diethyl ether:ethyl acetate (1:1) solution was added and a white solid formed on cooling. The crystals were filtered off and washed with a cold diethyl ether:ethyl acetate solution (1:1) and dried in a dessicator. Proton NMR showed the product N,N'-dimethyl-N,N'-di(4-chlorophenyl) malonamide. Alkylation of this malonamide was performed using the dried N,N'-dimethyl-N,N'-di(4-chlorophenyl) malonamide (1.9 g, 0.005 mol) dissolved in toluene (35 mL) at room temperature. Sodium hydride (0.20 g of a 60% dispersion in mineral oil, 0.005 mol) was washed with petroleum ether and suspended in toluene (10 mL). The N,N'-dimethyl-N,N'-di(4-chlorophenyl) malonamide solution was added to this suspension and refluxed (90°C) until hydrogen evolution ceased (*ca.* 1 h). 1-Bromotetradecane (1.51g, 0.005 mol) in toluene (2 mL) was added dropwise to the solution and refluxed for 2 days. The reaction was followed by TLC (thin layer chromatography) and the product was separated on a silica column with diethyl ether:ethyl acetate (1:1) solution. The diluent was evaporated and crystals formed on cooling. The melting point was 51-53°C and the product was characterised by elemental analysis and <sup>1</sup>H NMR, Table 1-2.

**TABLE 3.**  
The different malonamides investigated.

Structure	Name	Provider	Acronym
	N,N'-dimethyl-N,N'-dibutyltetradecyl malonamide (DMDBTDMA)	Panchim France	<b>BTD</b>
	N,N'-dimethyl-N,N'-dibutyloctadecyl malonamide (DMDBODMA)	Synthelec AB Sweden	<b>BOD</b>
	N,N'-dimethyl-N,N'-diphenyltetradecyl malonamide (DMDPHTDMA)	University of Reading England	<b>PHTD</b>
	N,N'-dimethyl-N,N'-di(4-chlorophenyl)tetradecyl malonamide (DMDCLPHTDMA)	University of Reading England	<b>CLPHTD</b>
	N,N'-dimethyl-N,N'-dicyclohexyltetradecyl malonamide (DMDCHTDMA)	University of Reading England	<b>CHTD</b>
	N,N'-dimethyl-N,N'-dioctylhexylethoxy malonamide (DMDOHEMA)	Panchim France	<b>OHEX</b>
	N,N'-dimethyl-N,N'-dibutyldodecylethoxy malonamide (DMDBDDEMA)	Panchim France	<b>BDDEx</b>
	N,N'-dimethyl-N,N'-dibutylundecylpropoxy malonamide (DMDBUDOPMA)	Panchim France	<b>BUDOPx</b>

### Experimental Procedure

The metal extractions were carried out in 3.5 mL test-tubes by manually shaking equal volumes of organic and aqueous phase for 5 min, a time which enable equilibrium to be reached. The aqueous solutions contained different nitric acid concentrations and 0.1M of the malonamides, dissolved in *tert*-butylbenzene, was used as the organic phase in the extractions. After centrifugation at 3500 rpm (2200g) for 5 min, samples of each phase were withdrawn for analysis. When metal extraction was considered,  $\gamma$ -spectrometry with a HPGe-detector (*EG&G ORTEC*) was used to determine the ratio of the radioactivity in the two phases (D-value) and for the nitric acid extractions, the samples from each phase, after extraction equilibrium, were titrated with 0.1M NaOH. The organic phase was titrated in ethanolic media. Water concentration in the organic phase after extraction was determined with the Karl-Fischer method using Pt-electrodes and a *Radiometer* ABU91 Autoburette. A two-component system for volumetric titrations was used, Hydranal-Titrant 5 with a capacity of  $5.00 \pm 0.002$  mg H<sub>2</sub>O/mL and Hydranal-solvent. A *Radiometer* SAM90 sample station was used to prevent disturbances from humid air.

The basicities of the different malonamides were determined by titrations in acetonitrile media, using 0.1M HClO<sub>4</sub> in anhydrous acetic acid as the titrant. The outer salt-bridge in a double junction Ag/AgCl reference electrode (*Radiometer* REF251) was changed to 0.1M LiClO<sub>4</sub> in acetonitrile, and was used with a conventional glass electrode (*Radiometer* pHG201). The titrations were conducted with a *Radiometer* ABU91 Autoburette and a SAM90 sample station was used to prevent disturbances from humid air. The malonamides (0.1M) were dissolved in *tert*-butylbenzene and 0.3 mL of this solution was added to 45 mL acetonitrile. 15  $\mu$ mol of imidazole was also added in order to eliminate disturbances of possible impurities in the acetonitrile. Pyridine together with 15  $\mu$ mol of imidazole were used as reference substances and were titrated before each titration, to adjust for drift in electrode potential. The HNP (half-neutralisation potential) for pyridine was set at a constant value (138mV) and measured HNPs were adjusted by adding or subtracting any deviation from this value. Three titrations were performed for each ligand. The HNP was used as a measure for basicity; the higher the HNP, the lower the basicity.

### Quantum mechanic calculations

The starting models were built using the CERIUS2 software [5]. The semi-empirical calculations were carried out with the MOPAC6 program [6], and the *ab initio* single point calculations were carried out using the Gaussian 94 software and Hartree-Fock methods using two different basis sets [7]. The structures were first geometry optimised using a 3-21G basis set. The frequency calculations, required for the  $\Delta G$  calculations, were then carried out using these optimised structures but with a 6-31G\* or 6-31G basis set. All calculations were carried out on a Silicon Graphics Origin 2000 at Reading University.

## RESULTS AND DISCUSSION

### Basicity Measurements

The ability of malonamides to extract metal ions or nitric acid is related to the basicity of the molecule. Low basicity of the ligand is considered to give good metal extraction since the competition between proton and metal ion is less severe than with a more basic ligand. The basicity of the malonamide is influenced by its structure and substituents of different electronegativity can therefore be introduced in the molecule to cause changes in the basicity.

Bifunctional phosphorous based extractants, like carbamoylmethyl-phosphonates, -phosphinates, and -phosphine oxides as well as monoamides and monodentate phosphorous based ligands show an opposite correlation between metal extraction and basicity compared to the malonamides, at least at low acidities. A better metal extraction is observed with the extractants of highest basicity [8-12]. However, competition between protons and metal cations for the binding site in CMPO derivatives result in a decrease in metal extraction at higher acidities and thus the less basic CMPO derivatives show a better metal extraction than the more basic ones above a certain acidity. The extraction with CMPO derivatives is reported to be very dependent on the diluent used and the relations stated above are certainly not valid in all diluents [13].

The basicities of a few malonamides have, therefore, been determined experimentally by titrations in acetonitrile media [14]. The potential at the half-

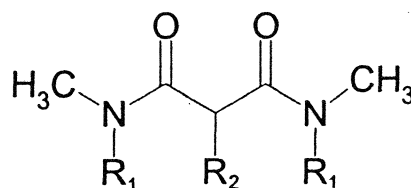


FIGURE 1. General structure of the studied malonamides.

TABLE 4.  
Basicity (HNP) of the different malonamides measured by titration in acetonitrile media.

R <sub>1</sub>	R <sub>2</sub>	Ligand	HNP(mV)
butyl	-C <sub>14</sub> H <sub>29</sub>	BTD	332±3
cyclohexyl	-C <sub>14</sub> H <sub>29</sub>	CHTD	332±5
butyl	-C <sub>3</sub> H <sub>6</sub> OC <sub>11</sub> H <sub>23</sub>	BUDOPx	346±1
butyl	-C <sub>2</sub> H <sub>4</sub> OC <sub>12</sub> H <sub>25</sub>	BDDEx	352±3
octyl	-C <sub>2</sub> H <sub>4</sub> OC <sub>6</sub> H <sub>13</sub>	OHEx	356±6
phenyl	-C <sub>14</sub> H <sub>29</sub>	PHTD	490±4
4-chlorophenyl	-C <sub>14</sub> H <sub>29</sub>	CLPHTD	529±6

neutralisation volume (HNP) was taken as a measure for basicity. The measured HNPs are listed in Table 4, and the higher the HNP the less basic the molecule. It was not possible to measure the basicity of BOD in acetonitrile media owing to solubility problems. The -C<sub>18</sub>H<sub>37</sub> group attached to the central carbon in BOD might be too long to achieve sufficient solubility in acetonitrile compared to the rest of malonamides studied. Since all the substituents in this molecule are alkyl groups, the basicity would be expected to be similar to BTD and CHTD.

The 4-chlorophenyl substituted malonamide, CLPHTD, is thus the least basic malonamide and the cyclohexyl- and butyl substituted malonamides, BTD and CHTD, are the most basic ones. The electron withdrawing effect of the phenyl groups, which are substituted on the nitrogens in the malonamide, results in the large difference in basicity between phenyl substituted and alkyl substituted malonamides. The effect is even more apparent in CLPHTD where the electron withdrawing chlorine in the *para* position on the phenyl group influences the basicity on the carbonyls. There is a big difference in basicity between the

malonamides with aromatic groups on the nitrogen and those with non-aromatic groups. There is also a significant difference in basicity for the malonamides with non-aromatic groups on the nitrogens and substituted with oxyalkyl groups or alkyl groups on the central carbon ( $R_2$ ). Lower basicities are observed for the malonamides substituted with oxyalkyl groups.

The position of the ether oxygen in the alkoxy group on the central carbon also has an effect on the basicity. The only difference in structure between BUDOPX and BDDEX is that the oxygen in the oxyalkyl group on the central carbon is positioned after the second carbon in BDDEX and after the third carbon in BUDOPX. The nitrogen substituents and the total number of carbons are the same. The basicity of BUDOPX is slightly higher than that of BDDEX which indicates that an oxygen further away from the carbonyl oxygens has a smaller effect on the basicity, Table 4. The titration method for basicity determination of malonamides has been verified in acetic anhydride media and the same basicity order was achieved when four of the malonamides were titrated [15].

#### Metal Extraction

The extraction of trivalent americium and europium with the different malonamides studied shows the same extraction behaviour as previously presented in that extraction increases with increasing nitric acid concentration [1-4]. All malonamides, except PHTD and CLPHTD, show a maximum in extraction at about 8M nitric acid concentration, see Figure 2. The extraction decreases thereafter, owing to the competition between metal ions and protons for the coordination site, and the competition is more severe for the malonamides with higher basicity than for the less basic molecules.

The continuous increase in extraction for PHTD and CLPHTD at all nitric acid concentrations studied, compared to CHTD, has been explained by steric effects [4], but the lower basicity of these malonamides probably also influences the steep increase in metal extraction. The order of extraction ability for the malonamides as seen in Figure 2, is inversely correlated with the order of basicity in Table 4, the lower the basicity the higher the metal extraction. The malonamides with non-aromatic groups on the nitrogens but substituted with an oxyalkyl group on the central carbon have a lower basicity and higher metal extraction, than malonamides which have alkyl groups attached to the central carbon.

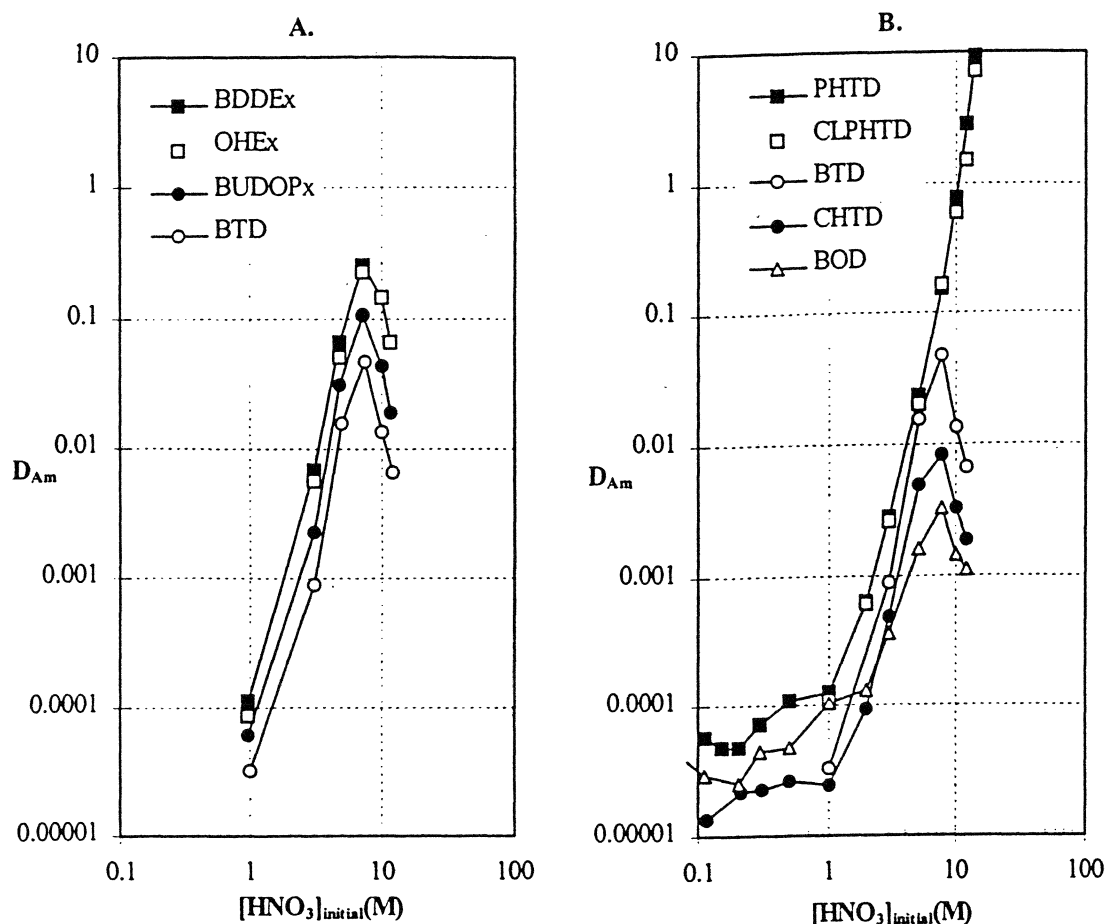


FIGURE 2. Extraction of Am(III) from nitric acid solution with 0.1M of the different malonamides in *tert*-butylbenzene (room temperature). Extraction data for PHTD, CHTD and BTD was presented previously [15]. BTD is shown in both graphs for comparison.

Malonamides are used as coextractants for trivalent actinides and, as seen in Table 5-6, the extraction of Am(III) and Eu(III) is quite similar when extracted from nitric acid solution with 0.1M of the malonamides in *tert*-butylbenzene. The separation factor,  $D_{Am}/D_{Eu}$ , is less than 2 for all nitric acid concentrations investigated.

The extraction studies were performed at a low malonamide concentration (0.1M) which results in rather low D-values. Higher concentration of malonamides will, however, give D-values higher than 1 which is sufficient for process development purposes.

TABLE 5.

Extraction of Am(III) and Eu(III) by 0.1M of BTD and CLPHTD in *tert*-butylbenzene from nitric acid solution.

[HNO <sub>3</sub> ] (M)	BTD		CLPHTD	
	D <sub>Am</sub>	D <sub>Eu</sub>	D <sub>Am</sub>	D <sub>Eu</sub>
1	(3.3±0.6)·10 <sup>-5</sup>	(3.0±0.2)·10 <sup>-5</sup>	(1.1±0.1)·10 <sup>-4</sup>	(6.0±0.1)·10 <sup>-5</sup>
3	(9.0±0.2)·10 <sup>-4</sup>	(4.7±0.1)·10 <sup>-4</sup>	(2.6±0.1)·10 <sup>-3</sup>	(1.0±0.1)·10 <sup>-3</sup>
5	(1.6±0.1)·10 <sup>-2</sup>	(8.3±0.1)·10 <sup>-3</sup>	(2.0±0.1)·10 <sup>-2</sup>	(8.4±0.2)·10 <sup>-3</sup>
7.5	(4.7±0.1)·10 <sup>-2</sup>	(3.2±0.1)·10 <sup>-2</sup>	(1.7±0.1)·10 <sup>-1</sup>	(6.4±0.1)·10 <sup>-2</sup>
10	(1.4±0.1)·10 <sup>-2</sup>	(1.1±0.1)·10 <sup>-2</sup>	(5.8±0.2)·10 <sup>-1</sup>	(3.1±0.1)·10 <sup>-1</sup>
12	(6.7±0.3)·10 <sup>-3</sup>	(7.0±0.1)·10 <sup>-3</sup>	1.5±0.1	(8.9±0.1)·10 <sup>-1</sup>

TABLE 6.

Extraction of Am(III) and Eu(III) by 0.1M of the oxyalkylated malonamides in *tert*-butylbenzene from nitric acid solution.

[HNO <sub>3</sub> ] (M)	BDDEX		BUDOPx	
	D <sub>Am</sub>	D <sub>Eu</sub>	D <sub>Am</sub>	D <sub>Eu</sub>
1.0	(1.1±0.1)·10 <sup>-4</sup>	(6.6±0.2)·10 <sup>-5</sup>	(6.1±0.4)·10 <sup>-5</sup>	(4.4±0.1)·10 <sup>-5</sup>
3.1	(6.8±0.1)·10 <sup>-3</sup>	(3.8±0.1)·10 <sup>-3</sup>	(2.3±0.1)·10 <sup>-3</sup>	(1.2±0.1)·10 <sup>-3</sup>
4.8	(6.5±0.2)·10 <sup>-2</sup>	(3.8±0.1)·10 <sup>-2</sup>	(3.1±0.2)·10 <sup>-2</sup>	(1.7±0.1)·10 <sup>-2</sup>
7.2	(2.5±0.1)·10 <sup>-1</sup>	(1.9±0.1)·10 <sup>-1</sup>	(1.1±0.1)·10 <sup>-1</sup>	(7.0±0.1)·10 <sup>-2</sup>
9.9	(1.4±0.1)·10 <sup>-1</sup>	(1.4±0.1)·10 <sup>-1</sup>	(4.3±0.2)·10 <sup>-2</sup>	(3.7±0.1)·10 <sup>-2</sup>
12	(6.5±0.2)·10 <sup>-2</sup>	(7.2±0.1)·10 <sup>-2</sup>	(1.9±0.1)·10 <sup>-2</sup>	(1.9±0.1)·10 <sup>-2</sup>

[HNO <sub>3</sub> ] (M)	OHEX	
	D <sub>Am</sub>	D <sub>Eu</sub>
1.0	(8.6±0.4)·10 <sup>-5</sup>	(4.8±0.1)·10 <sup>-5</sup>
3.1	(5.7±0.2)·10 <sup>-3</sup>	(3.3±0.1)·10 <sup>-3</sup>
4.8	(5.0±0.1)·10 <sup>-2</sup>	(2.9±0.1)·10 <sup>-2</sup>
7.2	(2.3±0.1)·10 <sup>-1</sup>	(1.5±0.1)·10 <sup>-1</sup>
9.9	(1.4±0.1)·10 <sup>-1</sup>	(1.3±0.1)·10 <sup>-1</sup>
12	(6.6±0.2)·10 <sup>-2</sup>	(6.9±0.1)·10 <sup>-2</sup>

It is highly likely, as demonstrated by several single crystal determinations, that the malonamides coordinate to the metals via the carbonyl oxygens in a bidentate manner and the nitrogens are not involved in the coordination [16]. X-ray crystallographic studies have also shown that the etheral oxygen atom, in

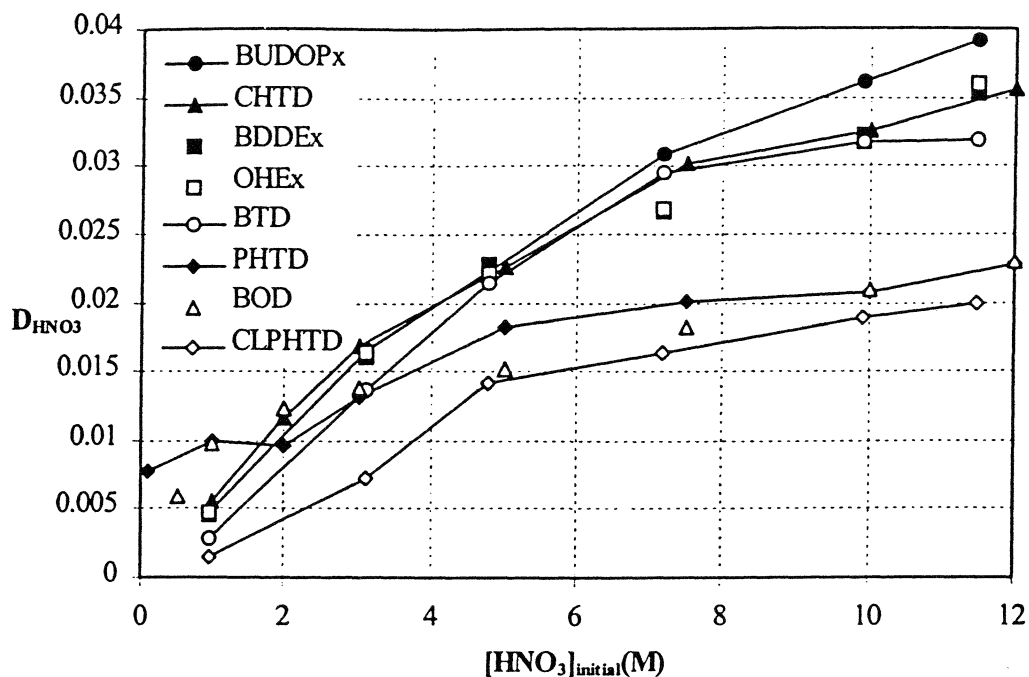


FIGURE 3. Nitric acid extraction with 0.1M of the different malonamides in *tert*-butylbenzene (room temperature).

oxyalkylated malonamides, remains unbonded to the metal while the malonamide is coordinated only through the two carbonyl oxygen atoms [17]. Polydentate extractants that coordinate to the metal with nitrogen atoms, like TPTZ (tripyrindyl triazine) or terpyridine, have however shown good separation efficiency,  $D_{Am}/D_{Eu} \approx 10$ , for trivalent actinides over lanthanides, possibly owing to a more covalent character of the actinide-nitrogen bond compared to the lanthanide-nitrogen bond [18,19].

#### Nitric Acid Extraction and Protonation

Possible protonation of the malonamide needs to be taken into account when metal extraction from relatively high nitric acid concentrations is considered. During the extraction, the proton or nitric acid and the metal ion are competing for the same binding sites in the malonamide, the carbonyl oxygens. Previous studies have shown that protonation occurs on the carbonyl oxygens rather than on the nitrogens [16], and this is supported by *ab initio* calculations performed on protonated malonamides [15]. For nitric acid extraction, as presented in Figure 3,

the concentration of nitric acid or protons in the organic phase after extraction is also consistent with basicity data, higher nitric acid extraction for malonamides with high basicity and lowest for the least basic ligands.

The small difference in nitric acid extraction between the oxyalkyl substituted malonamides and BTM and CHTD is not enough to be explained by the difference in basicity. BUDOPX even shows the highest nitric acid extraction of all malonamides when extracted from 8-12M HNO<sub>3</sub> even though it is not the most basic molecule.

A higher nitric acid extraction by oxyalkylated malonamides compared to alkyl substituted malonamides was also found by Nakamura *et al.* [20]. The extra oxygen in the carbon chain on the central carbon might increase the nitric acid extraction owing to the possibility of forming hydrogen bonds or network hydrogen bonds involving water molecules, nitric acid molecules and other malonamides.

The average numbers of HNO<sub>3</sub> molecules per malonamide molecule in the organic phase after extraction with 0.1M malonamide from different nitric acid concentrations is shown in Table 7. Up to 4 molecules of nitric acid per each malonamide were observed when extracted from 12M nitric acid with the more basic molecules, while only 2-3 nitric acid molecules per malonamide were observed for CLPHTD, PHTD and also BOD. The nitric acid extraction with BOD is lower than expected from its basicity, but the long, lipophilic chain on the central carbon seems to influence the extraction of nitric acid.

The number of HNO<sub>3</sub> molecules per malonamide were shown to be independent of the malonamide concentration used [21]. The relatively large amount of HNO<sub>3</sub> in the organic phase indicates that there are several HNO<sub>3</sub>-malonamide species present. Modelling of nitric acid extraction data with CHTD and PHTD supports the presence in the organic phase of several HNO<sub>3</sub>-malonamide species such as L·HNO<sub>3</sub>, L<sub>2</sub>·HNO<sub>3</sub>, L·(HNO<sub>3</sub>)<sub>2</sub>, L·(HNO<sub>3</sub>)<sub>3</sub> and possibly also L·(HNO<sub>3</sub>)<sub>4</sub>, where L is the malonamide [11]. These species have been confirmed by IR spectroscopy studies [16, 22, 23].

TABLE 7.

Average number of HNO<sub>3</sub> molecules per malonamide molecule when extracted from different nitric acid concentrations with 0.1M malonamide in *tert*-butylbenzene (room temperature).

[HNO <sub>3</sub> ] (M)	Average number of HNO <sub>3</sub> molecules per malonamide molecule							
	BTD	BOD	PHTD	CLPHTD	CHTD	OHE <sub>x</sub>	BDDE <sub>x</sub>	BUDOP <sub>x</sub>
1	0.028	0.099	0.099	0.015	0.052	0.046	0.044	0.045
3	0.41	0.42	0.40	0.22	0.51	0.50	0.48	0.50
5	0.99	0.78	0.91	0.66	1.1	1.0	1.0	1.0
7.5	2.0	1.4	1.5	1.1	2.2	1.9	1.8	2.1
10	3.0	2.1	2.1	1.8	3.2	3.0	3.1	3.5
12	3.6	2.8	2.8	2.3	4.1	3.9	3.9	4.3

#### Water Extraction

Small amounts of water are present in the organic phase after extraction and the extracted water could either be extracted by the malonamide itself, malonamide-HNO<sub>3</sub> species or be solubilised by the different species present in the organic phase. Water has also been found in crystal structures of neodymium-trinitrato and ytterbium-trinitrato N,N'-dimethyl-N,N'-diphenylmalonamide complexes [4]. The water concentration in the organic phase extracted by PHTD and CHTD, was determined by the Karl-Fischer method. The amount of water extracted by the diluent, *tert*-butylbenzene, was negligible.

The average number of water molecules per malonamide extracted by CHTD increases constantly with increasing nitric acid concentration up to about 1 water molecule per malonamide at 12 M HNO<sub>3</sub>, Figure 4. The number of water molecules extracted from LiNO<sub>3</sub> solution is however constant, around 0.2 water molecules per malonamide, for all LiNO<sub>3</sub> concentrations studied and was the same for both CHTD and PHTD. This indicates that the larger amount of water extracted from higher nitric acid concentrations is solubilised or co-extracted by malonamide-HNO<sub>3</sub> species rather than extracted by the malonamide itself.

The water extracted from nitric acid solution with PHTD shows a rather different behaviour, Figure 5. The number of water molecules per malonamide increases with greater nitric acid concentration up to about 5M but is thereafter constant, at about 0.8 water molecules per malonamide.

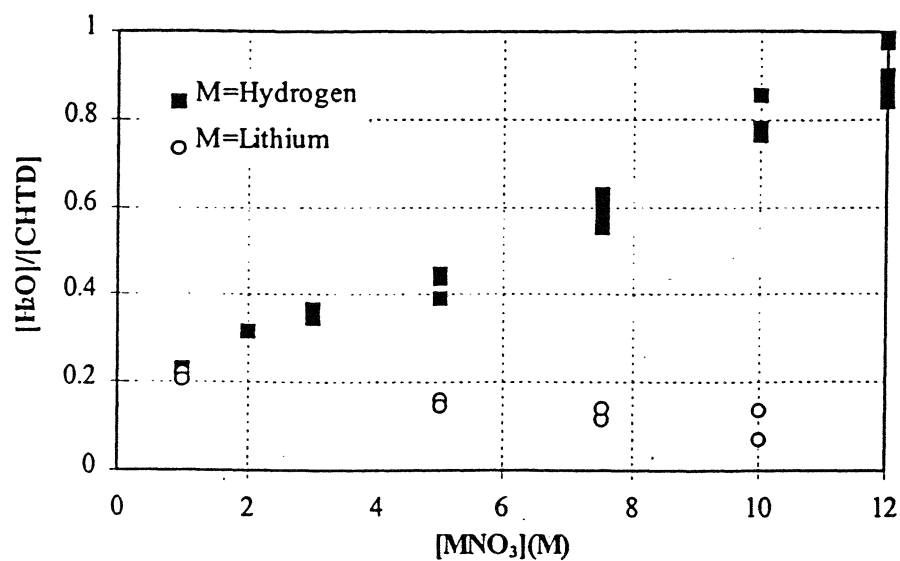


FIGURE 4. Average number of water molecules per malonamide molecule when extracted from  $\text{HNO}_3$  or  $\text{LiNO}_3$  with 0.3M CHTD in *tert*-butylbenzene (room temperature).

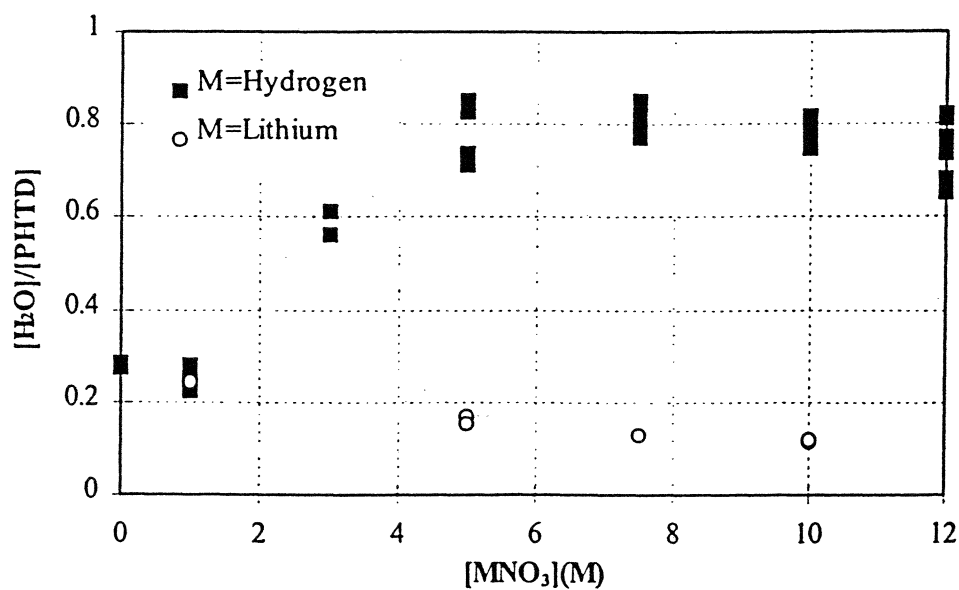


FIGURE 5. Average number of water molecules per malonamide molecule when extracted from  $\text{HNO}_3$  or  $\text{LiNO}_3$  with 0.3M PHTD in *tert*-butylbenzene (room temperature).

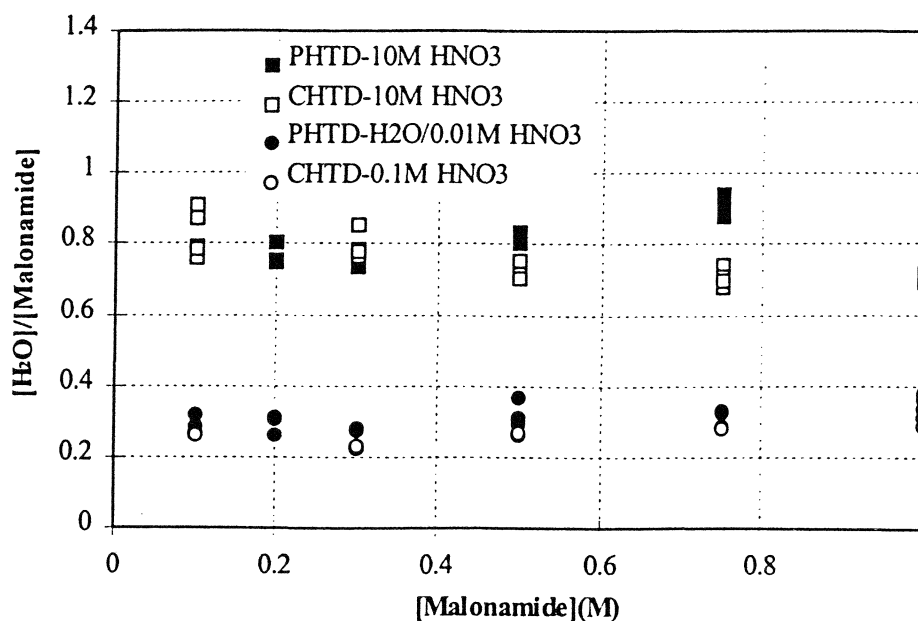


FIGURE 6. Average number of water molecules per malonamide molecule when extracted from HNO<sub>3</sub> or water with different malonamide concentration in *tert*-butylbenzene (room temperature).

The relationship between malonamide concentration and water extraction was studied at high and low acidities, Figure 6. Extraction from pure water was only conducted with PHTD up to 0.3M owing to disturbance from a third phase at higher malonamide concentrations. An acidity of 0.01M nitric acid was, therefore, used for higher PHTD concentrations and 0.1M nitric acid concentration was used for all CHTD concentrations at low acidity to eliminate third phase formation. No significant difference in extraction was observed when extracted from pure water compared to 0.1M HNO<sub>3</sub>. The amount of water extracted is almost independent of the malonamide concentration, a result which supports the assumption that the extracted water is solubilised or co-extracted by malonamide-HNO<sub>3</sub> species. About 0.3 water molecules per malonamide are extracted at low acidity.

The water in the organic phase, when extracted from aqueous solution of low acidity, could be modelled as extracted L·H<sub>2</sub>O and L<sub>2</sub>·H<sub>2</sub>O species up to at least 1M malonamide. However, Nigond *et al.* showed in previous studies that the water extraction with malonamide concentrations higher than 1M could not be explained by these species [16]. The increase was instead explained by a probable

change in a physical parameter such as the dielectric constant at higher malonamide concentrations. Their IR spectroscopic data showed no change in the carbonyl bands when water was present in the organic phase, which rather indicates water solubilisation in the organic phase than formation of hydrated species. A shift in the carbonyl spectra was also observed by  $^{13}\text{C}$  NMR which might indicate a weak hydrogen bond between carbonyl and water [16].

At high acidity, 10M  $\text{HNO}_3$ , about 0.8 water molecules per malonamide are extracted for all malonamide concentrations studied. A slight increase is, however, seen for PHTD at malonamide concentrations above 0.7M. Modelling of the extraction data showed that the water extraction at this high acidity could neither be explained by  $\text{L}_n \cdot (\text{H}_2\text{O})_m$  ( $n \leq 2$ ,  $m = 1$ ) species nor hydrated  $\text{L}_p \cdot (\text{HNO}_3)_q \cdot (\text{H}_2\text{O})_r$  ( $p \leq 2$ ,  $q = 1$ ,  $r = 1$ ) species.

#### Basicity Calculations

Some quantum mechanic calculations were carried out in order to investigate if calculated parameters, such as charge density, electric potential etc., could be related to the experimentally determined basicities. If an important chemical property like basicity, which is related to extraction ability, could be calculated it would simplify the design of future ligands.

As a first approach, semi-empirical single point calculations, using the MOPAC program [6], were carried out but no apparent correlation could be found between basicity and different calculated parameters like charge density on the binding site, electric potential, enthalpy of formation or total electronic energy. It was hard to calculate accurately the small differences in the molecular structure with the more simplified semi-empirical methods. A better result was achieved with *ab initio* methods using the Gaussian 94 software and a Hartree-Fock approach with a 3-21G basis set for the geometry optimisation and 6-31G\* basis set for the single point calculations. Several model structures of malonamides with different substituents were built from the molecular conformations found in crystal structures of related compounds. The long carbon chain at the central carbon which is needed to achieve enough lipophilicity in the extractions, was replaced

TABLE 8.

Average electric potential on the carbonyl oxygens for some different malonamides calculated by Gaussian 94 HF/6-31G\*, geometry optimised with 3-21G basis set.

R <sub>1</sub>	R <sub>2</sub>	Electric Potential (a.u.)
4-chlorophenyl	H	-22.3485
2,6-dichlorophenyl	H	-22.3526
phenyl	-CH <sub>2</sub> OC <sub>3</sub> H <sub>7</sub>	-22.3608
phenyl	H	-22.3609
cyclohexyl	H	-22.3610
phenyl	-C <sub>4</sub> H <sub>9</sub>	-22.3626

by a hydrogen atom or a shorter carbon chain to decrease the computation time. The introduction of a carbon chain on the central carbon was assumed to change the calculated parameter to the same extent for the different malonamides. Substituents that were expected to influence the charge distribution on the carbonyl groups were attached on the nitrogens and central carbons in the malonamides.

The charge density was expected to be related to the basicity but the electric potential was the only one of the different calculated parameters that could be correlated to the basicity. The most basic site in a molecule should correspond to the atom with the most negative electric potential and can, therefore, be used to compare the basicity of different molecules. The calculated electric potentials are shown in Table 8. They are ordered from the lowest electric potential (lowest basicity) to the highest electric potential (highest basicity).

The relative order of basicity is in good agreement with experimental data. The phenyl substituted malonamides have lower experimental basicities than those substituted with cyclohexyl groups. The malonamides with an oxyalkyl substituent on the central carbon (R<sub>2</sub>) is less basic than the malonamide substituted with an alkyl chain, which is in agreement with Table 8.

A more sophisticated approach was also considered, which involved the calculation of gas-phase basicity by using calculated thermodynamic quantities.

Gas-phase basicity is defined as the negative of the Gibbs free energy of the protonation reaction  $L + H^+ \rightleftharpoons LH^+$ , where L is the ligand. The more negative the  $\Delta G$  the more basic the molecule. Solvation effects was not considered and thus the relative order of free energy of protonation in solution is assumed to be close to the free energy in the gas phase. The method for calculating the free energies for the protonation reaction at 25°C is well established [24-26]. The following equations (1)-(4) are required.

$$\Delta G_R = \Delta H_R - T\Delta S_R \quad (1)$$

$$-T\Delta S_R = -298.15[S(LH^+) - S(L) - S(H^+)] \quad (2)$$

$$\Delta H_R = E(LH^+) - E(L) - E(H^+) + \Delta(PV) \quad (3)$$

$$E = E_{elec} + E_{ZPE} + (E - E_0) \quad (4)$$

$E_{elec}$  is the energy of the geometry optimised structure at 0 K,  $E_{ZPE}$  is the zero-point energy and  $(E - E_0)$  is the energy difference between 0 and 298.15 K. A correction factor of 0.91 is used to convert zero-point vibrational energy into heat of formation at 0 K [27]. The electronic energy for the proton is zero and the only energy term that contributes to  $E(H^+)$  is the translational energy which is equal to  $3/2RT$ . Since one mole of gas disappears in the reaction the  $\Delta(PV)$  term is equal to  $-RT$  and the entropy term of a free proton is equal to 7.76 kcal/mol [28, 29], equation (5) is obtained.

$$\Delta H_R = E(LH^+) - E(L) - 3/2RT - RT = E(LH^+) - E(L) - 0.889 \text{ kcal/mol} \quad (5)$$

The energies and entropies for the unprotonated (L) and protonated ( $LH^+$ ) malonamides were obtained from frequency calculations preceded by a full geometry optimisation, using the Gaussian 94 software.

The calculated  $\Delta G$  values in Table 9 are ordered from the least basic to the most basic structure. These calculated basicity data show the same relative order of basicity as the experimentally determined basicities. Malonamides with aromatic groups on the nitrogens show lower basicity than malonamides with non-aromatic

TABLE 9.

The difference free Gibbs energy for the protonation reaction of some different substituted malonamides (Gaussian94, HF/6-31G\*, full geometry optimisation).

R	R <sub>2</sub>	$\Delta G_R$ (kcal/mol)
4-chlorophenyl	H	-215.30
phenyl	H	-228.56
2,6-dichlorophenyl	H	-229.35
cyclohexyl	H	-230.71

TABLE 10.

The difference in Gibbs free energy for the protonation reaction of some different substituted malonamides (Gaussian94, HF/6-31G, full geometry optimisation).

R <sub>1</sub>	R <sub>2</sub>	$\Delta G_R$ (kcal/mol)
phenyl	-C <sub>2</sub> H <sub>4</sub> OCH <sub>3</sub>	-226.88
phenyl	-C <sub>4</sub> H <sub>9</sub>	-229.20

groups and a chlorine in *para* position on the phenyl results in even lower basicity.

The position of the chlorines on the phenyl groups seems to have a great influence on the basicities. The calculated basicity for the 2,6-dichlorophenyl derivative was shown to be even higher than the phenyl substituent. On the contrary, the electric potential data in Table 8 indicate that the phenyl substituted malonamide is more basic than the 2,6-dichlorophenyl derivative. There are, so far, no experimental data for the 2,6-dichlorophenyl ligand to verify either of these observations.

The calculated basicities for malonamides with an alkoxy- or alkyl group on the central carbon is also consistent with the experimentally determined basicity, Table 10. The malonamide substituted with an alkoxy group has a less negative  $\Delta G$ , less basic, than the malonamide with an alkyl group on the central carbon. In order to save computational time it proved necessary to obtain the result in Table 10 with the 6-31G basis set and not the 6-31G\* basis set as used in Table 9. The values in the two tables are therefore not directly comparable.

## CONCLUSIONS

Malonamides substituted with phenyl groups on the nitrogens showed to have the lowest basicity of all studied malonamides. Malonamides with non-aromatic substituents on the nitrogens and substituted with oxyalkyl groups on the central carbon showed lower basicity than malonamides with alkyl groups in this position. Malonamides are, as a group, more basic than phosphorous-based extractants and monoamides and the competition between protons and metal cations for the binding site is therefore observed at a lower acidity for malonamides [30]. A slight increase in basicity for the least basic extractants, such as phosphorous-based extractants and monoamides, result in an increase in the extractant strength since protons are not competing with the metal ions to a significant extent at this acidity. Organophosphorous extractants and monoamides thus show better metal extraction with the extractants with highest basicity, at least at low acidity. Malonamides, on the other hand, show a significant increase in the binding of a proton at the binding site when the basicity increases and this competition causes a decrease in metal extraction at a given pH. Malonamides with lowest basicity therefore show the best metal extraction.

However, CMPO derivatives show a similar relation as malonamides at high acidities [12]. CMPO derivatives have been suggested to act as monodentate ligands where the amide function act as an internal buffer for protons and protect the metal-phosphoryl bond from attack from protons [8]. The interaction of protons with the binding site will thus show up at a higher acidity for the CMPO derivatives than for the malonamides.

Work by Cuillerdier *et al.* indicate that the more basic malonamides were shown to give slightly better extraction than the less basic ones at low acidity, like the phosphorous based extractants and monoamides do [31]. This effect was not seen in this work, but these changes might be hard to observe for the malonamides studied since their interaction with protons is significant even at low acidity, due to their higher basicity.

More quantum chemical calculations and experimental basicity measurements on new malonamides are needed to verify the relation between calculated and experimental basicity.

### ACKNOWLEDGEMENTS

We wish to thank the Swedish Nuclear and Waste Management Co., SKB, and the European Union (NEWPART CT FI4I-CT96-0010) for the financial support and the High Performance Computer Centre (HPCC) at the University of Reading for the use of the SG Origin 2000.

### REFERENCES

- [1] NIGOND, L., Thèse de Doctorat D'Université de Clermont-Ferrand II, CEA-R-5610, 1992
- [2] MADIC, C. AND HUDSON, M.J., EUR 18038 EN, 1998
- [3] MUSIKAS, C., *Inorg. Chim. Acta*, **140**, 197 (1987)
- [4] CHAN, G.Y.S., DREW, M.G.B., HUDSON, M.J., IVESON, P.B., LILJENZIN, J.O., SKÅLBERG, M., SPJUTH, L. AND MADIC, C., *J. Chem. Soc., Dalton Trans.*, 649, (1997)
- [5] CERIU2, Molecular Simulations Inc., San Diego, California, USA
- [6] STEWART, J. J. P., MOPAC version 6.0, A Semi-Empirical Molecular Orbital Program, *J. Comp-Aided Mol. Design*, **4**, 45 (1991)
- [7] *Gaussian 94 (software), Revision A1*, FRISCH, M.J., TRUCKS, G.W., SCHLEGEL, H.B., GILL, P.M.W., JOHNSON, B.G., ROBB, M.A., CHEESEMAN, J.R., KEITH, T.A., PETERSSON, G.A., MONTGOMERY, J.A., RAGHAVACHARI, K., AL-LAHAM, M.A., ZAKRZEWSKI, V.G., ORTIZ, J.V., FORESMAN J.B., CIOSLOWSKI, J., STEFANOV, B.B., NANAYAKKARA, A., CHALLALCOMBE, M., PENG, C.Y., AYALA, P.Y., CHEN, W., WONG, M.W., ANDREWS, J.L., REPLOGLE, E.S., GOMPERS, R., MARTIN, R.L., FOX, D.L., BINKLEY, J.S., DEFREES, D.J., BAKER, J., STEWART, J.P., HEAD-GORDON, M., GONZALEZ, C., AND POPLE, J.A., Gaussian Inc., Pittsburgh, PA, 1995
- [8] KALINA, D.G., HORWITZ, E.P., KAPLAN, L., AND MUSCATELLO A.C., *Sep. Sci. Technol.*, **16**(9), 1127 (1981)
- [9] MASON, G.W., AND GRIFFIN, H.E., in Am. Chem. Soc. series no. 117, Actinide Separations, Navratil J.D., and Shulz, W.W., Eds., Washington D.C., 1980, p. 89

- [10] ROZEN, A.M., NIKIFOROV, A.S., NIKOLOTOVA, Z.I., AND KARTESHEVA, N.A., *Soviet Atomic Energy*, 59(6), 982 (1985)
- [11] SIDDALL III, T.H., *J. Phys. Chem.*, 64, 1863 (1960)
- [12] HORWITZ, E.P., AND CHIARIZIA, R., In Separation Techniques in Nuclear Waste Management, Chapter 1, Carleson, T.E., Chipman, N.A., Wai, C.M., Ed., CRC Press, Inc., Florida, 1996
- [13] CHIARIZIA, R., AND HORWITZ, E.P., *Solvent Extr. Ion Exch.* 10(1), 101-118 (1992)
- [14] FRITZ, J.S., *Anal. Chem.*, 25(3), 407 (1953)
- [15] SPJUTH, L., LILJENZIN, J.O., HUDSON, M.J., DREW, M.G.B., IVESON, P.B. AND MADIC C., *Proceedings in International Solvent Extraction Conference, Barcelona 1999*
- [16] NIGOND, L., MUSIKAS, C., AND CUILLERDIER, C., *Solvent Extr. Ion Exch.* 12(2), 261 (1994)
- [17] IVESON, P.B., DREW, M.G.B., HUDSON, M.J., AND MADIC, C., *J. Chem Soc. Dalton*, submitted (1999)
- [18] VITORGE, P., Thèse de Doctorat Thèse a l'Université Pierre et Marie Curie,, CEA-R-5270, 1984
- [19] HAGSTRÖM, I., SPJUTH, L., LILJENZIN, J.O., SKÅLBERG, M., HUDSON, M.J., IVESON, P.B., MADIC, C., CORDIER, P.Y., HILL, C., AND FRANCOIS, N., *Solvent Extr. Ion Exch.* 17(2), 221 (1999)
- [20] NAKAMURA, T., MATSUDA, Y., AND MIYAKE, C., in Materials Research Society Symposium Proceedings, 353(2), 1293-1300, 1995
- [21] SPJUTH, L., LILJENZIN, J.O., SKÅLBERG, M., HUDSON, M.J., CHAN, G.Y.S., DREW, M.G.B., FEAVIOUR, M., AND MADIC, C., *Radiochimica Acta*, 78, 39 (1997)
- [22] MUSIKAS, C., AND HUBERT, H., *Solvent Extr. Ion Exch.* 5(1), 151 (1987)
- [23] TIAN, Q. Z., AND HUGHES, M. A., *Hydrometallurgy*, 36(3), 315 (1994)
- [24] ZHANG, K., ZIMMERMAN, D.M., CHUNG-PHILLIPS, A., CASSADY C.J., *J. Am. Chem. Soc.*, 115, 10812, (1993)
- [25] JEBBER, K.A., ZHANG, K., CASSADY, C.J., CHUNG-PHILLIPS, A., *J. Am. Chem. Soc.* 118, 10515 (1996)
- [26] ZHANG, K., CASSADY C.J., CHUNG-PHILLIPS, A., *J. Am. Chem. Soc.*, 116, 11512 (1994)
- [27] GREV, R.S., JANSSEN, C.L. AND SCHAEFER, H.F.III., *J. Chem. Phys.* 95(7), 5128 (1991)
- [28] STULL, D.R. AND PROPHET, H., in JANAF Themodynamical Tables, *Nat. Stand. Ref. Data Ser.*, *Nat. Bur. Stand.*, 37, 1971
- [29] AUE, D.H. AND BOWERS, M.T., In Gas-Phase Ion Chemistry, Vol.2, Bowers, M.T., Ed., Academic Press, New York, 1979, p. 1
- [30] CONDAMINES, N., AND MUSIKAS, C., *Solvent Extr. Ion Exch.* 6(6), 1007 (1988)

- [31] CUILLERDIER, C., MUSIKAS, C., HOEL, P., NIGOND, L., AND VITART, X.,  
Sep. Sci. Technol. 26(9), 1229 (1991)

Received by Editor  
June 8, 1999

# Appendix

## V

**Influence of Organic Phase Composition  
on the Extraction of Trivalent Actinides**

**Mikael Nilsson  
2000**

**EXAMENSARBETE 20 P**

**DEPARTMENT OF NUCLEAR CHEMISTRY  
CHALMERS UNIVERSITY OF TECHNOLOGY  
GÖTEBORG  
SWEDEN  
00 11 24**

**Examinator: Prof. Jan-Olov Liljenzin  
Supervisors: Prof. Jan-Olov Liljenzin, Prof. Gunnar Skarnemark  
Christian Ekberg and Sofie Andersson**

## Abstract

Spent fuel from nuclear power reactors is one of the biggest issues concerning nuclear energy production systems. The real problem with the spent fuel is the fact that it is radioactive and contains nuclides with long half-lives. Instead of burying this problem for millions of years, as Swedish regulations direct, there are some methods to reduce this problem. One of these methods is transmutation.

In the transmutation process, radioactive waste with long half-life is reduced to short-lived or stable nuclides. This process demands a separation system with sufficiently high yield. Such a separation may be achieved by liquid-liquid extraction, but finding an efficient system requires large amounts of time and money.

In this diploma work a model that can be used to calculate the result of a liquid-liquid extraction without performing the actual experiment has been developed. The model is based on Hansen solubility parameters. Solubility parameters are used to describe the solubility characteristics of a substance and are derived from certain physical properties of the substance.

The model was applied to some measured extraction cases, where it performed quite well. Comparing the calculated values of distribution coefficients with those found experimentally gives a good agreement in most cases.

# Table of Contents

<b>1. Introduction.....</b>	<b>1</b>
<b>2. Transmutation.....</b>	<b>2</b>
<b>3. Separation.....</b>	<b>6</b>
3.1 Solvent extraction.....	6
3.2 Synergistic extraction.....	7
<b>4. Solubility parameters.....</b>	<b>10</b>
4.1 Hildebrand solubility parameter.....	10
4.2 Hansen solubility parameters.....	11
4.3 Applications for solubility parameters.....	14
<b>5. Experimental.....</b>	<b>16</b>
5.1 Extraction procedures.....	16
5.2 Radionuclides.....	18
5.3 Detection.....	19
<b>6. Results.....</b>	<b>21</b>
<b>7. Conclusions.....</b>	<b>27</b>
<b>8. Acknowledgements.....</b>	<b>28</b>
<b>9. References.....</b>	<b>29</b>
<b>Appendix.....</b>	<b>I</b>

## 1. Introduction

Nuclear reactors produce, apart from large amounts of energy, radioactive waste. A big issue concerning this waste is how and where to store it. The current solution in Sweden is to store it deep underground for a very long time. The problem with this kind of repository is that the waste must be stored for such a long time that there is no way to know what might happen during the time it will be stored. Another aspect is that the spent fuel still contains much unused energy and it may be seen as a waste of raw material to bury it for an unsurveyable future.

One alternative to this final storage concept is a method called transmutation. Transmutation is a way to reduce the storage time of radiotoxic material, by converting long-lived nuclides to short-lived or stable ones, from millions of years down to hundreds of years and at the same time gain energy. If the transmutation process is to be feasible it must be combined with partitioning, i.e. separation of the different elements in the spent nuclear fuel. Separation is usually performed by some means of extraction. As with all industrial processes, high efficiency must be attained. To achieve this, different extraction reagents and different compositions of extraction solvents must be thoroughly investigated.

It would be advantageous to be able to calculate the outcome of a separation based only on data from substances included in the extraction, i.e. without performing the actual experiment. This would give a tool for reducing the time needed for the thorough investigation mentioned earlier. Of course, interesting results must be verified experimentally.

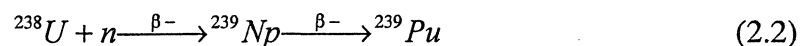
The purpose of this diploma work is to test different combinations of organic solvents in liquid-liquid extraction experiments. These extraction data are then used in an attempt to find a model that can express the degree of separation based on the solubility parameters of the involved organic solvents. Solubility parameter theory is widely used in the plastic and paint industry and thus data can be found for a large number of solvents.

## 2. Transmutation

When a thermal reactor is running the fission process can be summarised as:



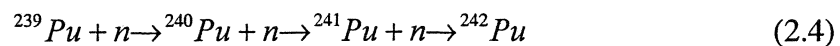
For each neutron used in the fission  $2-3(=\nu)$  new neutrons are released. These new neutrons can be used to split other  $^{235}\text{U}$  nuclei, which leads to a nuclear chain reaction system. Most of the uranium in the fuel is the  $^{238}\text{U}$ -isotope, which undergoes neutron capture in the reactor:



The  $^{239}\text{Pu}$  is fissile, i.e. can be split through fission, in a thermal reactor:



but it can also capture neutrons which leads to new Pu-isotopes:



Of these isotopes  $^{239}\text{Pu}$  and  $^{241}\text{Pu}$  are fissile in a thermal reactor. The other two isotopes decrease the neutron economy in the reactor making it less efficient.

The fuel elements are used to a much less than 100% burnup of the  $^{235}\text{U}$  originally present. This is due to the fission products and somewhat to the heavier non-fissile elements. During fission these fission products accumulate in the fuel and since some of them have very high neutron capture cross sections, they compete with the fission chain reaction for the neutrons. Instead of releasing new neutrons, the fission products absorb neutrons leading to a net decrease of neutrons in the reactor. In this way the fuel becomes "poisoned" with fission products and must therefore be removed from the reactor core and replaced with new fuel. The removed fuel elements are considered spent and according to Swedish regulations they are to be stored in an underground repository for millions of years until classified safe for the environment. Since there are still many fissile nuclides in the spent fuel, it could be seen as a waste of raw material to put it in a storage.

Spent reactor fuel contains about 35 different elements. Most of the fuel still consists of uranium but there is also some plutonium (0.9 %) and fission products (3.3%). Actinides, other than U and Pu, are also present in spent fuel, a result of neutron capture followed by  $\alpha$ - or  $\beta$ -decay.

The actinides and some of the fission products are long-lived and are the main reason why the spent fuel has to be stored for such a long time.

Through a well tested reprocessing system called the Purex process fission products and all actinides except for U and Pu are removed from the spent fuel. The U and Pu can then be used to make MOX-fuel (MOX = Mixed OXide)[1], which can be used as fuel in a standard thermal reactor since  $^{239}\text{Pu}$  and  $^{241}\text{Pu}$  are fissile. As the fission products are removed there will be no problems with the “poisoning” mentioned earlier. Fission products are of course produced anew and reprocessing of the MOX-fuel is soon necessary. This will allow a higher degree of fission efficiency regarding the  $^{235}\text{U}$ -isotope. After the MOX-fuel has been recycled 2-3 times it contains such high amounts of the Pu isotopes,  $^{240}\text{Pu}$  and  $^{242}\text{Pu}$ , that it can not be used efficiently in a thermal reactor. One way to deal with this is to run this MOX-fuel in a fast breeder reactor (FBR), which uses fast neutrons instead of thermal. These fast neutrons can split  $^{240}\text{Pu}$  and  $^{242}\text{Pu}$  efficiently and after some time in the FBR the MOX-fuel can be brought back to the thermal reactor cycle. The FBR can with some small alterations be used to produce Pu with a high concentration of the  $^{239}\text{Pu}$ -isotope, i.e. weapons grade Pu, a fact that has made the FBR’s unpopular and even prohibited. This concludes the U and Pu reprocessing cycle.

What is now left from the Purex process are fission products, of which the majority is short-lived, and some actinides. These left-overs could be considered as waste and stored as mentioned before or it could be reprocessed and reused through transmutation. Transmutation is, roughly put, a method for transforming long-lived radiotoxic isotopes into short-lived or stable ones and at the same time gain energy. This would not only raise the efficiency of the nuclear fuel usage but also reduce the amount of waste and the time it has to be stored. The complete cycle of nuclear reactors and transmutation is shown in fig 2.1.

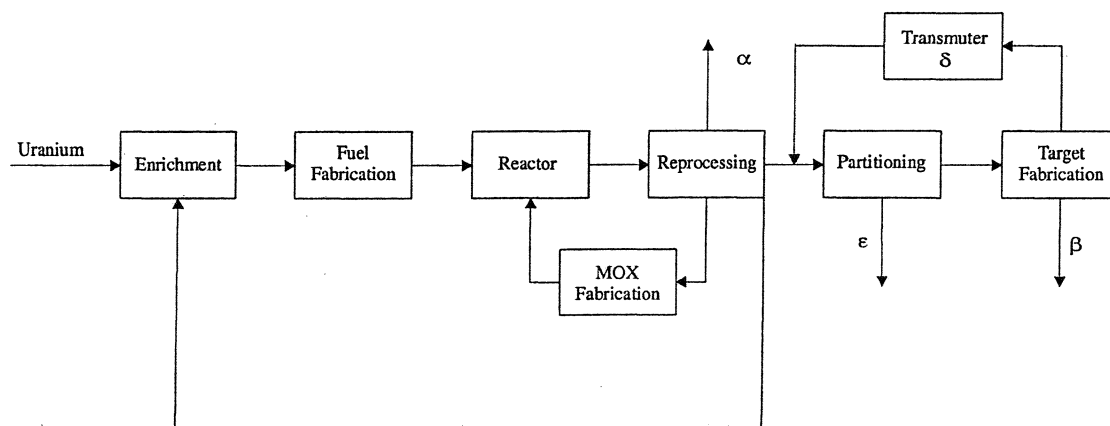
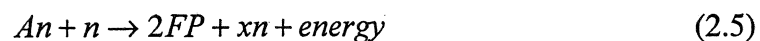


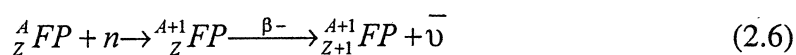
**Figure 2.1** Fuel cycle with partitioning and transmutation operations (modified from [2])

In a similar way as uranium is fissioned in the original fuel, most actinides can be split through neutron induced fission. The first thing to accomplish is therefore to separate the actinides from the fission products because of the “poisoning” mentioned earlier. This is carried out in a partitioning step through some means of separation (see chapter 3 and fig 2.2). The fraction containing the actinides can be used as fuel in special contraptions, similar to a thorium reactor (fig 2.2), where they are fissioned [2]:



The actinides are considered transmuted by fission and new neutrons are released that can be used for further transmutation reactions. Since new FP’s are produced when transmuting actinides, a partitioning step must be carried out once in a while to ensure efficient burnup.

The final fraction containing the fission product is still considered long-lived in a radiotoxic sense. The long-lived fission products, for example  $^{90}\text{Sr}$  and  $^{137}\text{Cs}$ , can be transmuted into short-lived or stable isotopes by charged particle or neutron irradiation. Through this method the fission products undergo neutron capture and subsequent  $\alpha$ -,  $\beta$ - or  $\gamma$ -decay, for example [2]:



In the reaction  $\bar{\nu}$  denotes an antineutrino.

This neutron capture can take place in the same reactor in which the actinides are fissioned. In the end there will be some waste that has to be stored but the amount has been reduced significantly.

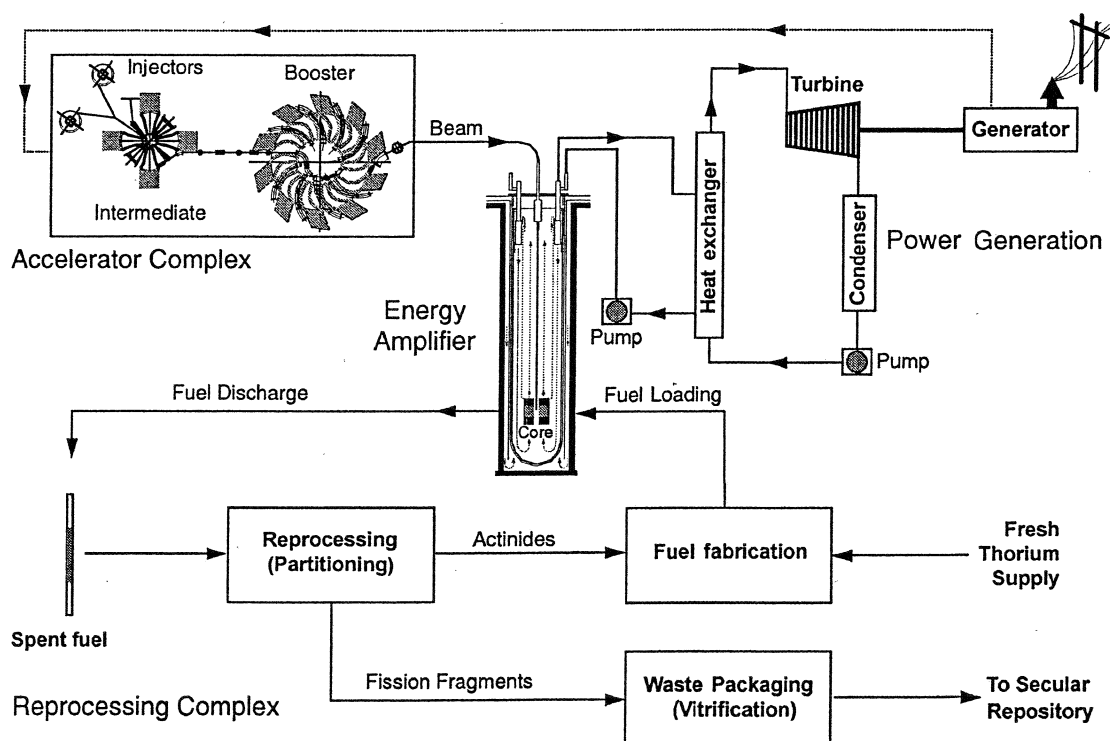


**Figure 2.2** *A conceivable thorium reactor. If actinides are recycled in this system, it can be considered as a transmutation facility. The accelerator creates a beam of protons which radiates liquid lead in the core leading to spallation in the lead which yields around 17 fast neutrons per spallation. These neutrons are used for fission of actinides or neutron capture for fission products. The lead is cooled in a heat exchanger creating steam which runs the turbine.*

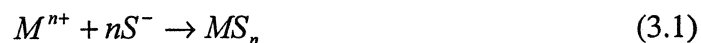
### 3. Separation

#### 3.1 Solvent extraction

The purpose of solvent extraction is to remove a specific element or substance from one solution and introducing it in another solution, thereby separating the element or substance from other elements or substances in the original solution. An extraction system consists of two phases that are almost immiscible. In this work they are assumed to be completely immiscible. In many cases an extracting reagent is added to the system in order to facilitate the extraction. This extracting reagent might be one of several kinds of reagents e.g. chelating reagents or ion exchange reagents. One of the two phases is usually aqueous and the other phase is organic.

In laboratory scale, the extraction itself may be performed by contacting the phases in some container, e.g. shaking in a test tube. After that the two phases are allowed to separate, either with the help of some device, e.g. a centrifuge, or by gravity. A sample is then taken from each phase and measured upon to get the distribution of the desired element between the two phases, i.e. if the extraction properties of the extraction system were good or not.

In the case of a metal ion,  $M^{n+}$ , being extracted from the aqueous phase, an organic or inorganic ligand,  $S^-$ , can bind to the ion giving an uncharged complex:



This complex will be distributed between the two phases and its distribution can be expressed as a distribution ratio,  $D_M$ , for that particular complex in that particular extraction system [3]:

$$D_M = \frac{[M]_{tot,org}}{[M]_{tot,aq}} = \frac{\text{Total concentration of } M \text{ in the organic phase}}{\text{Total concentration of } M \text{ in the aqueous phase}} \quad (3.2)$$

The distribution ratio depends on the hydrophilic/hydrophobic character of the complex and of the ligand concentration,  $[S^-]$ .

If a radioactive metal ion is to be extracted the distribution ratio,  $D_M$ , is easily calculated by measuring the specific radioactivity in each phase and use the fact that the concentration of a radioactive isotope is proportional to the specific radioactivity [3]:

$$D_M = \frac{[M]_{tot,org}}{[M]_{tot,aq}} = \frac{\text{Specific radioactivity in the organic phase}}{\text{Specific radioactivity in the aqueous phase}} = \frac{S_{org}}{S_{aq}} \quad (3.3)$$

### 3.2 Synergistic extraction

In the solvent extraction of a metal ion (M) synergistic extraction by using an acidic chelating extractant (HA) and a neutral ligand (S) has proven to be very effective [4].

The synergistic extraction is built up in two main processes. First the metal ion, M, and the acidic chelating extractant, HA, forms a neutral complex,  $MA_n$ , which is extracted into the organic phase. Then  $MA_n$  is bound to m molecules of S forming an adduct,  $MA_nS_m$ , in the organic phase [5].

This diploma work discusses the synergistic extraction of trivalent metal ions with 2-bromodecanoic acid (fig.3.1) as the acidic chelating extractant, HA, and the neutral ligand 2,2':6,2''-terpyridine (fig. 3.2), S, called terpy .

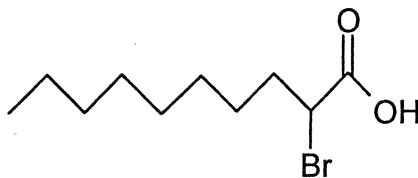


**Figure 3.1** 2-Bromodecanoic acid.

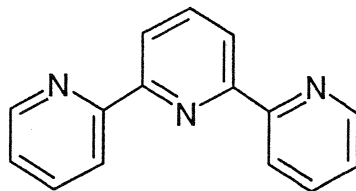


**Figure 3.2** 2,2':6,2''-terpyridine

When terpy is transferred to the aqueous phase it can be protonated as follows [4]:



The overlining means that the element or specie is in the organic phase. Recent work indicates that terpy may bind a third proton [6].

The protonisation of terpy is graphically described in fig. 3.3.

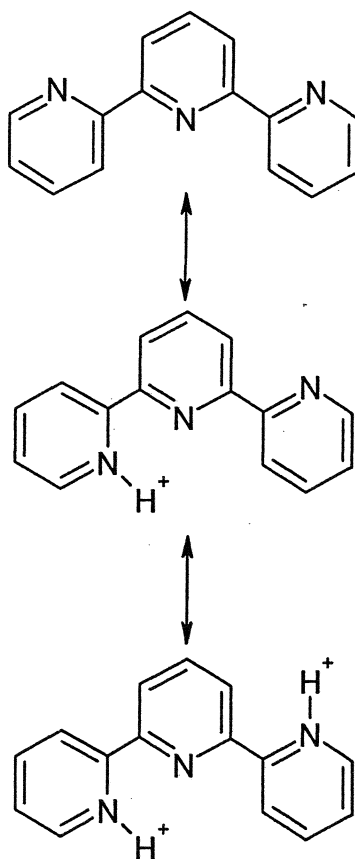


**Figure 3.3** The protonisation of terpy

The 2-bromodecanoic acid is transferred to the aqueous phase where it dissociates:



As stated earlier complexation occurs between the M(III)-ions and A<sup>-</sup> in the aqueous phase. The neutral complex is then distributed between the phases:



In non polar diluents 2-bromodecanoic acid is known to dimerise [7]:



This makes it possible for metallic complexes containing both dimerised 2-bromodecanoic acid and terpy to be formed in the organic phase:



As the mechanism suggests a range of different mixed complexes can be present. The distribution ratio of the trivalent metal ion can be described as [4]:

$$D = \frac{\sum_{m=0}^M \sum_{n=0}^N [\overline{MA_3(HA)_{2m}S_n}]}{\sum_{x=0}^X [MA_x^{3-x+}]} = \frac{[M]_{tot,org}}{[M]_{tot,aq}} \quad (3.9)$$

## 4. Solubility parameters

A solvent, usually a liquid, is a substance that is able to dissolve other substances forming a homogenous mixture, a solution. The dissolved substance is called the solute and is in most cases considered to be the component present in the smallest amount.

Liquids (and solids) differ from gases in the sense that the molecules of the liquid (or solid) are held together, a phenomenon known as cohesion, in a confined space by certain intermolecular forces. The molecules are attracted to each other on an intermolecular level.

If a solution is to be formed the solvent molecules must overcome the intermolecular forces between the solute molecules and vice versa. This will make the different molecules find their way between and around each other, resulting in a homogenous mixture, a solution. This mixing works best when the intermolecular attractions of the components are similar. If the attractions are different to some extent, the strongly attracted molecules will cling together, rejecting any mixing with the weakly attracted ones, resulting in immiscibility.

### 4.1 Hildebrand solubility parameter

The relation between intermolecular attractions and solubility is reflected in the Hildebrand solubility parameter, which is a numerical value that indicates the solvency behaviour of a specific solvent. The Hildebrand solubility parameter,  $\delta$ , is defined as [8]:

$$\delta = \sqrt{c} \quad (4.1)$$

where  $c$  is the cohesive energy density of a substance.

The cohesive energy density is related to the heat of vaporisation of a liquid:

$$c = \frac{\Delta H_m - RT}{V_m} \quad (4.2)$$

$\Delta H_m$  = heat of vaporisation per mole

$R$  = gas constant

$T$  = temperature

$V_m$  = molar volume

The heat of vaporisation is the energy required to separate the molecules in a liquid from each other, turning the liquid into gas (vapour). This energy can be translated as the amount of energy that holds the molecules together. Thus the Hildebrand solubility parameter is based on the assumption that the same intermolecular attractive forces have to be overcome to vaporise a liquid as to dissolve it:

$$\delta = \left[ \frac{\Delta H_m - RT}{V_m} \right]^{1/2} \quad (4.3)$$

Similar to the miscibility problems with components of different intermolecular attraction, immiscibility will occur if the solubility parameters of the components differ too much.

## 4.2 Hansen solubility parameters

Even though solubility behaviour can be described with the Hildebrand parameter, greater accuracy is reached if the attraction forces between the molecules in a solvent is divided into different contributions. One method is to consider the total attraction force as a sum of van der Waals, polar and hydrogen bonding forces. According to this theory, three values are determined for each substance and homogenous solutions are predicted if all three values are similar.

The most widely used three component system is the parameter system developed by Charles M. Hansen 1966. Hansens parameters split the total Hildebrand values into the three parts mentioned above: dispersion, polar and hydrogen bonding [8]:

$$\delta_t^2 = \delta_d^2 + \delta_p^2 + \delta_h^2 \quad (4.4)$$

$\delta_t^2$  = total Hildebrand value

$\delta_d^2$  = dispersion component

$\delta_p^2$  = polar component

$\delta_h^2$  = hydrogen bonding component

Or described as cohesive energy density:

$$\frac{\Delta E_{t,m}}{V_m} = \frac{\Delta E_{d,m}}{V_m} + \frac{\Delta E_{p,m}}{V_m} + \frac{\Delta E_{h,m}}{V_m} \quad (4.5)$$

$\Delta E_{t,m}$  = total cohesive energy per mole of a liquid

$\Delta E_{d,m}$  = dispersion energy per mole

$\Delta E_{p,m}$  = polar energy per mole

$\Delta E_{h,m}$  = hydrogen bonding energy per mole

Hansen initially described the dispersion component by assuming that  $\Delta E_{d,m}$  for a particular substance was equal to the heat of vaporisation of the homomorph of that substance. The homomorph of a molecule is the nonpolar molecule most closely resembling it in size and shape [8]. Thus the dispersion parameter of a substance is equal to the Hildebrand parameter for the nonpolar homomorph:

$$\delta_d = \delta_{t(\text{Homomorph})} \quad (4.6)$$

This dispersion value is then subtracted from the Hildebrand value of the actual substance, giving the sum of the polar and hydrogen bonding parameters:

$$\delta_t^2 - \delta_d^2 = \delta_p^2 + \delta_h^2 \quad (4.7)$$

Later on Hansen used solubility and pigment suspension data from around 10 000 observations to make more accurate determinations of the dispersion parameter.

The hydrogen bonding component can be approximated using the fact that the energy of the OH-O bond is 20 900 joules per mole (indicated by infrared spectroscopy) [9]. From there one can simply assume that 20 900 joules of the energy of vaporisation of a substance is due to each alcohol group the molecule contains. The hydrogen bonding parameter is:

$$\delta_h^2 = \frac{20900N}{V_m} \quad (4.8)$$

$N$  = number of alcohol groups in the molecule

A method for calculating the cohesive energy contributing from permanent dipoles has been developed by Böttcher [10]:

$$W_m = -\frac{4\pi}{3} \cdot \frac{\rho \cdot N_A}{M} \cdot \frac{\epsilon_0 \epsilon - 1}{2\epsilon_0 \epsilon + n_D^2} \cdot \frac{n_D^2 + 2}{3} \mu^2 \quad (4.9)$$

Where, for the condensed phase:

$W_m$  = cohesion energy density of permanent dipoles per mole

$\rho$  = density

$M$  = molecular weight

$N_A$  = Avogadro's number

$\epsilon$  = dielectric constant, static value

$n_D$  = index of refraction for the sodium-D line

$\mu$  = dipole moment

To fit the definition of the polar parameter the energy is divided by the molar volume and it all ends up to [11]:

$$\delta_p^2 = \frac{W_m}{V_m} = \frac{12108}{V_m^2} \cdot \frac{\epsilon_0 \epsilon - 1}{2\epsilon_0 \epsilon + n_D^2} \cdot (n_D^2 + 2) \mu^2 \quad (4.10)$$

A number of procedures for calculating Hansen solubility parameters using structural group contributions have been developed. These procedures provide a fast and easy way to get an approximation of the solubility behaviour of a substance, if nothing but the structure of the molecule is known.

### 4.3 Applications of solubility parameters

For a regular solution the activity of solute A,  $a_A$ , in solvent B can be expressed as

[12]:

$$RT \ln(a_A) = RT \ln(x_A) + V_{m,A} \Phi_B^2 (\delta_A + \delta_B)^2 \quad (4.11)$$

$x$  = molar fraction

$$\Phi = \text{volume fraction: } \Phi_i = \frac{V_i}{\sum_n V_n}$$

A regular solution is defined as a solution where there are no interactions between solute and solvent, and association and molecular orientation do not change when the solution is formed. If the difference in molar volume between the solute and the solvent is taken into account, the activity for the solute is:

$$RT \ln(a_A) = RT \left[ \ln(\Phi_A) + \Phi_B \left( 1 - \frac{V_{m,A}}{V_{m,B}} \right) \right] + V_{m,A} \Phi_B^2 (\delta_A - \delta_B)^2 \quad (4.12)$$

The Hildebrand value is then divided into three parameters as described above. This will give the expression:

$$RT \ln(a_A) = RT \left[ \ln(\Phi_A) + \Phi_B \left( 1 - \frac{V_{m,A}}{V_{m,B}} \right) \right] + V_{m,A} \Phi_B^2 \left[ (\delta_{d,A} - \delta_{d,B})^2 + (\delta_{p,A} - \delta_{p,B})^2 + (\delta_{h,A} - \delta_{h,B})^2 \right] \quad (4.13a)$$

The activity for a substance in a specific phase can be written as:

$$RT \ln(a_{A,i}) = RT \left[ \ln(\Phi_{A,i}) + \Phi_i \left( 1 - \frac{V_{m,A}}{V_{m,i}} \right) \right] + V_{m,A} \Phi_i^2 \left[ (\delta_{d,A} - \delta_{d,i})^2 + (\delta_{p,A} - \delta_{p,i})^2 + (\delta_{h,A} - \delta_{h,i})^2 \right] \quad (4.13b)$$

$i$  = aq, org

At equilibrium, the activity of A is assumed to be equal in both phases:

$$RT \ln(a_{A,aq}) = RT \ln(a_{A,org}) \quad (4.14)$$

If it also is assumed that the volume fractions of water in the aq-phase and organic solvent in the org-phase both are 1,  $\Phi_{aq} = \Phi_{org} = 1$ , and considering the relation:

$$D_A = \frac{\Phi_{A,org}}{\Phi_{A,aq}} \quad (4.15)$$

the distribution,  $D_A$ , can be described as:

$$\ln(D_A) = V_{m,A} \left[ \frac{1}{V_{m,org}} - \frac{1}{V_{m,aq}} + \frac{1}{RT} (\Delta_{d,A,aq} + \Delta_{p,A,aq} + \Delta_{h,A,aq} - \Delta_{d,A,org} - \Delta_{p,A,org} - \Delta_{h,A,org}) \right] \quad (4.16)$$

$$\Delta_{d,A,aq} = (\delta_{d,A} - \delta_{d,aq})^2$$

$$\Delta_{p,A,aq} = (\delta_{p,A} - \delta_{p,aq})^2$$

$$\Delta_{h,A,aq} = (\delta_{h,A} - \delta_{h,aq})^2$$

$$\Delta_{d,A,org} = (\delta_{d,A} - \delta_{d,org})^2$$

$$\Delta_{p,A,org} = (\delta_{p,A} - \delta_{p,org})^2$$

$$\Delta_{h,A,org} = (\delta_{h,A} - \delta_{h,org})^2$$

If the composition of the aqueous phase is assumed to be constant equation 4.16 becomes:

$$\ln(D_A) = V_{m,A} \left[ \frac{1}{V_{m,org}} - \frac{1}{V_{m,aq}} + \frac{1}{RT} (K - \Delta_{d,A,org} - \Delta_{p,A,org} - \Delta_{h,A,org}) \right] \quad (4.17)$$

$$K = \Delta_{d,A,aq} + \Delta_{p,A,aq} + \Delta_{h,A,aq} \quad (4.18)$$

Equation 4.17 has 5 unknown parameters:  $K$ ,  $V_{m,A}$ ,  $\delta_{d,A}$ ,  $\delta_{p,A}$  and  $\delta_{h,A}$ . If a number of extraction experiments are carried out, the unknown parameters could be found by applying some parameter fitting algorithm on equation 4.17.

Equation 4.17 can, with all constants known, be used for estimating the distribution of substance A that would be obtained in a liquid-liquid extraction experiment, provided the aqueous phase is identical to the one used in the “fitting” experiments and Hansens solubility parameters are known for the organic solvent(s).

## 5. Experimental

### 5.1 Extraction procedures

Extraction of americium, curium and promethium was investigated using 2,2':6,2''-terpyridine(terpy) and  $\alpha$ -bromodecanoic acid as complexing agents.

The aqueous phase was the same during all experiments and consisted of about 0.1 Mcpm per cm<sup>3</sup> each of <sup>241</sup>Am, <sup>244</sup>Cm and <sup>147</sup>Pm in 0.05 M HNO<sub>3</sub>. The organic phase was made up of one or more different organic solvent(s) in which  $\alpha$ -bromodecanoic acid and terpy were dissolved to a concentration of 1 M and 0.1 M respectively. If there were more than one organic solvent present in the organic phase the volume ratio between them was 1. The different solvents used, and  $\alpha$ -bromodecanoic acid along with its solubility parameters, are listed in Table 5.1. Combinations of solvents tested, for those experiments where more than one organic solvent was present in the organic phase, are listed in Table 5.2.

2,5 ml of each phase was added to a test tube. It was shaken for 5 minutes and the phases were allowed to settle. 1ml of the aqueous phase was removed for liquid scintillation counting and 200 $\mu$ l of each phase was taken for measurement on a NaI(Tl) detector, the former for detection of  $\alpha$  and  $\beta$  and the latter for  $\gamma$  detection. The specific radioactivity from each radionuclide and phase was obtained and distribution values could be calculated. Each extraction case was carried out five times if there was only one solvent in the organic phase and three times for the other extraction cases. Mean values and standard deviation for the specific activity was calculated, as well as standard deviation for the values of distribution.

*Table 5.1. A list of substances used in the experiments. All parameter values was found in [13], if not stated otherwise*

Different organic substances	Hansen solubility parameters in (cal/cm <sup>3</sup> ) <sup>1/2</sup>		
	$\delta_d$	$\delta_p$	$\delta_h$
2,2':6,2''-Terpyridine	8,65 <sup>a</sup>	3,85 <sup>a</sup>	4,52 <sup>a</sup>
Alfabromodecanoic acid	8.17 <sup>a</sup>	0.99 <sup>a</sup>	3.39 <sup>a</sup>
Xylene	8.60	0.9 <sup>b</sup>	1.2 <sup>b</sup>
Toluene	8.80	0.68	0.98
Cyclohexane	8.21	0	0.10
n-Hexane	7.28	0	0
Nitrobenzene	9.78	4.20	2.00
Chloroform	8,70	1,52	2,79
Tertbutyl benzene	8,35 <sup>c</sup>	0,32 <sup>d</sup>	0 <sup>e</sup>
Benzene	9.00	0	0.98
Carbon tetrachloride	8.70	0	0.29
Chlorobenzene	9.29	2.10	0.98
Ethyl benzene	8.70	0.29	0.68

<sup>a</sup>: Parameter value calculated from group molar contributions[14]

<sup>b</sup>: Parameter value from Charles Tenant & Company Ltd[15]

<sup>c</sup>: Parameter value calculated from heat of vaporisation using: (equation 4.3 - equation 4.10)

<sup>d</sup>: Parameter value calculated from refractive index using equation 4.10

<sup>e</sup>: Parameter value calculated using equation 4.8

*Table 5.2 Different combinations of organic solvents experimented with, in cases where more than one solvent was present in the organic phase*

**Combinations of organic solvents tested**

---

Cloroform / Tertbutyl benzene  
 Clorobenzene / Xylene  
 Ethyl benzene / Clorobenzene  
 Cyclohexane / Toluene  
 Nitrobenzene / n-Hexane  
 Benzene / Carbon tetrachloride  
 Benzene / Carbon tetrachloride / Toluene  
 Cyclohexane / Chloroform / Chlorobenzene

**5.2 Radionuclides**

$^{241}\text{Am}$  decays through  $\alpha$ -radiation with subsequent  $\gamma$ -radiation. The half-life for  $^{241}\text{Am}$  is 432.7 years and notable energies for detection are:

keV	$\alpha$ (%)
5388.40	1.4
5443.01	12.8
5485.70	85.2
5511.61	0.20
5544.25	0.34

keV	$\gamma$ (% of the total $\alpha$ -decay)
59.54	35.7

$^{244}\text{Cm}$  also decays through  $\alpha$ -emission with subsequent  $\gamma$ -radiation. Its half-life is 18.11 years and notable  $\alpha$ -energies are:

keV	$\alpha$ (%)
5762.84	23.6
5804.96	76.4

The  $\gamma$ -energies for the  $^{244}\text{Cm}$  decay are too small for measurement in the NaI(Tl) scintillator.

$^{147}\text{Pm}$  decays through  $\beta$ -radiation with subsequent  $\gamma$ -radiation. It has a half-life of 2.62 years,  $E_{\beta,\text{max}}$  is 224 keV and notable  $\gamma$ -energies are:

keV	$\gamma$ (% of total $\beta$ -decay)
76.14	$1.03 * 10^{-8}$
121.26	0.00285
197.39	$3.4 * 10^{-7}$

### 5.3 Detection

The liquid scintillation detector used was a 1219 Rackbeta liquid scintillation counter from LKB Wallac. The sample taken from the aqueous phase was mixed with 10 ml Emulsifier-Safe<sup>TM</sup> scintillation fluid to make a suitable scintillation cocktail for liquid scintillation. Every pulse detected adds a count to a specific channel, each channel representing a small energy interval. This means that nuclides with similar energies might result in one large peak instead of several smaller, which is the case with the  $^{241}\text{Am}$ - and  $^{244}\text{Cm}$ -isotopes (fig 5.1). Each sample was measured for 150 seconds and the results were divided into two different energy intervals, "windows". The first interval ranged from channel 1 to 550 and was used for detection of  $\beta$ -radiation from  $^{147}\text{Pm}$ , and the second ranged from channel 575 to 800 and was used for detection of  $\alpha$ -radiation from  $^{241}\text{Am}$  and  $^{244}\text{Cm}$ .

Figure 5.1

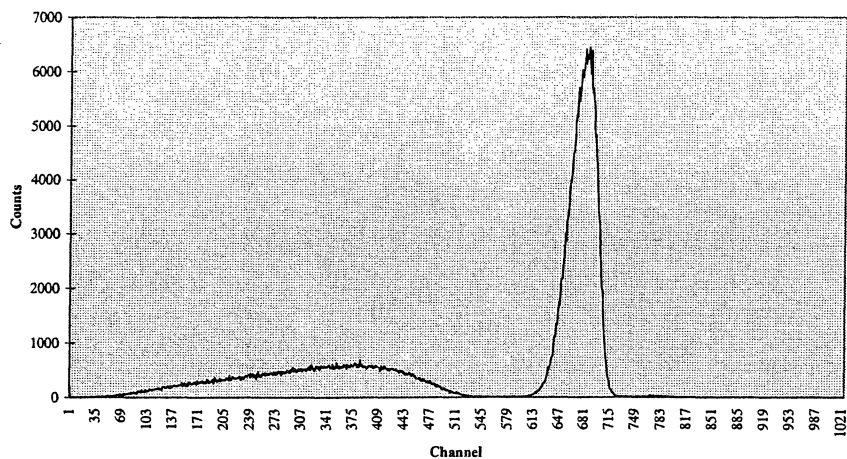


*Figure 5.1 Plot from a measure of the standard in the liquid scintillator. The first peak is a characteristic  $\beta$ -peak originating from  $^{147}\text{Pm}$ . The other peak is an  $\alpha$ -peak from both  $^{241}\text{Am}$  and  $^{244}\text{Cm}$  together.*

The NaI(Tl) detector was a Gamma Counter 4000 from Intertechnique. This scintillator only detects  $\gamma$ -radiation in an energy interval preset by the user. This interval was set so that the scintillator did not detect any  $\gamma$ -radiation from  $^{244}\text{Cm}$ , only from  $^{241}\text{Am}$ . Each sample was measured in the detector for 20 min. This gave the specific activity of  $^{241}\text{Am}$  in the samples, which could then be subtracted from the large  $\alpha$ -peak obtained from the liquid scintillation to find the specific activity of  $^{244}\text{Cm}$ .

With the specific activity known for every radionuclide, D-values were calculated using equation 3.1b.

## 6. Results

Experiments show that there is a distinct difference in the distribution of metal complexes between different organic phases. Am and Cm are always easier extracted to the organic phase than Pm i.e. Am and Cm have higher D-values. A common trend is that the actinides, Am and Cm, are separated from the lanthanide, Pm, with a factor of about 10 in most of the extraction cases. This actinide-lanthanide separation is observed in earlier experiments [4]. Specific activities, with their standard deviation, for each experiment are found in Appendix.

D-values obtained from liquid-liquid extractions with the organic phase consisting of only one solvent were used as data, along with the  $\delta_d$ -,  $\delta_p$ -,  $\delta_h$ - and  $V_{m,org}$ -values for each respective case, to find the 5 unknown constants for eq. 4.17 (discussed in chapter 4). This was done by fitting equation 4.17 to the data, by minimising the sum of squares of differences between theoretical predictions and experimental values. Obtained constants shown in table 6.1. All values of distribution constants experimentally found together with the standard deviation are plotted in graphs. Also plotted in the same graphs, for comparison, are the values of distribution calculated with the fitted model, see fig 6.1a, b, c.

The model gives a good agreement in most extraction cases except for the case where both nitrobenzene and n-hexane were present in the organic phase, see fig 6.1a, b, c. This disagreement is probably due to the strong polar contribution of nitrobenzene, which might induce other dipoles. Hansen solubility parameters does not take dipole-induced dipoles into contribution, and since the fitted model is based on these solubility parameters nitrobenzene gives a bad agreement.

Hansen solubility parameters for a mixture of substances were calculated using the formula:

$$\delta_{i,tot} = \sqrt{\frac{\delta_{i,1}^2 \cdot V_1 + \delta_{i,2}^2 \cdot V_2 + \dots + \delta_{i,n}^2 \cdot V_n}{V_1 + V_2 + \dots + V_n}} \quad (6.1)$$

$i = d, p$  or  $h$

$n =$  number of components

$V =$  volume of each component in the mixture

The molar volume for a mixture,  $V_{m,tot}$ , was calculated in a similar way:

$$V_{m,tot} = \frac{V_{m,1} \cdot V_1 + V_{m,2} \cdot V_2 + \dots + V_{m,n} \cdot V_n}{V_1 + V_2 + \dots + V_n} \quad (6.2)$$

The terpy dissolved in the organic phase was assumed not to effect the total volume of the organic phase.

The calculated Hansen solubility parameters and molar volumes used as data when fitting eq. 4.17 are shown in Table 6.2.

*Table 6.1 Constants used in equation 4.17, obtained from fitting.*

Constants for equation 4.17	A= Am- complex	A= Cm- complex	A= Pm- complex
$V_{m,A}$ (cm <sup>3</sup> /mole)	331.0	389.5	402.8
$K$ (cal/cm <sup>3</sup> )	42.29	43.54	37.63
$\delta_{dA}$ (cal/cm <sup>3</sup> ) <sup>1/2</sup>	6.10	5.82	6.19
$\delta_{pA}$ (cal/cm <sup>3</sup> ) <sup>1/2</sup>	1.82	1.82	1.60
$\delta_{hA}$ (cal/cm <sup>3</sup> ) <sup>1/2</sup>	0	0	0

*Table 6.2 Hansen solubility parameters and molar volumes for different organic phases*

Organic phase consists of 1 M $\alpha$ -bromo and 0.1 M terpy in:	$\delta_d$ (cal/cm <sup>3</sup> ) <sup>1/2</sup>	$\delta_p$ (cal/cm <sup>3</sup> ) <sup>1/2</sup>	$\delta_h$ (cal/cm <sup>3</sup> ) <sup>1/2</sup>	$V_{m,org}$ (cm <sup>3</sup> /mole)
Xylene	8.586	1.052	1.992	144.7
Toluene	8.743	0.914	1.896	131.7
Cyclohexane	8.281	0.687	1.688	133.2
Chloroform	8.664	1.511	2.991	111.2
Tertbutyl benzene	8.393	0.744	1.685	170.0
Benzene	8.901	0.687	1.896	117.6
Carbon tetrachloride	8.664	0.687	1.705	123.6
Chlorobenzene	9.132	1.982	1.896	127.7
Ethyl benzene	8.664	0.734	1.790	143.9

Am

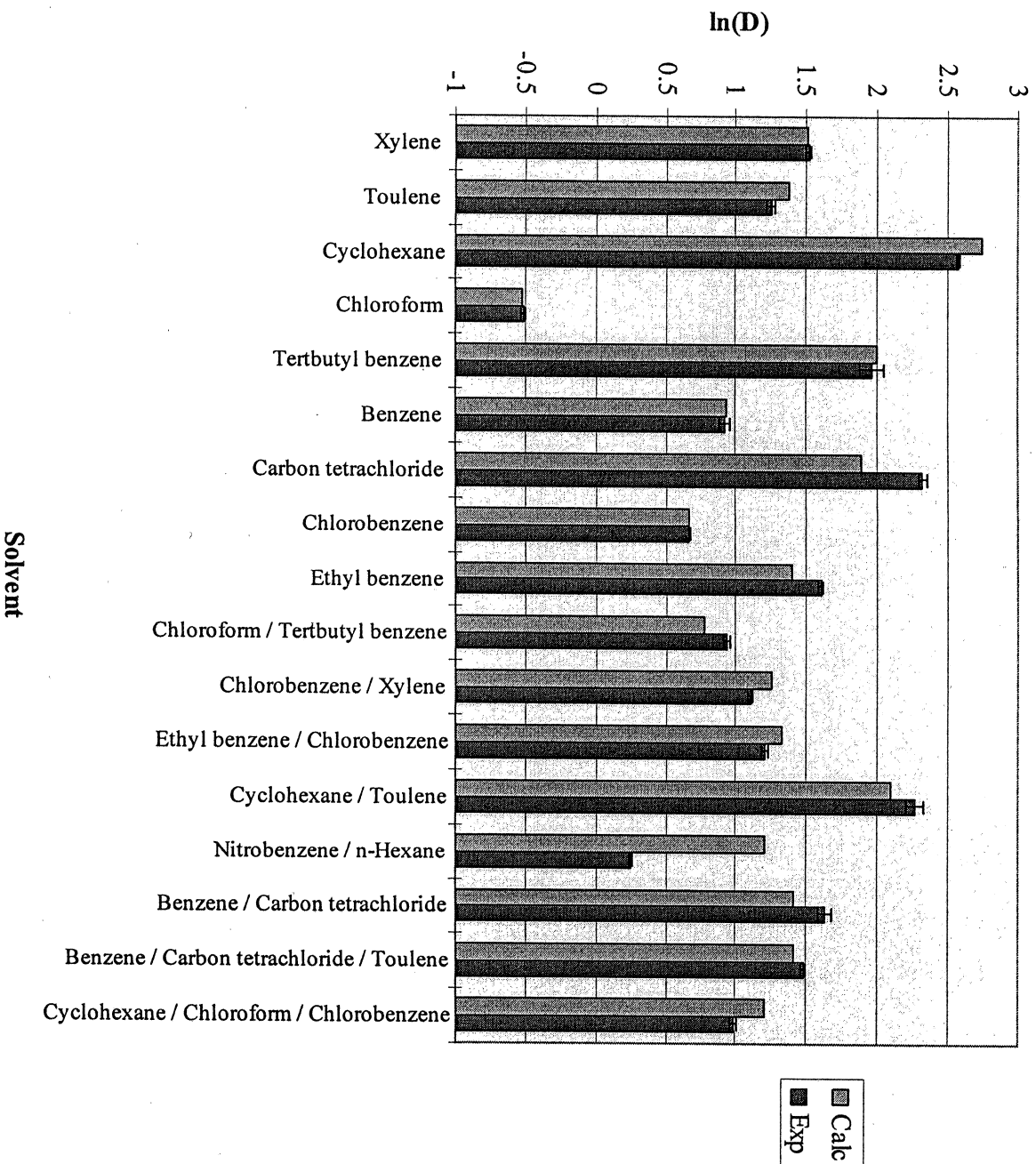
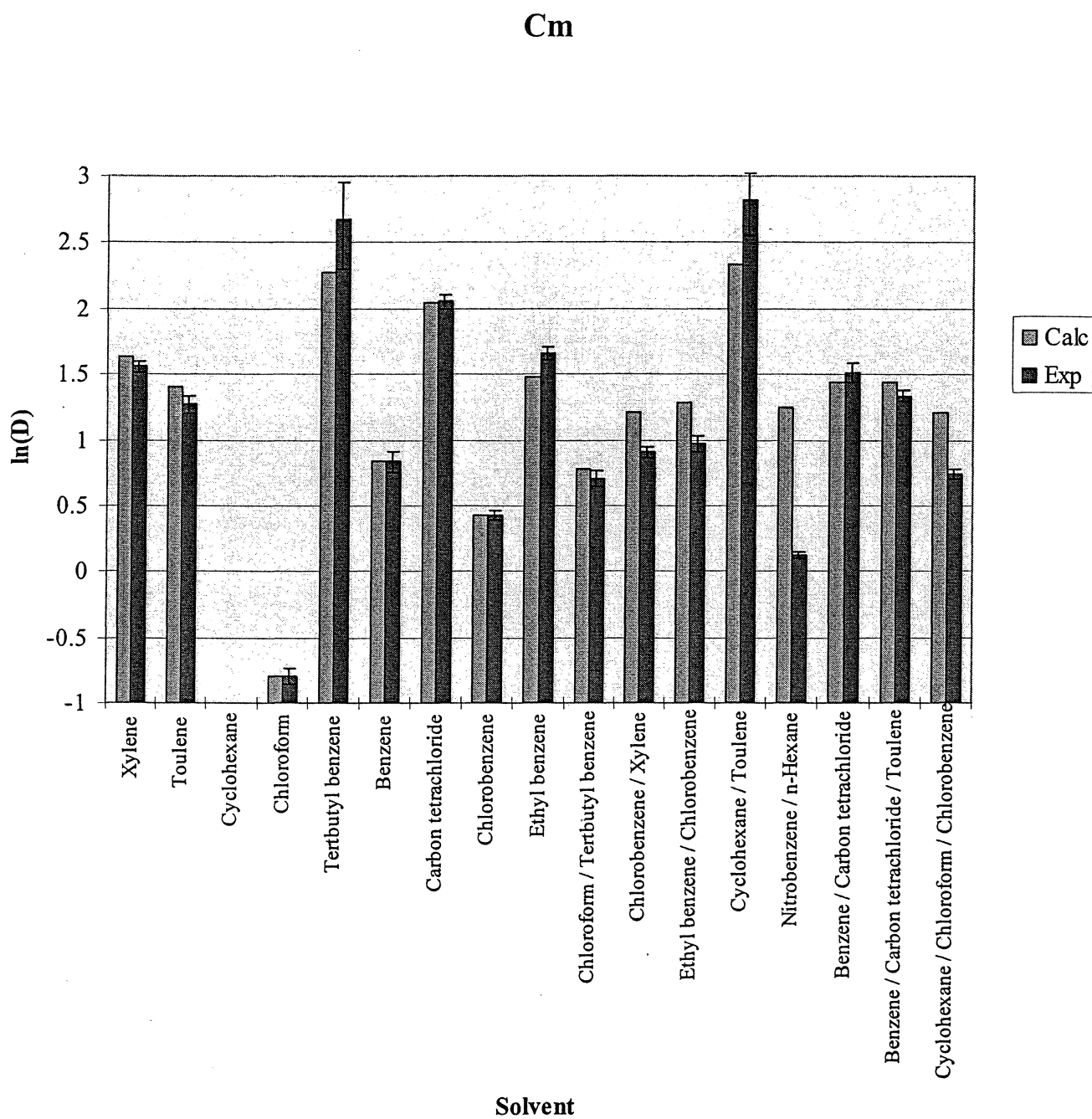


Figure 6.1a

Differences between calculated and experimental values of distribution for Am-complex.



**Figure 6.1b**

*Differences between calculated and experimental values of distribution for Cm-complex. No value is given for cyclohexane due to large uncertainties in the specific activities measured.*

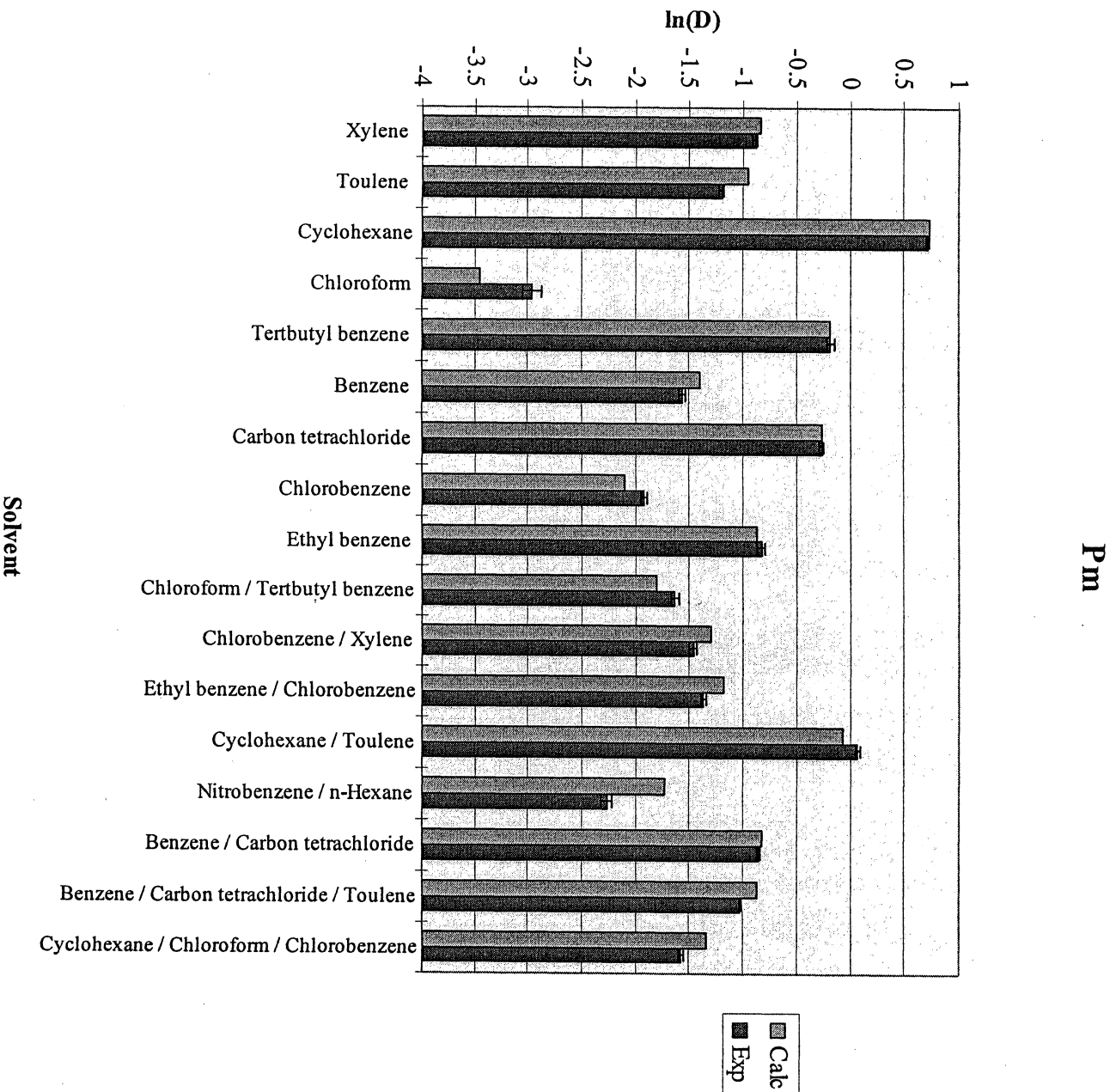


**Figure 6.1c** Differences between calculated and experimental values of distribution for P<sub>m</sub>-complex.

## 7. Conclusions

In this diploma work a model for calculating the result of a liquid-liquid extraction has been developed. This model is based on Hansens solubility parameters and requires very few input data. Solubility parameters and molar volumes for the substances in the organic phase are all that is needed to calculate the expected value of distribution in an extraction experiment. Since solubility parameters are widely used in the plastic and paint industry, data for most standard organic solvents can be found in tables produced by many of the industries in this branch.

The model was found to give a good agreement with experiments for most of the extraction cases tested. However, the model does not work well with nitrobenzene, which is a strong polar substance. This suggests that further development of the model is needed, perhaps by including dipole induced dipole interactions. The simplicity of the model makes it easy to expand and the results found so far indicate that it may be worth spending more time along this track.

## 8. Acknowledgements

I would like to thank my supervisors and friends, Prof. Jan-Olov Liljenzin, Prof. Gunnar Skarnemark, Christian Ekberg and Sofie Andersson for enduring all my questions and endless need for help. Thanks also to Allan Emrén for helping me understand the wonders of physical chemistry.

A special thanks to Dr. Stig Wingefors for helping me out with the solubility parameter concept and for improving the quality of my work with some constructive criticism.

Finally I would like to thank everyone at the department of nuclear chemistry for making this crazy place seem like a normal working habitat.

## 9. References

- [1]. Enarsson Å., Landgren A., Liljenzin J-O., Skålberg M., Spjuth L., Gudowski W., Wallenius J. "Partitioning and transmutation", (P&T) (1997), Status report
- [2]. Landgren A. "The Use of Aliquat-336 in a Partitioning and Transmutation Process and a Kinetic Study of the Oxidation of U(IV) to U(VI)", PhD Thesis, Department of Nuclear chemistry, Chalmers University of Technology (1999)
- [3]. Ekberg C. "Uncertainties in Actinide Solubility Calculations Illustrated using the Th-OH-PO<sub>4</sub> System", PhD Thesis, Department of Nuclear chemistry, Chalmers University of Technology (1999)
- [4]. Hagström I., Spjuth L., Enarsson Å., Liljenzin J-O., Skålberg M., Hudson M.J., Iveson P.B., Madic C., Cordier P.Y., Hill C. Francois N. "Synergistic Solvent Extraction of Trivalent Americium and Europium by 2-bromodecanoic Acid and Neutral Nitrogen-Containing Reagents", Solvent Extraction and Ion Exchange, 17(2), (1999), 221-242
- [5]. Suzuki N., Satake S., Tsukahara S. "Synergic Extraction of Lanthanoids(III) with Thenoyltrifluoroacetone and Terpyridine", J. Radioanalytical and Nuclear Chem. vol 172, No2(1993), 239-248
- [6]. Andersson S. *et al.*, Personal communication
- [7]. Vitorge P. Thesis University Pierre et Marie Curie, 80-83
- [8]. Burke J. "Solubility Parameters", The Book and Paper group annual / Washington D.C Book and pap 1982-. vol 3 (1984), 13-58

- [9]. Pimentel G.C., McCiellan A.L. "The Hydrogen Bond", W.H. Freeman and Co., San Francisco (1960), Chap. 7
- [10]. Böttcher C.J.F. "Theory of Electric Polarization", Elsevier. New York (1952), chap 5, 153-159
- [11]. Hansen C., Skaaup K. "Some Aspects of the Three Dimensional Solubility Parameter", Dansk Kemi 48 (1967), 81-84
- [12]. Wakahayashi T., Oki S., Omori T., Suzuki N. "Some Applications of the Regular Solution Theory to Solvent Extraction-I", J. Inorg. Nucl. Chem. vol 26 (1964), 2255-2264
- [13]. Hansen C. "Hansen Solubility Parameters: A Users Handbook", CRC Press (2000)
- [14]. Barton A.F.M. "CRC Handbook of Solubility Parameters and Other Cohesion Parameters", CRC Press (1991), chap 6, 182-185
- [15]. Charles Tenant & Company (London) Ltd.  
Web site: <http://www.ctennant.co.uk/proddata/tp00006a.htm>

## Appendix

Table A.1 Specific activity in  $\text{cpm}/\text{cm}^3$  for each phase.

Xylene		Toluene	
Am (aq)	19905±336	Am (aq)	24722±638
Am (org)	90478±764	Am (org)	86032±863
Cm (aq)	16719±682	Cm (aq)	20733±1340
Cm (org)	79295±1397	Cm (org)	73903±1851
Pm (aq)	82885±571	Pm (aq)	89242±434
Pm (org)	34179±779	Pm (org)	26892±641

Cyklohexane		n-Hexane	
Am (aq)	7843±121	Am (aq)	8447±282
Am (org)	102568±569	Am (org)	101945±507
Cm (aq)	934±737	Cm (aq)	3623±334
Cm (org)	94281±1472	Cm (org)	92088±846
Pm (aq)	38188±633	Pm (aq)	47766±156
Pm (org)	78230±840	Pm (org)	68858±364

Nitrobenzene		Chloroform	
Am (aq)	90666±844	Am (aq)	68930±437
Am (org)	19903±1068	Am (org)	41116±661
Cm (aq)	82862±1493	Cm (aq)	65593±1133
Cm (org)	12223±2004	Cm (org)	29759±1644
Pm (aq)	115795±593	Pm (aq)	110309±293
Pm (org)	626±800	Pm (org)	5753±500

T.b.benzene		Benzene	
Am (aq)	13632±1086	Am (aq)	31634±995
Am (org)	96988±1582	Am (org)	79149±1220
Cm (aq)	6049±1887	Cm (aq)	28732±2026
Cm (org)	87861±2669	Cm (org)	66320±2538
Pm (aq)	63227±1321	Pm (aq)	94743±378
Pm (org)	52821±1528	Pm (org)	19792±583

CCl <sub>4</sub>		Trich.ethylene	
Am (aq)	9878±334	Am (aq)	26575±251
Am (org)	100652±729	Am (org)	84228±476
Cm (aq)	10737±582	Cm (aq)	27321±648
Cm (org)	83839±1264	Cm (org)	67571±1160
Pm (aq)	64427±586	Pm (aq)	92130±208
Pm (org)	49393±791	Pm (org)	21804±413

Ch.benzen		Ethyl benzene	
Am (aq)	37479±208	Am (aq)	18568±338
Am (org)	73047±433	Am (org)	92017±563
Cm (aq)	37491±835	Cm (aq)	15076±703
Cm (org)	57351±1347	Cm (org)	78917±1214
Pm (aq)	99817±217	Pm (aq)	78634±927
Pm (org)	14653±423	Pm (org)	34284±1131

*Table A.2 Combinations of solvents used as organic phase with indexes.*

Combinations of organic solvents tested	Index
Cloroform / Tertbutyl benzene	A
Clorobenzene / Xylene	B
Ethyl benzene / Clorobenzene	C
Cyclohexane / Toluene	D
Nitrobenzene / n-Hexane	E
Benzene / Carbon tetrachloride	F
Benzene / Carbon tetrachloride / Toluene	G
Cyclohexane / Chloroform / Chlorobenzene	H

*Table A.3 Specific activity in cpm/cm<sup>3</sup> for each phase when more than one organic solvent was used in the organic phase.*

A		B	
Am (aq)	31281±699	Am (aq)	27735±481
Am (org)	79266±924	Am (org)	83163±706
Cm (aq)	30856±1630	Cm (aq)	27193±1115
Cm (org)	62593±2140	Cm (org)	67162±1627
Pm (aq)	94548±536	Pm (aq)	92183±675
Pm (org)	18444±741	Pm (org)	21246±880

C	
Am (aq)	26942±569
Am (org)	89334±895
Cm (aq)	24121±1219
Cm (org)	63949±1830
Pm (aq)	90665±262
Pm (org)	23122±467

D	
Am (aq)	10935±625
Am (org)	105341±951
Cm (aq)	4964±943
Cm (org)	83106±1555
Pm (aq)	54982±777
Pm (org)	58805±982

E	
Am (aq)	50751±216
Am (org)	65010±541
Cm (aq)	41560±402
Cm (org)	47106±1014
Pm (aq)	102714±302
Pm (org)	10598±507

F	
Am (aq)	18894±908
Am (org)	96868±1234
Cm (aq)	15951±1029
Cm (org)	72715±1640
Pm (aq)	79511±345
Pm (org)	33801±550

G	
Am (aq)	21462±379
Am (org)	94149±704
Cm (aq)	18518±701
Cm (org)	70456±1312
Pm (aq)	83173±173
Pm (org)	29790±378

H	
Am (aq)	31666±573
Am (org)	84424±898
Cm (aq)	28464±740
Cm (org)	59573±1352
Pm (aq)	93401±207
Pm (org)	19267±411

Reprinted from

# Talanta

---

Talanta 51 (2000) 231–246

## Assessment of uncertainty in parameter evaluation and prediction

G. Meinrath<sup>a,b,c,\*</sup>, C. Ekberg<sup>d</sup>, A. Landgren<sup>d</sup>, J.O. Liljenzin<sup>d</sup>

<sup>a</sup> Faculty of Chemistry and Physics, Institute of Inorganic Chemistry, Technical University Mining Academy Freiberg, D-09596 Freiberg, Germany

<sup>b</sup> Department of Hydrogeology, Faculty of Geology, Technical University Mining Academy Freiberg, D-09596 Freiberg, Germany

<sup>c</sup> RER Consultants, Schießstattweg 3a, D-94032 Passau, Germany

<sup>d</sup> Department of Nuclear Chemistry, Chalmers University of Technology, S-41296 Gothenburg, Sweden



ELSEVIER